A BIOMIMETIC APPROACH TO ACTIVE SELF-MICROENCAPSULATION OF PROTEINS IN POLY (DL)-LACTIC-CO-GLYCOLIC ACID

by

Ronak B. Shah

A dissertation submitted in the partial fulfillment
of the requirements for the degree of
Doctor of Philosophy
(Pharmaceutical Sciences)
in the University of Michigan
2015

Doctoral Committee:

Professor Steven P. Schwendeman, Chair
Research Professor Gregory E. Amidon
Professor Joerg Lahann
Associate Professor Naír Rodríguez-Hornedo

DEDICATION

To my father, mother, and sister,

to whom I will be forever and deeply indebted

for their unconditional

love and support.

न होगा यक-बयाबां मांदगी से ज़ौक़ कम मेरा
हबाब-ए मौजह-ए रफ़्तार है नक़्श-ए क़दम मेरा

- Mirza Ghalib

ACKNOWLEDGEMENTS

The list of people to whom I will be forever indebted for their kindness and generosity is rather long and tedious, but I will make an effort to acknowledge some of the people who have helped me during my time at the University of Michigan.

I will like to start by thanking Dr. Steven P. Schwendeman for giving me an opportunity to work in his research group and his continued support during my doctoral work. I am grateful to him for his wisdom, patience and giving me the chance to explore ideas independently. His insightful questions, thoughtful advice, and ability to fit research problems into the larger context of the field, were crucial for my work.

I would also like to thank the members of my committee. Dr. Gregory Amidon has always been very supportive, accessible, and encouraging. His advice, insight, and suggestions were very valuable. Dr. Naír Rodríguez-Hornedo has been a great resource, providing thoughtful insight and suggestions about my work. I am very thankful for her support and guidance. I am also thankful to Dr. Benedict Lucchessi for helping me approach my research from the standpoint of medical practitioners and patient convenience. In addition, I would like to thank Dr. Joerg Lahann for agreeing to be on my committee as a cognate member. His insightful comments and questions have been very useful. The committee as a whole has been very supportive and I have gained immensely from my discussions with them. Dr. Anna Schwendmen has also been a great

source of help and encouragement. Finally, I would also like to thank Dr. David Putnam for his mentorship and support during my time at Cornell.

I would like to extend my sincere thanks to all the members of the Schwendeman lab with whom I had the pleasure of working with. I am grateful to Dr. Kashappa Desai, Dr. Samuel Reinhold, Dr. Ying Zhang and Dr. Andreas Sophocleous for training and helping me when I initially joined the lab. I would also like to thank my fellow graduate students in the lab for their support and help. In addition, I would like to thank our lab manager, Karl Olsen for his help in carrying out my work.

Here, I would also like to thank all my friends and colleagues for their friendship and company. I had the pleasure of meeting and being friends with some remarkable people during graduate school. Their companionship and kindness greatly enriched my graduate school experience. I would also like to thank all the support and administrative staff at the College of Pharmacy and the Biointerfaces Institute who often went out of their way to help me. I would like to acknowledge the various sources of funding which have supported me including, Savitaben Chotubhai fellowship, Warner Lambert/Park Davis fellowship, the College of Pharmacy, and the National Institute of Health (NIH EB 08873 and NIH HL 68345).

I would like to acknowledge the support and love my family has extended. I will like to extend a very heartfelt thanks to Sejal, Nimisha, Utpal and Niraj. Finally, I would like to thank my father, mother, and sister for their unconditional love. I continue to draw from

their support the resolve to follow my dreams. Their kindness and thoughtfulness inspires me to be a better person, and I am thankful to have them in my life.

I am a part of all that I have met;
Yet all experience is an arch wherethro'
Gleams that untravell'd world whose margin fades
For ever and forever when I move.
How dull it is to pause, to make an end,
To rust unburnish'd, not to shine in use!
As tho' to breathe were life! Life piled on life
Were all too little, and of one to me
Little remains: but every hour is saved
From that eternal silence, something more,
A bringer of new things; and vile it were
For some three suns to store and hoard myself,
And this gray spirit yearning in desire
To follow knowledge like a sinking star,
Beyond the utmost bound of human thought.

- (Ulysses, Alfred Tennyson)

TABLE OF CONTENTS

LIST OF TABLES

LIST OF FIGURES

ABSTRACT

Poly (DL)-lactic-co-glycolic acid (PLGA) based delivery systems have been used extensively for the delivery of a range of therapeutic molecules. Here, a biomimetic approach to organic solvent-free microencapsulation of proteins based on the self-healing capacity of poly PLGA microspheres is developed to overcome issues associated with delivery of proteins. The biomimetic approach involves incorporation of biomaterials in the microparticles, which would actively bind and sequester growth factors, thereby improving the loading and stability during encapsulation and subsequent release. To screen BPs, aqueous solutions of BP [high molecular weight dextran sulfate (HDS), low molecular weight dextran sulfate (LDS), chondroitin sulfate (CS), heparin (HP), hyaluronic acid (HA), chitosan (CH)] and model protein lysozyme (LYZ) were combined in different molar and mass ratios, at 37 °C and pH 7. LDS and HP were found to bind > 95% LYZ at BP:LYZ > 0.125 w/w, whereas HDS and CS bound > 80% LYZ at BP:LYZ of 0.25–1 and < 0.33, respectively. The BP-PLGA microspheres (20–63 μm) were prepared by a double water–oil–water emulsion method with a range of BP content, and trehalose and $MgCO_3$ to control microclimate pH and to create percolating pores for protein. Biomimetic active self-encapsulation (ASE) of proteins [LYZ, vascular endothelial growth factor165 (VEGF) and fibroblast growth factor (FgF-20)] was accomplished by incubating blank BP-PLGA microspheres in low concentration protein solutions at ~ 24 °C, for 48 h. Pore closure was induced at 42.5 °C under mild agitation for 42 h. Formulation parameters of BP-PLGA microspheres and loading conditions were studied to optimize protein loading and subsequent release. Hyaluronic acid (HA)-PLGA

microsphere formulations were developed with HA of 66, 357 and 1010 kDa M_w. In the absence of $MgCO_3$, LYZ loading was found to increase with HA M_w and content. This effect on LYZ loading was dampened by the addition of $MgCO_3$ to HA-PLGA microspheres. Based on poor LYZ loading (< 2 % w/w of LYZ) and undesirable release kinetics, HA-PLGA microspheres were determined to be not suitable for developing a biomimetic approach to protein encapsulation. In contrast sulfated BP-PLGA microspheres were capable of loading LYZ (~ 2–7% w/w), VEGF (~ 4% w/w), and FgF-20 (~ 2% w/w) with high efficiency. Protein loading was found to be dependent on the loading solution concentration, with higher protein loading obtained at higher loading solution concentration within the range investigated. Loading also increased with content of sulfated BP in microspheres. Release kinetics of proteins was evaluated *in-vitro* with complete release media replacement. Rate and extent of release were found to depend upon volume of release (with non-sink conditions observed < 5 ml release volume for ~ 18 mg loaded BP-PLGA microspheres), ionic strength of release media and loading solution concentration. HDS-PLGA formulations were identified as having ideal loading and release characteristics. These optimal microspheres released ~ 73–80% of the encapsulated LYZ over 60 days, with > 90% of protein being enzymatically active. Nearly 72% of immunoreactive VEGF was similarly released over 42 days, without significant losses in heparin binding affinity in the release medium. Using circular dichroism, isothermal titration calorimetry, differential scanning calorimetry, and intrinsic fluorescence, we compared protein-biopolymer interactions to commonly used polyions like phytic acid (PA) and sucrose octasulfate (SO). We explored the potential of using biopolymers as stabilizing agents for the development of pharmaceutical

formulations of proteins. The interactions were found to be enthalpically driven and BPs were identified for their ability to stabilize proteins.

CHAPTER 1 INTRODUCTION

1.1 Motivation

The past decade has seen an increase of protein/peptide drugs being developed as pharmaceutical therapies for an array of diseases such as cancers, heart ailments and metabolic disorders [1, 2]. Complex macromolecular protein and peptide pharmaceutical formulations are generally not suitable for oral administration, as protein drugs tend to degrade during their passage through the gastrointestinal tract (GI) and are poorly absorbed across the GI mucosa. Systemic delivery is associated with increased costs and potential side effects/toxicity due to the absence of site-specific targeting methodologies. Therefore great effort has been spent on developing suitable delivery methods for administering these drugs [3] as their efficacy is closely related to drug stability and delivery. In addition, sky-rocketing healthcare costs make it essential to develop inexpensive yet robust delivery systems, especially with the possible launch of biosimilar generics in the near future. Thus, a number of drug delivery systems have been developed since the 1980's to explore delivery of bioactive protein drugs [1, 4, 5]. Numerous local/regional and targeting modalities/strategies have also been used in conjugation with these systems to enhance delivery and efficacy.

Biodegradable microparticles composed of natural or synthetic polymers have emerged as suitable delivery systems for controlled release of proteins, peptides, growth factors, small molecules and chemotherapeutic agents [6-11]. Poly (lactic-co-glycolic acid) (PLGA)-based polymers possess highly desirable qualities such as biodegradability and favorable non-immunogenic characteristics, when employed to fabricate systems for drug delivery. PLGA has been incorporated in numerous products approved by the United States Food and Drug Administration, making it an attractive polymer for developing new delivery systems. A major drawback of the polymer is the acidic environment when delivering acid liable drugs, which is commonly created by the build-up of degradation products in PLGA [11]. However, this issue has largely been overcome by incorporation of poorly soluble basic additives and other pH-modifying species into the polymer. A number of formulation methods have been explored to improve drug stability, loading, release characteristics, and processing [4, 12].

Additional considerations of protein encapsulation in microparticles are protein exposure to the organic/aqueous interface, shear, air/liquid interface, organic solvents and high temperatures [13, 14]. These factors combine to make protein encapsulation one of the two major issues in the development of controlled-release formulations for protein drugs, along with instability during *in vivo* release [11]. Our group has developed an encapsulation technique 'self-healing microencapsulation', which circumvents many of the traditional stresses polymer-encapsulated proteins are exposed to, and offers a substantial stability advantage over them [15, 16].

Recently our group has developed a novel active self-encapsulation method, which is capable of microencapsulating proteins safely with high efficiency by simple mixing of porous PLGA and the protein of interest [17]. In this work, we expand on the active self-encapsulation paradigm by introducing a biomimetic approach. This would be brought about by incorporating biomaterials in the microparticles, which would actively bind and sequester growth factors, thereby improving the loading and stability during encapsulation and subsequent release. The bio-mimetic approach will be adopted to exploit the unique interactions between growth factors and biomaterial like glycosaminoglycans, which are known to sequester and stabilize growth factors *in vivo.*

1.2 Age of Biologics

Biologics are rapidly emerging as a major class of drug products with expected sales of nearly $200 billion by 2017, representing 19-20% of total market value [2]. Proteins, antibodies and vaccines account for a total sales of ~ $108 billion in 2012, with 29 blockbusters amongst their ranks [1, 2]. In addition, sky-rocketing healthcare costs make it essential to develop inexpensive yet robust formulations, especially with the expected growth of biosimilars in the near future. A number of challenges associated with formulation development need to be addressed for this to happen. Stability and aggregation of biologics in solution is one of the major challenges being faced during production and storage of injectable biologics [18, 19]. Aggregation causes not only loss of therapeutic dosage, but could also lead to hazardous immunogenic reactions [20-22].

1.3 Controlled Release Formulations

Sustained drug levels in the blood or target tissue for 1-3 months following a single injection has been a much cherished aim for numerous drug companies for delivery of their polypeptide drugs. This long duration is not so readily attainable by non-PLGA systems, which do not have commercial precedence and lack the so-called "real world biomaterial" status. Peptide/protein modification and no-invasive strategies have typically been limited to weekly dosing, due to limitations associated with the half-life of the therapeutic agent. However, in order to accomplish 1-3 month controlled release, typically high total doses would have to be delivered via the polymer system. Once administered to the body, the polymer would react with water to bring about polymer erosion and degradation and subsequent release of the drug.

1.3.1 Biodegradable Polymer Delivery Systems

As newer molecules have been formulated for a wide variety of diseases and therapies, they demand different properties for optimal delivery. A very large number of natural and synthetic polymers have been developed over the years for the delivery of pharmaceutically active compounds [7, 8, 11, 23-26]. A range of biodegradable biopolymers has been developed to meet these challenges [6-11]. Of these, only a few reach the clinic and beyond in large part because of the high costs and risk associated with placing unproven biomaterials in pharmaceutical LAR (long acting release) products. In addition, others fail because of poor drug-polymer compatibility, inherent

polymer toxicity, immunogenicity, low drug loading and poor preclinical performance [5].

In spite of these obstacles, some promising clinical results have been reported. For example, Locetron®, a poly (ether-ester) microsphere formulation for the delivery of interferon α2b, had promising phase II trials [27, 28]. PhaseBio pharmaceuticals has reported promising clinical results for Lucemera® and Insumera®, which are based on its propriety elastin-like polypeptide delivery system [29]. The extensively studied polycaprolactone polymer has been a part of FDA-approved therapies in the past, making it a possible candidate for developing controlled release products [30]. Poly(d,l-lactide-*co*-hydroxymethyl glycolide) (PLHMGA) microspheres have been shown to strongly inhibit acidic conditions compared to equivalent PLGAs [31] and have been reported to release stable octreotide over 60 days [32]. Copolymerization of hydrophobic polymers (e.g. PLGA and PLA) with hydrophilic polymers also has been accomplished to overcome the issue of acidic degradation [5]. A polyoxalate based polymer system has been shown to be biodegradable, biocompatible, and provide better cell viability as compared to PLGA [33]. Polyketal copolymers have been shown to deliver imatinib effectively, but the inflammatory response warrants further investigation [34].

As it is evident, new polymers promising better therapeutic outcomes are many but the challenges remain the same, namely safety and efficacy. This, lead to a number of new biodegradable polymers to be developed over the years, but they have faced regulatory and clinical hurdles. Judicious and early use of cellular and animal studies need to be

adopted to ensure that biocompatibility issues are overcome for the timely development of safe and effective drug delivery systems. Another plausible factor limiting the alternatives to PLGA is the gap between the research work carried out developing new polymers and the developmental work in the pharmaceutical industry. Most new polymer systems are tested exclusively in preclinical studies, and rarely undergo further clinical research and development. These materials fall into the "valley of death", which arguably impedes development of new discoveries into therapies [35, 36]. Thus, in the absence of robust characterization and developmental work and a more straightforward regulatory path to close this gap, the industry usually prefers to work with very well characterized and polymeric biomaterials like PLGA, already used in FDA approved parenteral and implantable products, to avoid delays, risks and high costs associated with regulatory approval.

1.4 PLGA Microsphere Systems

1.4.1 Traditional Microsphere Formulations

The emulsion-solvent evaporation method is the most common method of preparing polymer microspheres. Four types of emulsion-solvent evaporation methods: oil-in-oil (O/O), oil-in-water (O/W), water-in-oil in water (W/O/W), and solid in-oil in water (S/O/W) are widely used. The W/O/W emulsion-based encapsulation method is the double emulsion process and has been shown to be ideal for water soluble proteins and peptides [37]. The method involves dissolving the drug in an aqueous solution and the

polymer in an organic solution. After mixing the solutions vigorously, an emulsion is created. This emulsion is added to a larger volume of aqueous solution that contains an emulsifier (e.g. polyvinyl alcohol). The suspension is then stirred and the organic solvent removed via evaporation or extraction. The microspheres are then washed, collected and dried [12].

Pores are an artifact of the emulsion based manufacturing process. Honeycomb or sponges like structures, with visible surface pores are seen in microspheres. Percolating pores with interconnecting networks are defined as a pore network having access to the polymer surface on two sides of the microsphere. These porous spaces are locations where water or organic solvent were present before lyophilization, preventing hydrophobic polymer occupation. The porosity, a measure of the total amount of empty space, is important because it has been shown to correlate with the amount of drug release during the initial release [38]. The extent of pore formation in w/o/w emulsion microspheres has been found to be dependent on a number of processing parameters. The rate of organic solvent evaporation and the polymer concentration are very important factors determining the porosity [12]. The composition and size of the inner aqueous phase was found to play a role in porosity. Additional parameters include the volume of the inner water phase, osmotic pressure difference between dispersed phase and continuous phase, ionic strength and type of emulsifier used [39].

1.4.2 Stability Concerns

The prevalent microsphere formulation methods have a number of drawbacks, particularly for delivery of proteins and other bio-macromolecules [10, 40]. The major issues are instability during encapsulation and release [38]. Additional problems include effective sterilization and variability within and across the different formulations. Unlike small molecules, protein/macromolecules are not only sensitive to chemical modifications but to minute physical modifications. These physical changes include aggregation, denaturation, precipitation and a change in their native conformation [41].

The manufacturing process, especially the encapsulation stage is known to be extremely harsh. The issues arise due to aforementioned organic/aqueous interface [42], shear, air/liquid interface, temperature change and others. As proteins consist of hydrophilic and hydrophobic domains, they are surface-active and end up aggregating at the various interfaces created during the manufacturing process [42, 43]. Any exposure to organic solvents is also known to bring about denaturation [44]. Methods like ultrasonification or mechanical shear, used to disperse the protein in the polymer phase, introduces energy into the system leading to localized temperature extremes and subsequent denaturation [45]. Traditionally, microspheres prepared with the protein in the first emulsion, face stability issues when they are lyophilized prior to storage. To overcome this, a number of cryopreservants have been used to maintain the bioactivity of the protein encapsulated [46]. The stability issues are reported to arise due to freezing and dehydration of the microsphere and the encapsulated protein.

When microspheres are placed in a release environment, they become hydrated with water uptake in the typical range of 20-100% of microsphere weight [13]. Both the polymer and protein are exposed to water during rehydration which leads to destabilization [46]. Protein molecules become more flexible and reactive, and are thus less stable [47]. Surprisingly at low and high moisture levels, aggregation is at minimum and it tends to maximize at intermediate moisture levels [48]. The aqueous pores in the PLGA microparticles consist of a distribution of 'microclimates', exposing the protein to unique and diverse set of environments created by the different levels of water penetration, polymer degradation and number of acidic moieties. In the literature, the microclimate differs remarkably across all formulations. Some formulations have been reported to possess neutral microclimate [49], while others have reported acidic microclimates [50-52]. Very low pH at physiological temperature is very detrimental to the proteins. Extremely low or high pH can lead to the protein developing a large positive and negative net charge respectively, leading to possible denaturation due to strong intra-chain repulsion. In addition, acidic moieties can cleave the peptide bond and lead to protein hydrolysis.

Model proteins like BSA and lysozyme have been reported to degrade over time in PLGA microparticles [38, 53]. This is crucial as some of the proteins/bio-macromolecules are very expensive and losses due to acidic hydrolysis would seriously hinder development of microparticle formulations. There are also safety concerns, e.g., regarding the immunogenicity of protein aggregates. To overcome this issue, a number of

bases (such as $Mg(OH)_2$, $MgCO_3$, $ZnCO_3$) have been added to the polymer solution in an effort to diminish these effects by increasing the pH [38]. Possible interactions between the PLGA and proteins, primarily during absorption have been reported, and can be attributed to hydrophobic interactions between the two. The extent of interaction has not been quantified, but is estimated to be limited to 10% of the loaded protein [13].

The other causes of protein instability during release include presence of water soluble oligomers, chemical reactivity and chemical changes like deamidation and oxidation [54]. It is believed that these factors only have a smaller role in the destabilization process for most proteins. Thus, any strategy to improve the stability would best be focused on the issues previously discussed first, and thereafter focused on the residual instability issues.

A major issue with commercialization of microparticle formulation is the need for sterilization. This is especially challenging, as it involves neutralizing all microorganisms, without compromising the encapsulated protein. Traditional sterilization techniques like heat, filtration, chemical sterilization and others are not applicable. Heating would damage the polymer and protein. Filtration would not be effective, as it cannot eliminate organisms inside the microparticle. Treatment with ethanol, ethylene oxide and other chemicals is not effective as they cannot sterilize all microorganisms and would damage the polymer matrix. This leaves radiation as the only viable option for sterilization. However, irradiation has been shown to cause polymer degradation, proportional to radiation dosage, although this loss does not preclude product development. Reports also indicate that irradiation causes potential aggregation and

difference in release profiles [55]. Irradiation of clonazepam, BSA and ovalbumin when encapsulated in PLGA microspheres has led to formation of free radicals [41]. Recently we have shown that it is possible to sterilize ASE microsphere formulations by gamma irradiation, allowing for bulk manufacturing of protein loaded ASE [56].

There is considerable variability among the microparticle formulations produced by the different research groups. Each group has its own protocol, equipment, process, environment, and location, which could be responsible for the variability.

1.5 Recent Advances

1.5.1 Self Encapsulation by Passive Diffusion

Polymers in solution can be very mobile enabling them to repair internal damages such as fracture or indentation. This process of intrinsic repair is called 'self-healing'. Wool and O'Connor [57] have proposed an eloquent theory consisting of five stages which are 1) surface rearrangement, 2) surface approach, 3) wetting, 4) diffusion, and 5) randomization. Investigations in our lab have shown that observed pore closing phenomenon is believed to occur in much the same manner as traditional self-healing systems [39]. The healing process is initiated by the changes at the edges of the cracks, which then approach another surface. Wetting involves formation of an interface between the two surfaces. This is followed by movement of polymers and intermingling. Using

this behavior, our group developed an encapsulation paradigm which addresses some of the issues with protein instability during encapsulation and sterilization [15]. This paradigm uses a 'self-encapsulation' method, which minimizes initial burst. It was hypothesized that the unknown pore closing mechanism may be a form of polymer self-healing, in which surface entanglements, facilitated by a temperature above the Tg, entangled and strengthened through random motion, and further driven by an attempt to minimize interfacial tension, allow polymer rearrangement and pore closing to take place [39]. The study also demonstrated improved protein stability over a traditional emulsion-based encapsulation technique and possibilities of incorporating additives to improve release characteristics. Thus, self-healing microencapsulation may hold a significant advantage in delivering proteins that are known to be highly unstable.

1.5.2 Active Self Encapsulation

Active self- encapsulation overcomes some of the loading efficiency issues associated with passive self-encapsulation by incorporating a protein trapping agent. The method relies on a) incorporation of a substance in the PLGA pores, which strongly binds the protein (e.g., alum absorption of vaccine antigens) [17] and b) self-healing the PLGA pores by raising temperature above the hydrated glass transition temperature of the polymer (i.e., in the vicinity of physiological temperature). The following important features of active self-encapsulation have been identified: a) outstanding protein stability during encapsulation owing to the absence of organic solvents, high shear, and other protein-denaturing stresses, b) the ability to encapsulate at high loading (>1 % w/w) from

low protein concentrations (< 1 mg/mL), c) long-term controlled release with excellent protein stability, and d) the ability to encapsulate without drying the protein. Alum has been shown to be able to effectively absorb and retain antigen from low concentration solutions [17]. The optimized formulations were shown to release stable antigen over 28 days.

1.6 Biomimetic Active Self Encapsulation Paradigm

In this study, I propose to incorporate biopolymers (BP) in the microspheres, which actively bind and sequester growth factors (GFs) [58-67]. The biomimetic approach would presumably enhance the stability of encapsulated protein during the loading and subsequent release [59, 61, 66]. BPs can also potentially enhance the biological effect of the protein by acting as co-factors. Exploiting the unique interactions between GFs and glycosaminoglycans, known to sequester and stabilize growth factors *in vivo;* BPs are used as trapping agents here to promote uptake of proteins from aqueous solution and to improve encapsulation efficiency. This work explores the potential and promise of the biomimetic approach in overcoming some of the limitations associated with stability and loading during encapsulation and subsequent release. Several BPs were selected for this purpose, namely hyaluronic acid, chondritin sulfate, heparin, chitosan and dextran sulfate. These BPs are members of the glycosaminoglycan (GAG) family or have similar structural moieties (e.g. - dextran sulfate and chitosan).

1.6.1 Biopolymers

Angiogenic growth factors are engaged in multiple interactions in the extracellular environment and on the extra-cellular surface. They bind to a variety of free or immobilized proteins, polysaccharides, and complex lipids present in the extracellular milieu and these interactions may affect their stability, integrity, bioavailability and diffusion [12]. They are found in body fluids as circulating complexes or immobilized in the ECM and in the sub-endothelial lamina of micro-and macrovasculature [58]. The ECM is largely composed of complex polysaccharides, with glycosaminoglycans (GAGs) being one of the major classes of polysaccharides. They are known to bind and regulate a number of distinct proteins, including chemokines, cytokines, growth factors, morphogens, adhesion molecules and enzymes [58]. GAGs are linear, generally sulphated, negtively charged polysaccharides with molecular weights in 10-100 kDa range [58]. Non-sulphated GAGs include hyaluronic acid (HA), whereas the sulphated include chondriton sulphate (CS), dermatran sulphate (DS), kertran sulphate (KS), heparin and heparin sulphate (HS).

1.6.1.1 Non Sulphated Glycosaminoglycans

1.6.1.1.1 Hyaluronic Acid

Hyaluronic acid (HA), is a polyanionic polysaccharide that consists of N-acetyl-D-glucosamine and β-glucoronic acid [68]. It is frequently referred to as hyaluronan because it exists *in vivo* as a polyanion and not in the protonated acid form. It is

distributed widely in vertebrates and is a major component of the cell coat of many strains of bacteria [67, 69].

HA is a unique GAG as it is neither sulfated nor bound to a core protein. In the ECM it is distributed as a long chain polymer (averaging 1-4 MDa) [70]. Its chemical structure was first elucidated by Weissman and Meyer in 1954 and has been significantly improved in the past decade. The unique viscoelastic nature of hyaluronan along with its biocompatibility and non-immunogenicity has led to its use in a number of cosmetic, medical, and pharmaceutical applications.

A significant amount of HA is found in synovial fluid, vitreous humor, cartilage, blood vessels, skin and umbilical cord. In its various forms and states, it is believed to play a role in tissue homeostasis, embryonic/tissue development, cell signaling cues, initiation and progression of pathological conditions, including aberrations of angiogenesis [69-71]. Of significant interest is its reported role in the mediation of angiogenesis via interaction with binding proteins and cell surface receptors, regeneration, wound healing and tumor invasion [68-70].

The biologic role and cellular interaction of HA is highly dependent on chain length. In tissues, long chain HA plays a role in maintaining a hydrated environment, regulates osmotic balance, acts as a shock absorber, space filler, and as a lubricant. At the same time, it can sequester and release growth factors and other biological signaling molecules [59]. Longer chains have been reported to inhibit proliferation of EC and disrupt newly-

formed EC layers [72]. HA oligomers are believed to cluster and activate receptors (e.g,CD-44, RHAMM, TLR-4) effectively, leading to inflammatory cytokine release and activation of inflammatory cells (e.g., EC's and smooth muscular cells) and their subsequent proliferation, migrations and tissue healing/remodeling [71]. Thus through their interaction with receptors, HA oligomers can induce neo-angiogenesis and sprout formation, both vital processes for tissue repair and growth.

1.6.1.1.2 Sulphated Glycosaminoglycans

The highly sulphated analogues, heparin and HS, have been studied extensively due to their well understood functions in anti-coagulation. Heparin is known to be highly evolutionarily conserved with similar structures found in a broad range of vertebrate and invertebrate organisms [63].

Heparin consists of repeating units of 1→4 linked pyranosyluronic acid and 2-amino-2-deoxyglucopyranose (glucosamine) residues [60]. The uronic acid residues typically consist of 90%L-idopyranosyluronic acid (L-iduronic acid) and 10%D-glucopyranosyluronic acid (D-glucuronic acid).

Various growth factors bind to the ECM of target tissues by forming tight complexes with sulphated-glycosaminoglycans [73]. Variations of the fine structure of the GAG chains may allow cells to control their responses to individual growth factors and to change the specificity of their response to different members of the growth factor family.

Reports indicate that GAG's mediate the activity of FGF-2 by inducing dimer formation and transient dimerization though specific interactions with FGF-2 and its receptor [74, 75]. No significant change in the structure of FGF-2 was observed upon binding. Sulphated-GAG's bind to different VEGF isoforms, exerting multifaceted effects. They contribute to VEGF accumulation in the ECM and acts as EC core-receptors for VEGF [65].

The effect of GAG's on VEGF165 would depend upon the size of the chains, high molecular weight chains increase VEGF binding to receptors while the lower molecular weight chains inhibit pro-angiogenic activity of VEGF165.

1.6.1.1.3 Chitosan

Chitin, poly[h(1α4)-2-acetoamido-2-deoxy-D-glucopyranose], is one of the most abundant natural polysaccharides and is present in crustacea, insects, fungi, and yeasts. Deacetylation of chitin by alkali produces chitosan (CH). The molecular structure of CH is believed to be a copolymer of N-acetyl-glucosamine and glucosamine; usually the glucosamine content is more than 90% [67].

Since CH has an amino group in the repeating unit, it affords ammonium groups in aqueous acidic media, at neutral pH. Owing to its cationic nature, CH spontaneously forms water-insoluble complexes with anionic polyelectrolytes [67]. Therefore, CH has been used mainly as a flocculent for the treatment of wastewater. However, it has been

increasingly used in biomedical and pharmaceutical fields because of its favorable properties of good biocompatibility, low toxicity, and biodegradability.

1.6.2 Protein-Glycosaminoglycans Interactions

The specificity of GAG-protein interactions is governed by the ionic interactions of the sulfate and carboxylate groups of GAGs with the basic amino acids on the protein as well as the optimal structural fit of a GAG chain into the binding site of the protein. The topology and distribution of the basic amino acids of the GAG binding site on the protein influences its specificity in molecular recognition of GAG sequences [60]. The binding affinity of the interaction depends on the ability of the oligosaccharide sequence to provide optimal charge (orientation of sulfate groups) and surface (van der Waals contact) complimentarity with the protein, which is governed by the three-dimensional structure and conformation of GAGs [60].

Co-crystal structures of HS-oligosaccharides have highlighted the ionic interactions between specific sulfate groups and carboxylate groups of HS with the basic amino acids in the GAG binding site on the protein [60]. However, ionic contacts are not sufficient to explain the optimal structural fit of a GAG oligosaccharide to the binding site of the protein that influences the affinity of the interaction. From the standpoint of GAG conformation, it can be envisioned that protein binding would induce local distortions in an otherwise uniform helical structure of GAGs, which are manifested as changes in the glycosidic torsion angles. These conformational changes would enable an optimal

structural fit in terms of both ionic and van der Waals contact between the oligosaccharide motif and the protein.

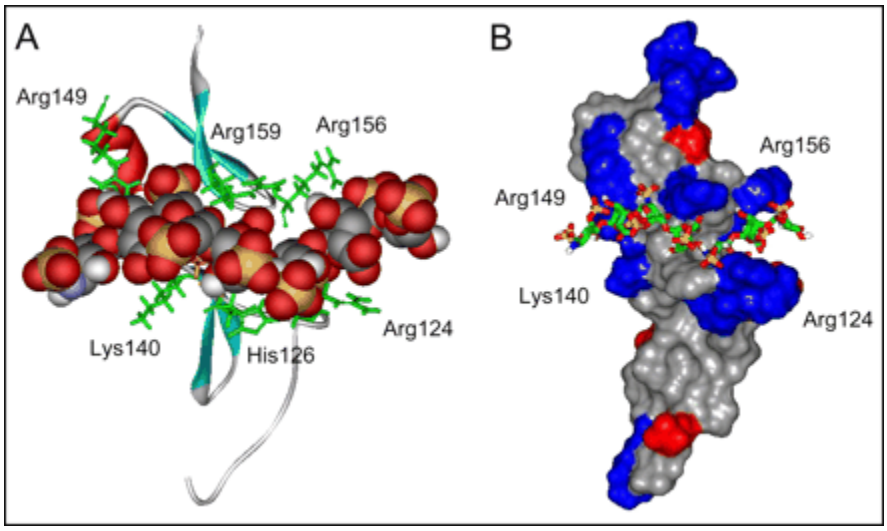

Figure 1-1 : Model of heparin/HS docking with VEGF165 heparin binding domain [77].

Strong ionic interactions are expected between GAGs and proteins [58]. Clusters of positively charged basic amino acids on proteins form ion pairs with spatially defined negatively charged sulphate or carboxylate groups on heparin chains. Glycosaminoglycans interact with residues that are prominently exposed on the surface of proteins. The main contribution to binding affinity comes from ionic interactions between the highly acidic sulphate groups and the basic side chains of arginine, lysine and, to a lesser extent, histidine [63]. The interactions of GAGs with proteins also involve a variety of different types of interactions, including van der Waals (VDW) forces, hydrogen bonds, and hydrophobic interactions with the carbohydrate backbone. It has also been observed that heparin-binding domains contain amino acids such as asparagine

and glutamine, which are capable of hydrogen bonding. The affinity of heparin-binding proteins for heparin/HS was also enhanced due to the presence of polar residues with smaller side chains like serine and glycine.

1.7 Proteins

1.7.1 VEGF (Vascular Endothelial Growth Factor)

VEGF is one of the most well studied growth factor involved in EC migration, mitogenesis, sprouting and tube formation. Upregulated VEGF and VEGF receptor mRNA has been detected in the tips of invasive angiogenic sprouts and antibody blockade of VEGF significantly decreases micro-vessel growth [78]. Its alternate splice variants and isoforms are known to bind to receptor tyrosine kinase (VEGFR-1 and VEGFR-2). These isoforms differ by their amino acid length and, most importantly, their ability to bind cellular heparan sulfates (HS). The latter feature is critical to VEGF biology. Loss of heparin binding results in a substantial loss of mitogenic activity [79]. VEGF121 is an acidic polypeptide that does not bind heparin; VEGF165 is secreted but a significant fraction remains bound to the cell surface and ECM. In contrast, VEGF189 and VEGF206 bind to heparin with greater affinity than VEGF165 and are almost completely sequestered in the extracellular matrix (ECM) [80].

Figure 1-2 : Rendering of heparin-binding domain of VEGF165 (Protein Data Base).

VEGFs may become available to endothelial cells by at least two different mechanisms: free proteins (VEGF 121 and VEGF 165) or following protease activation and cleavage of the longer isoforms. As a result, VEGF levels are tightly regulated and even minor changes can have profound physiological effects. Native VEGF is heparin binding, homodimeric glycoprotein of 45,000 daltons (45kDa). The properties of native VEGF (i.e. VEGF found *in vivo*) closely correspond to those of VEGF165 [79]. The VEGF165 variant binds to neuropilin, is involved in capillary morphogenesis, and is required for EC filopodial tip directionality during angiogenesis [78]. Precise dosing of VEGF is essential, as it is associated with side effects like gastrointestinal toxicity, hypothyroidism, proteinuria, coagulation disorders, neurotoxicity, impaired wound healing and excessive chaotic neovascularization [74].

Recombinant human vascular endothelial growth factor (rhVEGF) behaves similar to native VEGF in terms of its binding to heparin and its biological activity. RhVEGF is a homodimeric protein consisting of 165 amino acids per monomer with a molecular weight of 38.3 kDa and a pI of 8.5. The protein consists of 2 domains, a receptor-binding domain (residues 1-110) and a heparin-binding domain (residues 111-165) [81].

1.7.2 FgF-20 (Fibroblast Growth Factor 20)

Fibroblast growth factors (FgFs) play vital roles in angiogenesis, morphogenesis, tissue re modeling and carcinogenesis. The common forms are FGF-1 (acidic FGF) and FGF-2 (basic FGF) bind to the receptor tyrosine kinases i.e FGFR-1 and FGFR-2, respectively. FGF-2 has been shown to enhance VEGF production and VEGF is involved in the FGF-2 induced expression of placental growth factors, demonstrating the crosstalk between growth factors [82]. Also, FGF-2 has been shown to induce synthesis of collagen, fibronectin, and proteoglycans by EC's, demonstrating its crucial role in ECM remodeling [83]. FGFs mediate signals via four structurally related receptor tyrosine kinases on cell surfaces (FGFR-1, 2, 3 and 4) to induce numerous biological effects. One of the best-characterized functions of FGFs is the induction of new blood vessels. In brief, formation and sprouting of new capillaries involves endothelial cell proliferation and cell migration, as well as breakdown of surrounding ECM components. Together with the vascular endothelial growth factor (VEGF), FGFs are the most important regulators of these processes. bFGF may participate in angiogenesis in two primary ways: by modulating endothelial cell activity and by regulating VEGF expression.

FGF-20 is 211-amino-acid polypeptide with the FGF-core domain and known to be preferentially expressed in the substantia niagra of the brain [84]. A hydrophobic region was found in the FGF-core domain of FGF-20; however, no typical N-terminal signal sequence was found as in some other members of the FgF family. Its monomeric mass is 23 kD but it usually exists as a non-covalent dimer in solution. FgF-20 can be potentially used as a therapeutic to prevent oral mucositis, a common side effect of radio or chemo therapy. The therapeutic effect is due to FgF-20's ability to promote epithelial and mesenchymal cell proliferation. It is also reported to be involved in developing treatments for neurodegenerative pathologies like Parkinson's disease [85]. FgF-20 has been reported to be notoriously unstable and difficult to work with [86, 87].

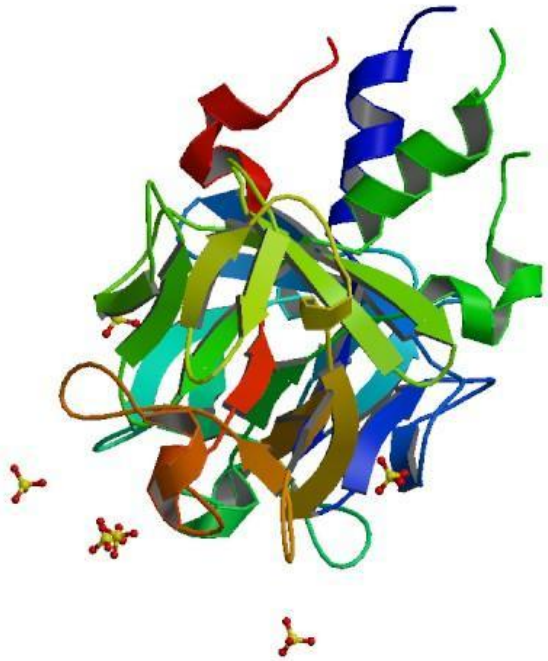

Figure 1-3 : Rendering of FgF-20 structure (RCSB Protein Data Base)

1.7.3 Lysozyme

Lysozyme (LYZ) is a very well studied and extensively characterized enzyme, which acts as a guardian by attacking cell walls of bacteria. It is found in numerous body secretions, and is often the first line of defense against infections. We propose to use LYZ as a model protein as, it is a basic highly soluble protein, and has heparin binding activity [88], similar to VEGF and FgF-20. LYZ and VEGF have reported pI values of 11.35 [89] and 8-8.5 [90] ; whereas FgF-20 has a theoretically calculated pI of 8.9 [91].

1.8 References

1. Dimitrov, D., *Therapeutic Proteins*, in *Therapeutic Proteins*, V. Voynov and J.A. Caravella, Editors. 2012, Humana Press. p. 1-26.
2. Rickwod, S., M. Kleinrock, and M. Nunez-Gaviria, *The Global Use of Medicines:Outlook through 2017*, 2013, IMS Institute for Healthcare Informatics.
3. Zhao, H. and E. Topp, *Recent U.S. patents on protein drug formulation: 2000-2007.* Recent Patents on Drug Delivery Formulation, 2008. **2**(3): p. 200-208.
4. Malik, D., et al., *Recent advances in protein and peptide drug delivery systems.* Current Drug Delivery, 2007. **4**(2): p. 141-151.
5. Brown, L.R., *Commercial challenges of protein drug delivery.* Expert Opinion on Drug Delivery, 2005. **2**(1): p. 29-42.
6. Nair, L.S. and C.T. Laurencin, *Biodegradable polymers as biomaterials.* Progress in Polymer Science, 2007. **32**(8–9): p. 762-798.
7. Grund, S., M. Bauer, and D. Fischer, *Polymers in Drug Delivery—State of the Art and Future Trends.* Advanced Engineering Materials, 2011. **13**(3): p. B61-B87.
8. Zhang, Y., H.F. Chan, and K.W. Leong, *Advanced materials and processing for drug delivery: The past and the future.* Advanced Drug Delivery Reviews, 2013. **65**(1): p. 104-120.
9. Karp, J.M. and R. Langer, *Development and therapeutic applications of advanced biomaterials.* Current Opinion in Biotechnology, 2007. **18**(5): p. 454-459.
10. Okada, H. and H. Toguchi, *Biodegradable microspheres in drug delivery.* Crit Rev Ther Drug Carrier Syst, 1995. **12**(1): p. 1-99.
11. *Controlled Drug Delivery: Designing Technologies for the Future*. ACS Symposium Series, ed. R.J.M. Kinam Park. Vol. 752. 2000: American Chemical Society. 478.
12. Jain, R., *The manufacturing techniques of various drug loaded biodegradable poly (lactide-co-glycolide)(PLGA) devices.* Biomaterials, 2000. **21**(23): p. 2475-90.
13. Schwendeman, S.P., *Recent advances in the stabilization of proteins encapsulated in injectable PLGA delivery systems.* Critical Reviews in Therapeutic Drug Carrier Systems, 2002. **19**(1): p. 73-98.
14. Wu, F. and T. Jin, *Polymer-based sustained-release dosage forms for protein drugs, challenges, and recent advances.* AAPS PharmSciTech, 2008. **9**(4): p. 1218-1229.
15. Reinhold, S.E., et al., *Self-Healing Microencapsulation of Biomacromolecules without Organic Solvents.* Angewandte Chemie International Edition, 2012. **51**(43): p. 10800-10803.
16. Reinhold, S.E. and S.P. Schwendeman, *Effect of polymer porosity on aqueous self-healing encapsulation of proteins in PLGA microspheres.* Macromolecular Bioscience, 2013. **13**(12): p. 1700-10.
17. Desai, K.G.H. *Active Self-microencapsulating PLGA Microspheres for Controlled Release of Vaccine Antigens: A New Paradigm for Low-cost, Safe, and Effective Antigen Delivery*. in *Controlled Release Society*. 2010.

18. Jiskoot, W., et al., *Protein instability and immunogenicity: Roadblocks to clinical application of injectable protein delivery systems for sustained release.* Journal of Pharmaceutical Sciences, 2012. **101**(3): p. 946-954.
19. Schwendeman, S.P., et al., *Injectable controlled release depots for large molecules.* Journal of Controlled Release, 2014. **190**(0): p. 240-253.
20. Rosenberg, A., *Effects of protein aggregates: An immunologic perspective.* AAPS J, 2006. **8**(3): p. E501-E507.
21. Wang, W., et al., *Immunogenicity of protein aggregates—Concerns and realities.* International Journal of Pharmaceutics, 2012. **431**(1–2): p. 1-11.
22. Hermeling, S., et al., *Structure-Immunogenicity Relationships of Therapeutic Proteins.* Pharmaceutical Research, 2004. **21**(6): p. 897-903.
23. Langer, R. and D.A. Tirrell, *Designing materials for biology and medicine.* Nature, 2004. **428**(6982): p. 487-492.
24. Pillai, O. and R. Panchagnula, *Polymers in drug delivery.* Current Opinion in Chemical Biology, 2001. **5**(4): p. 447-451.
25. Liechty, W.B., et al., *Polymers for Drug Delivery Systems.* Annual Review of Chemical and Biomolecular Engineering, Vol 1, 2010. **1**: p. 149-173.
26. Langer, R.S. and N.A. Peppas, *Present and future applications of biomaterials in controlled drug delivery systems.* Biomaterials, 1981. **2**(4): p. 201-14.
27. WA Long, D.T., K Tchernev, and others., *Controlled-release-interferon-alpha2b + ribavrin reduces flu-like symptoms >50% and provides equivalent efficacy in comparison to weekly pegylated-interferon-alpha2b + ribavirin in treatment-naive-genotype-1-chronic-hepatitis-C: results from EMPOWER, a randomized-open-label-12-week-comparison in 133 patients.* , in *45th Annual Meeting of the European Association for the Study of the Liver (EASL 2010).*2010: Vienna, Austria.
28. De Leede, L.G., et al., *Novel controlled-release Lemna-derived IFN-alpha2b (Locteron): pharmacokinetics, pharmacodynamics, and tolerability in a phase I clinical trial.* J Interferon Cytokine Res, 2008. **28**(2): p. 113-22.
29. Rio, C.L.d., et al., *VASOMERA™, A novel vpac2-selective vasoactive intestinal peptide agonist, enhances contractility and decreases myocardial demand in dogs with both normal hearts and with pacing-induced dilated cardiomyopathy.* Journal of the American College of Cardiology, 2013. **61**(10_S).
30. Woodruff, M.A. and D.W. Hutmacher, *The return of a forgotten polymer—Polycaprolactone in the 21st century.* Progress in Polymer Science, 2010. **35**(10): p. 1217-1256.
31. Liu, Y. and S.P. Schwendeman, *Mapping Microclimate pH Distribution inside Protein-Encapsulated PLGA Microspheres Using Confocal Laser Scanning Microscopy.* Molecular Pharmaceutics, 2012. **9**(5): p. 1342-1350.
32. Ghassemi, A.H., et al., *Controlled Release of Octreotide and Assessment of Peptide Acylation from Poly(D,L-lactide-co-hydroxymethyl glycolide) Compared to PLGA Microspheres.* Pharmaceutical Research, 2012. **29**(1): p. 110-120.
33. Kim, S., et al., *Polyoxalate Nanoparticles as a Biodegradable and Biocompatible Drug Delivery Vehicle.* Biomacromolecules, 2010. **11**(3): p. 555-560.

34. Yang, S.C., et al., *Polyketal copolymers: A new acid-sensitive delivery vehicle for treating acute inflammatory diseases.* Bioconjugate Chemistry, 2008. **19**(6): p. 1164-1169.
35. Butler, D., *Translational research: crossing the valley of death.* Nature, 2008. **453**(7197): p. 840-2.
36. Carmichael, M., *Why Don't More Medical Discoveries Become Cures?*, in *Newsweek*2010: USA.
37. Gopferich, A., M.J. Alonso, and R. Langer, *Development and Characterization of Microencapsulated Microspheres.* Pharmaceutical Research, 1994. **11**(11): p. 1568-1574.
38. van der Walle, C., G. Sharma, and M. Kumar, *Current approaches to stabilising and analysing proteins during microencapsulation in PLGA.* Expert Opinion on Drug Delivery, 2009. **6**(2): p. 177-186.
39. Reinhold, S., *Self-healing polymers microencapsulate biomacromolecules without organic solvents*, 2009, University of Michigan.
40. van de Weert, M., W.E. Hennink, and W. Jiskoot, *Protein Instability in Poly(Lactic-co-Glycolic Acid) Microparticles.* Pharmaceutical Research, 2000. **17**(10): p. 1159-1167.
41. Xu, F.-H. and Q. Zhang, *Recent advances in the preparation progress of protein/peptide drug loaded PLA/PLGA microspheres.* yao xue xue bao, 2007. **42**(1): p. 1.
42. Sah, H., *Protein behavior at the water/methylene chloride interface.* Journal of Pharmaceutical Sciences, 1999. **88**(12): p. 1320-1325.
43. Maa, Y.-F. and C.C. Hsu, *Protein denaturation by combined effect of shear and air-liquid interface.* Biotechnology and Bioengineering, 1997. **54**(6): p. 503-512.
44. Desai, U.R. and A.M. Klibanov, *Assessing the Structural Integrity of a Lyophilized Protein in Organic Solvents.* Journal of the American Chemical Society, 1995. **117**(14): p. 3940-3945.
45. Wang, J., K.M. Chua, and C.-H. Wang, *Stabilization and encapsulation of human immunoglobulin G into biodegradable microspheres.* Journal of Colloid and Interface Science, 2004. **271**(1): p. 92-101.
46. Carpenter, J.F., et al., *Rational Design of Stable Lyophilized Protein Formulations: Some Practical Advice.* Pharmaceutical Research, 1997. **14**(8): p. 969-975.
47. Putney, S.D. and P.A. Burke, *Improving protein therapeutics with sustained-release formulations.* Nature Biotechnology, 1998. **16**(2): p. 153-7.
48. Liu, W.R., R. Langer, and A.M. Klibanov, *Moisture-induced aggregation of lyophilized proteins in the solid state.* Biotechnology and Bioengineering, 1991. **37**(2): p. 177-184.
49. Cleland, J.L., et al., *Recombinant human growth hormone poly(lactic-co-glycolic acid) (PLGA) microspheres provide a long lasting effect.* Journal of Controlled Release, 1997. **49**(2-3): p. 193-205.
50. Shenderova, A., T.G. Burke, and S.P. Schwendeman, *The Acidic Microclimate in Poly(lactide-co-glycolide) Microspheres Stabilizes Camptothecins.* Pharmaceutical Research, 1999. **16**(2): p. 241-248.

51. Mäder, K., et al., *Non-invasive in vivo characterization of release processes in biodegradable polymers by low-frequency electron paramagnetic resonance spectroscopy.* Biomaterials, 1996. **17**(4): p. 457-461.
52. Mäder, K., et al., *Monitoring Microviscosity and Microacidity of the Albumin Microenvironment Inside Degrading Microparticles from Poly(lactide-co-glycolide) (PLG) or ABA-triblock Polymers Containing Hydrophobic Poly(lactide-co-glycolide) A Blocks and Hydrophilic Poly(ethyleneoxide) B Blocks.* Pharmaceutical Research, 1998. **15**(5): p. 787-793.
53. Schwendeman, S.P., Cardamone, M., Brandon, M. R., Klibanov, A. and Langer, R., *The stability of proteins and their delivery from biodegradable polymer microspheres,* in *Microparticulate Systems for the Delivery of Proteins and Vaccines,* S. Cohen, Bernstein, H., Editor. 1996, Marcel Dekker: New York. p. 1-49.
54. Zhu, G., S.R. Mallery, and S.P. Schwendeman, *Stabilization of proteins encapsulated in injectable poly (lactide- co-glycolide).* Nat Biotech, 2000. **18**(1): p. 52-57.
55. Crotts, G. and T.G. Park, *Preparation of porous and nonporous biodegradable polymeric hollow microspheres.* Journal of Controlled Release, 1995. **35**(2-3): p. 91-105.
56. Desai, K.-G., S. Kadous, and S. Schwendeman, *Gamma Irradiation of Active Self-Healing PLGA Microspheres for Efficient Aqueous Encapsulation of Vaccine Antigens.* Pharmaceutical Research, 2013. **30**(7): p. 1768-1778.
57. Wool, R.P., *Self-healing materials: a review.* Soft Matter, 2008. **4**(3): p. 400-418.
58. Gandhi, N.S. and R.L. Mancera, *The Structure of Glycosaminoglycans and their Interactions with Proteins.* Chemical Biology & Drug Design, 2008. **72**(6): p. 455-482.
59. Lai, P.-H., et al., *Acellular biological tissues containing inherent glycosaminoglycans for loading basic fibroblast growth factor promote angiogenesis and tissue regeneration.* Tissue Engineering, 2006. **12**(9): p. 2499-2508.
60. Raman, R., V. Sasisekharan, and R. Sasisekharan, *Structural Insights into Biological Roles of Protein-Glycosaminoglycan Interactions.* Chemistry & Biology, 2005. **12**(3): p. 267-277.
61. Pike, D.B., et al., *Heparin-regulated release of growth factors in vitro and angiogenic response in vivo to implanted hyaluronan hydrogels containing VEGF and bFGF.* Biomaterials, 2006. **27**(30): p. 5242-5251.
62. Riley, C.M., et al., *Stimulation of in vivo angiogenesis using dual growth factor-loaded crosslinked glycosaminoglycan hydrogels.* Biomaterials, 2006. **27**(35): p. 5935-5943.
63. Fromm, J.R., et al., *Pattern and Spacing of Basic Amino Acids in Heparin Binding Sites.* Archives of Biochemistry and Biophysics, 1997. **343**(1): p. 92-100.
64. Goerges, A.L. and M.A. Nugent, *pH Regulates Vascular Endothelial Growth Factor Binding to Fibronectin: A Mechnism for control of Extracellular Matrix Storage and Release.* Journal of Bioloical Chemistry, 2004. **279**(3): p. 2307-2315.

65. Goerges, A.L. and M.A. Nugent, *Regulation of Vascular Endothelial Growth Factor Binding and Activity by Extracellular pH.* Journal of Biological Chemistry, 2003. **278**(21): p. 19518-19525.
66. Jones, L.S., B. Yazzie, and C.R. Middaugh, *Polyanions and the Proteome.* Molecular & Cellular Proteomics, 2004. **3**(8): p. 746-769.
67. *Polysaccharides : Structural Diversity and Functional Versatility*, ed. S. Dumitriu. 2005, Hoboken: CRC Press.
68. Liao, Y.-H., et al., *Hyaluronan: pharmaceutical characterization and drug delivery.* Drug delivery, 2005. **12**(6): p. 327-342.
69. Pardue, E., S. Ibrahim, and A. Ramamurthi, *Role of hyaluronan in angiogenesis and its utility to angiogenic tissue engineering.* Organogenesis, 2008. **4**(4): p. 203-214.
70. Toole, B.P., *Hyaluronan: from extracellular glue to pericellular cue.* Nature Reviews. Cancer, 2004. **4**(7): p. 528-539.
71. Noble, P.W., *Hyaluronan and its catabolic products in tissue injury and repair.* Matrix Biology, 2002. **21**(1): p. 25-29.
72. West, D.C. and S. Kumar, *The effect of hyaluronate and its oligosaccharides on endothelial cell proliferation and monolayer integrity.* Experimental cell research, 1989. **183**(1): p. 179-196.
73. Distler, O., et al., *The molecular control of angiogenesis.* International Reviews of Immunology, 2002. **21**(1): p. 33-49.
74. Lazarous, D.F., et al., *Comparative effects of basic fibroblast growth factor and vascular endothelial growth factor on coronary collateral development and the arterial response to injury.* Circulation, 1996. **94**(5): p. 1074-1082.
75. Rusnati, M. and M. Presta, *Extracellular angiogenic growth factor interactions: an angiogenesis interactome survey.* Endothelium, 2006. **13**(2): p. 93-111.
76. Sinha, V., *Chitosan microspheres as a potential carrier for drugs* International journal of pharmaceutics, 2004. **274**(1-2): p. 1.
77. Robinson, C.J., et al., *VEGF165-binding Sites within Heparan Sulfate Encompass Two Highly Sulfated Domains and Can Be Liberated by K5 Lyase.* Journal of Biological Chemistry, 2006. **281**(3): p. 1731-1740.
78. Neufeld, G., et al., *Vascular endothelial growth factor (VEGF) and its receptors.* FASEB J., 1999. **13**(1): p. 9-22.
79. Houck, K.A., et al., *Dual regulation of vascular endothelial growth factor bioavailability by genetic and proteolytic mechanisms.* Journal of Biological Chemistry, 1992. **267**(36): p. 26031-26037.
80. Yoon, Y.-s., et al., *Therapeutic myocardial angiogenesis with vascular endothelial growth factors.* Molecular and Cellular Biochemistry, 2005. **264**(1): p. 63-74.
81. Zhang, L., *Controlled Release of Angiogenic Growth Factors from Poly(Lactic-Co-Glycolic Acid) Implants for Therapeutic Angiogenesis*. 2009.
82. Vernon, R.B. and E.H. Sage, *A Novel, Quantitative Model for Study of Endothelial Cell Migration and Sprout Formation within Three-Dimensional Collagen Matrices.* Microvascular Research, 1999. **57**(2): p. 118-133.

83. Taipale, J. and J. Keski-Oja, *Growth factors in the extracellular matrix.* The FASEB journal, 1997. **11**(1): p. 51-59.
84. Kirikoshi, H., et al., *Molecular Cloning and Characterization of Human FGF-20 on Chromosome 8p21.3-p22.* Biochemical and Biophysical Research Communications, 2000. **274**(2): p. 337-343.
85. Itoh, N. and H. Ohta, *Roles of FGF20 in dopaminergic neurons and Parkinson's disease.* Front Mol Neurosci, 2013. **6**(15).
86. Maity, H., C. Karkaria, and J. Davagnino, *Effects of pH and arginine on the solubility and stability of a therapeutic protein (Fibroblast Growth Factor 20): relationship between solubility and stability.* Curr Pharm Biotechnol, 2009. **10**(6): p. 609-25.
87. Fan, H., et al., *Effects of pH and polyanions on the thermal stability of fibroblast growth factor 20.* Mol Pharm, 2007. **4**(2): p. 232-40.
88. Smith, S.A., et al., *Conserved Surface-Exposed K/R-X-K/R Motifs and Net Positive Charge on Poxvirus Complement Control Proteins Serve as Putative Heparin Binding Sites and Contribute to Inhibition of Molecular Interactions with Human Endothelial Cells: a Novel Mechanism for Evasion of Host Defense.* Journal of Virology, 2000. **74**(12): p. 5659-5666.
89. Wetter, L. and H. Deutsch, *Immunological Studies On Egg White proteins: IV. Immunichemical and Physical studies of Lysozyme.* Journal of Biological Chemistry, 1951(192): p. 231-236.
90. Ferrara, N., et al., *Purification and cloning of vascular endothelial growth factor secreted by pituitary folliculostellate cells*, in *Methods in Enzymology*, J.P.M. David Barnes, Gordon H. Sato, Editor. 1991, Academic Press. p. 391-405.
91. Kozlowski, L.P. *Isoelectric Point Calculator*. 2007-2013 8/03/2014]; Available from: http://isoelectric.ovh.org

CHAPTER 2 Evaluating Biopolymers as Trapping Agents for Proteins

2.1 Abstract

The purpose of this study was to screen glycosaminoglycan-like biopolymers (BP) for use in long-term controlled release formulations that deliver therapeutic growth factors. Aqueous solutions of BP sodium salts [high molecular weight dextran sulfate (HDS), low molecular weight dextran sulfate (LDS), chondroitin sulfate (CS), heparin (HP)] and model protein lysozyme (LYZ) were combined in different molar and mass ratios. In most cases, insoluble complexes were obtained instantly upon mixing aqueous solutions of BP and LYZ. HP and LDS exhibited a very high efficiency in LYZ binding as the BP: LYZ mass ratio was raised > 1. In the case of HDS and CS, LYZ binding efficiency reached a local maximum and fell as the BP : LYZ was increased. BP-LYZ complexes formed at higher BP : LYZ ratios tended to release LYZ at a faster rate over 100 h compared to those at lower ratios. LYZ release also varied with ionic strength, the rate and extent of release increased steadily with increasing ionic strength (e.g., 0 – 0.9 M NaCl). Comparing differences between LDS and HDS, the rate and extent of release of LYZ was higher for HDS across all BP : LYZ ratios and ionic strength tested. LDS-LYZ and HP-LYZ complexes released highly active LYZ over 100 h. Hence, we identified suitable BPs for developing BP-PLGA microspheres for controlled release.

2.2 Introduction

Angiogenic growth factors are found in body fluids as circulating complexes or immobilized in the extra cellular matrix [1, 2]. Complex polysaccharides, like glycosaminoglycans (GAGs) are known to bind and regulate growth factors. GAGs are linear, generally sulphated, negatively charged polysaccharides with molecular weights in 10-100 kDa range [3]. Non-sulfated GAGs include hyaluronic acid (HA), whereas the sulfated include chondriton sulfate (CS), dermatan sulfate (DS), ketran sulfate (KS), heparin (HP) and heparin sulfate.

The proposed biomimetic approach involves incorporating the GAG like biopolymers (BPs) in PLGA microspheres, which are known to actively bind, sequester, and stabilize growth factors (GFs*) in-vivo* [2-11]. BPs can also potentially enhance the biological effect of the protein by acting as co-factors [2, 4, 6]. Incorporation of BPs into the pores of the self-healing PLGA microspheres would presumably enhance the protein loading efficiency as well as its stability during the encapsulation and subsequent release, by protein immobilization. Note that the biomimetic complexation of human growth hormone with Zn^{2+} in the Nutropin Depot formulation, as occurs naturally in the pituitary, has been used successfully to achieve excellent stability of the encapsulated protein during spray-congealing encapsulation and long-term release [12, 13]. Several BPs were selected in this work as trapping agents for biomimetic ASE, namely, hyaluronic acid, chondritin sulfate, heparin, chitosan and dextran sulfate.

Here, we screened GAG and GAG like BP's to develop biomimetic approach for delivery of growth factors (GF). To develop the biomimetic self-healing strategy, we studied the binding of BPs (total of 6) to a model basic enzyme with positive net charge at neutral pH, lysozyme (LYZ). The BPs used in this study are members of the glycosaminoglycan (GAG) family or have similar structural moieties (e.g., dextran sulfate and chitosan).

HA is a poly-anionic polysaccharide consisting of N-acetyl-D-glucosamine and β-glucoronic acid. It is found in synovial fluid, vitreous humor, cartilage, blood vessels, skin, and the umbilical cord [14]. Acting as a kind of extracellular glue, it is believed to play a vital role in the homeostasis, tissue development, cell signaling, regeneration, wound healing and tumor invasion [15, 16]. Its unique viscoelastic nature along with its biocompatibility and non-immunogenicity has led to its use in a number of cosmetic, medical, and pharmaceutical applications. Among the sulfated BPs, heparin [(1→4) pyranosyluronic acid 2-amino-2-deoxyglucopyranose] has been widely studied due to its well understood role in anti-coagulation pathway [5]. Chondroitin sulfate, polysaccharide chain of alternating units of N-acetylgalactosamine and glucuronic acid [β-glucuronic acid-(1→ 3)N-acetyl-β-galactosamine] is the most abundant GAG in the body. Found in the cartilage, tendon, ligament, and aorta it binds to proteins and forms proteoglycan aggregates [3, 11]. A number of growth factors bind to the ECM of target tissues by forming tight complexes with sulfated-glycosaminoglycans [17]. Chitin, poly[h(1α4)-2-acetoamido-2-deoxy-D-glucopyranose], is one of the most abundant natural polysaccharides and is present in crustaceans, insects, fungi, and yeasts. Deacetylation of chitin by alkali produces Chitosan (CH). The molecular structure of CH is believed to be

a copolymer of N-acetyl-glucosamine and glucosamine; usually the glucosamine content is more than 90% [11]. Dextran sulfates are derived from dextran (linear backbone of α-linked d-glucopyranosyl repeating units) via sulfation. The long history of the safety of dextrans has allowed them to be used as additives to food and chemicals, and in pharmaceutical and cosmetics manufacturing [18].

Ionic interactions are known to govern the specificity of GAG-protein interactions [2]. The carboxylate and sulfate groups of GAG's interact with the basic amino acid residues on the protein to create optimal structural fits of biding sites. Thus, the distribution and topology of the basic resides dictates the specificity of interactions and location of binding sites on the protein [5, 8]. For strong binding affinity, oligosaccharide sequences on the GAG have to provide optimal charge (orientation of sulfate groups) and surface (van der Waals contact) [3, 5]. Typically, GAGs interact with amino acid residues that are prominently exposed on the surface of proteins, with the three-dimensional structure and conformation of GAGs playing a crucial role. Arginine, lysine and, to a lesser extent, histidine are involved in the ionic interactions with highly acidic sulfate groups present on the GAG chains [8].

2.3 Materials and Methods

2.3.1 Materials

High molecular weight (~ 500 kDa) dextran sulfate (HDS), low molecular weight (~15.5 kDa) dextran sulfate (LDS), chondroitin sulfate (~ 63 kDa, shark cartilage) (CS), porcine heparin (~18 kDa) (HP) sodium salts were purchased from Sigma-Aldrich. Chitosan (~ 61 kDa) was also from Sigma-Aldrich. Lysozyme (chicken egg white) and magnesium carbonate were also purchased from Sigma-Aldrich. Sodium hyaluronate (HA) powders were obtained as a gift from Lifecore Biomedical (MN, USA). All other reagents, common solvents, and supplies were obtained from Sigma-Aldrich, unless otherwise specified.

2.3.2 Preparation of BP-LYZ Complexes

Aqueous solutions of BPs (HDS, LDS, CS, HP, HA of ~66 kDa, and CH) and LYZ, were combined at a total BP + LYZ concentration of 1 mg/ml in different mass ratios (0.09, 0.11, 0.14, 0.20, 0.33, 1, 2, 3, 5 w/w), at pH 7 and 24 °C. After 3 h of incubation, the free LYZ was quantified by UV spectroscopy at 282 nm and size exclusion chromatography (SE-HPLC), as described below.

2.3.3 Quantification of LYZ

2.3.3.1 Size Exclusion (SE) Chromatography

SE chromatography was performed using high performance liquid chromatography (HPLC). The mobile phase consisted of 0.1 M sodium phosphate with 0.3 M sodium sulfate at pH 6.7 at the rate of 0.8 ml/min and 0.4 ml/min for SE-HPLC. Samples and standards were injected onto TSKgel G2000SWxl (Tosoh Bioscience, USA) on HPLC system. Protein detection by UV was done at 214 and 282 nm. Retention times of roughly 11 min were observed for LYZ during SE-HPLC.

2.3.3.2 UV Spectroscopy

Quantification of protein was carried out with Synergy 2 microplate reader (Biotek, USA) at 214 and 282 nm with appropriate standards and controls, using 96 well plates (Corning, USA).

2.3.4 Release Kinetics of BP-LYZ Complexes

LYZ and BP solutions were combined to form BP-LYZ complexes with initial w/w BP:LYZ ratios (0.33, 0.14, 0.11 and 0.7). The amount of bound LYZ was evaluated by SE-HPLC. Release kinetics of complexes in the absence of PLGA was determined in 1 ml PBS at pH 7.4 with complete replacement of release media at 37 °C, and LYZ quantification via SE-HPLC. Similarly, release kinetics and complex stability in special

cases were analyzed in PBS + 0.3M NaCl, PBS + 0.6 M NaCl and PBS + 0.9 M NaCl at pH 7.4.

2.3.5 LYZ Activity Assay

The activity of LYZ in solution was determined by Enzchek® lysozyme assay (Life Technologies, USA) as per the protocol provided. As CS was found to interfere with the assay, activity data for CS containing formulations are not reported.

2.4 Results and Discussion

Biopolymers were screened for their ability to act as protein trapping agents in order to enhance efficiency of ASE in PLGA via the biomimetic approach. Ideal characteristics for such BPs include the ability to a) absorb protein from aqueous solution and ideally provide a synergistic effect along with the protein, b) stabilize the bound protein and release the bound protein when PLGA pores open, and c) not alter self-healing characteristics when formulated with PLGA.

2.4.1 BP-LYZ Binding

BPs were analyzed for their ability to bind to LYZ (Figure 2-1). HDS and CS binding to LYZ was quantified in the 0-5 (w/w BP:LYZ) range. The binding data has an optimum LYZ binding (~ 100 %) at HDS:LYZ of ~ 0.1 (w/w), with sharp reductions on the LYZ

binding on both sides of the optimum ratio. Similarly, optimum CS to LYZ (~ 100 %) binding was also seen at ~ 0.1 CS:LYZ ratio, with sharp declines on both sides of the optimum value. These sharp declines could possibly be attributed to the cross-linking behavior between BP and LYZ, at optimum binding ratios, which are governed by the charges on the interacting species, polymer size, shape, and pH of the solution, for example [19, 20].

When HP and LDS binding to LYZ (0-5 w/w, BP:LYZ) was investigated, > 95% of the LYZ was bound above ~ 0.1 BP:LYZ across the range of ratios investigated. This is in contrast to HDS and CS, which displayed an optimum LYZ binding efficiency at a BP:LYZ ratio of ~ 0.1. The highest binding efficiency was observed at low ratios BP:LYZ, and decreased as the ratio increased. It is important to note that as compared to M_w of HDS and CS, LYZ has similar M_w to HP and LDS. This could potentially provide some hints to the difference in the binding behavior observed.

HA binding to LYZ was studied over 0-50 (HA:LYZ, w/w). The binding efficiency was found to be the highest at the lowest mass ratios of HA:LYZ, and decreased as the ratio was increased to 10. The efficiency increased to ≈ 18% at around a HA:LYZ mass ratio of 49. A similar trend was seen in the case of CH as the binding efficiency decreased from 68% to 28% at around a CS:LYZ mass ratio of 1 and then increased to ≈ 100% as the ratio increased to 25. The increase in LYZ binding in case of CH around the minimum value of LYZ binding is much sharper when compared to the change in binding in case of HA.

Molar ratios were similar to mass ratios in the cases of LDS, HP, and HA binding to LYZ. HDS with average M_w of 500 kDa has a very narrow HDS:LYZ molar ratio (≈ 0.001) for achieving ~ 100% LYZ binding. Similarly, for CS:LYZ a narrow molar ratios (~ 0.03) were observed for optimum LYZ binding.

It is noted that HA formed gels, when combined with LYZ solutions, whereas the sulfated BPs formed visible precipitates. CH had very poor solubility (< 3 mg/ml) in 10 mM phosphate buffer solution at pH 7. Thus, because of its poor solubility CH was not a suitable candidate for developing BP-PLGA formulations with high w/w CH content.

Thus, based on the binding data, BP-PLGA microspheres were expected to sequester proteins into the microspheres from the aqueous protein solution during microencapsulation. Based upon the binding efficiencies, LDS and HP were expected to perform well in BP-PLGA microspheres as they have excellent binding at BP:LYZ mass ratios of > 0.13, whereas HDS and CS formulations would have to be optimized to bring about high loading and encapsulation efficiency of protein uptake from aqueous solution during ASE.

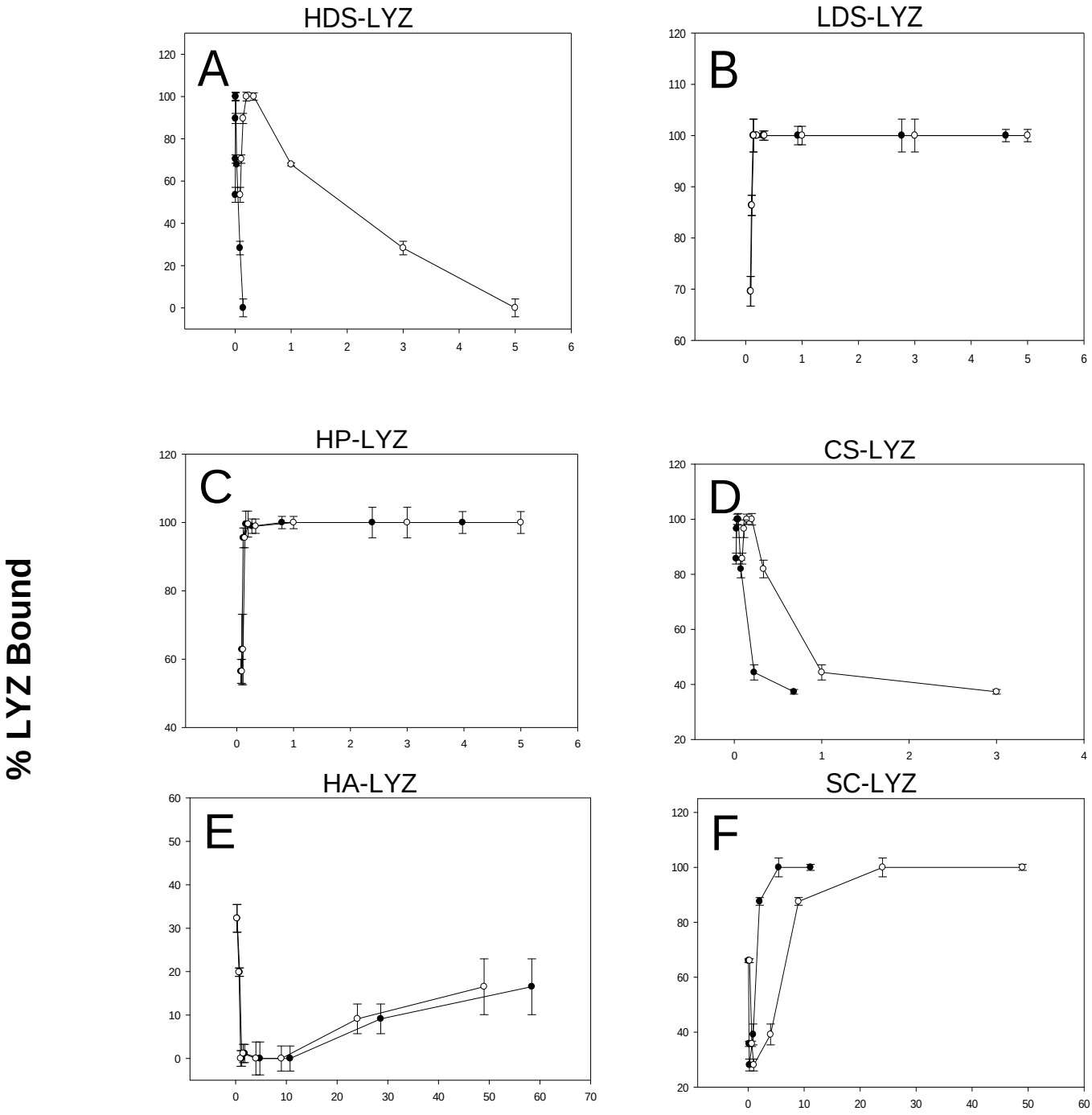

Figure 2-1: BP-LYZ binding profiles after 3hrs at 24°C. LYZ profiles quantified by UV at 280nm (A-C, E-F) and SEC-HPLC (D). The values are expressed as mean ± SD, n=3. Mass (—○—) and Molar Ratios (—●—) of BP:LYZ

2.4.2 BP-LYZ Complexes

After screening for the ability to bind LYZ, the next step was to check the stability of sulfated BP-LYZ complexes and evaluate the release kinetics of the bound LYZ. Ideally, BP-LYZ complexes would be able to release all of the bound protein in an active form and with suitable release kinetics.

2.4.2.1 Release Kinetics of BP-LYZ Complexes

BP:LYZ complexes were formed by combining BP and LYZ solutions at different mass ratios. The complexes were incubated in PBS, at pH 7.4 and 37 °C. Release kinetics was evaluated with complete release media replacement and quantified by SE-HPLC (Figure 2-2).

This was done to determine if the initial ratio of BP:LYZ could govern the stability and release kinetics of LYZ. It was important to study this ratio as it could provide some insight into the possible behavior to be expected when biomimetic self-encapsulation of BP-PLGA microspheres with a range of % BP (w/w), would be brought about at different protein concentrations.

2.4.2.2 Effect of Initial BP:LYZ on Release Kinetics

The extent of LYZ released across complexes of a given BP formed at different BP:LYZ, were found to be similar after 100 h in 1ml of PBS (pH 7.4), at 37 °C (Figure 2-2). HDS-LYZ complexes were seen to release ~ 20-40 % over 40 h and the difference in extent of release disappeard at 100 h, as all complexes were seen to release ~ 60 % of the bound LYZ. Similar differences were seen also across LDS-LYZ complexes over the first 40 h, when ~ 25-60 % of the bound LYZ. Over 100 h, LDS complexes released ~ 75-80 % of the bound LYZ. The difference in LYZ release extent was more pronounced in LDS-LYZ complexes formed at different initial mass ratios, when compared to HDS-LYZ complexes. HDS-LYZ complexes were also seen to have a smaller burst release when compared to LDS-LYZ. LDS-LYZ and HDS-LYZ complexes formed at a BP:LYZ ratio of 0.07 had significantly faster rate and extent of release compared to complexes formed at higher ratios. Generally, LDS-LYZ complexes were seen to release LYZ at a faster rate, when compared to HDS-LYZ complexes, over 100 h.

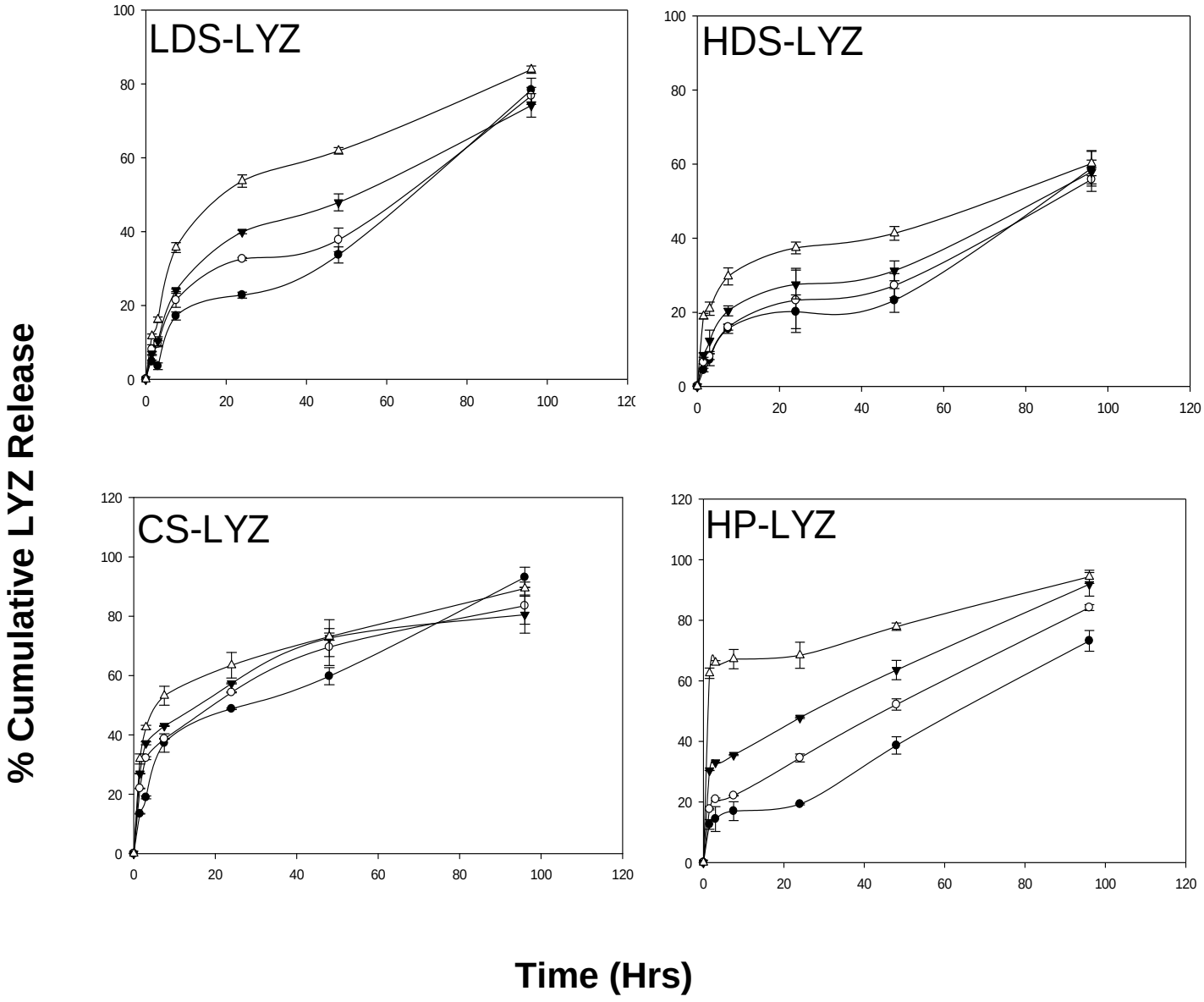

Figure 2-2: : LYZ release profiles in 1ml PBS (pH 7.4) at 37 °C from BP-LYZ complexes formed at BP:LYZ of 0.33 (-●-), 0.14 (-○-), 0.11 (-▼-) and 0.07 (-Δ-) quantified by SE-HPLC at 282 nm. The values are expressed as mean ± SE; n=3.

CS-LYZ complexes were found to have comparatively similar LYZ release kinetics over 100 h. Complexes were seen to release ~ 50-60 % over 40 h, which increased to ~ 78-90 % LYZ released over 100 h. HP-LYZ complexes released ~ 30-65 % over 40 h and ultimately ~ 60-83 % of the bound LYZ over 100h. HP-LYZ complexes formed at lower

HP:LYZ ratios had faster LYZ release over 100 h when compared to the complexes formed at higher HP:LYZ. In addition, HP-LYZ complexes were noted to have some of the highest burst release across all BP-LYZ complexes. HP-LYZ complex formed at 0.07 (HP:LYZ) released ~ 60 % of the bound LYZ within the first few hour of the release study.

Across all BPs, complexes formed at lower BP:LYZ ratios had the highest burst release. Overall, HDS-LYZ complexes had the lowest rate and extent of release at ~ 55-60% over 100 h, making them an excellent candidate for developing long-acting release formulations. Based on the data, it is possible that LYZ loaded HP-PLGA microspheres would have a higher burst release, when compared to other BPs.

2.4.2.3 Effect of Ionic Strength on Release Kinetics

To evaluate the stability of BP-LYZ complexes and study the role of electrostatic interactions on complex stability and release kinetics, the ionic strength of the release media was varied. *In-vitro* release of LYZ loaded BP-PLGA complexes was quantified in 1ml of PBS+0.3 M NaCl, PBS+0.6 M NaCl and PBS+0.9M NaCl. Due to the electrostatic component of the BP-LYZ interaction, the rate and extent of LYZ released was expected to increase with ionic strength of the release media. This was verified, as the rate and extent of LYZ release was found to increase across almost all the complexes,

with increasing ionic strength. Complexes formed with lower BP:LYZ, were generally found to have the fastest release kinetics with the largest burst release.

After 25 h, ~ 30-55 % of the bound LYZ was released from HDS-LYZ complexes in PBS+0.3M NaCl (Figure 2-3). In PBS+0.6M NaCl, ~ 35-60 % LYZ was released, whereas ~ 60-78 % of bound LYZ was released. Similarly, LDS-LYZ complexes were found to release ~ 20-50 % in PBS+0.3M NaCl, ~ 30-50 % in PBS+0.6M NaCl and ~ 50 70 % of the bound LYZ was released in PBS+0.9M NaCl (Figure 2-4). HP-LYZ complexes had some of the highest burst release across all the complexes studied. Clear differences in extent and release kinetics of LYZ were seen for complex formed at HP:LYZ (w/w). Also, in case of HP-LYZ complex formed at 0.11 (w/w), faster LYZ release kinetics was observed in PBS+0.6M NaCl, compared to that in PBS+0.9M NaCl (Figure 2-5). In addition, release kinetics of complexes formed at 0.14, 0.11, and 0.7 (w/w) were similar in PBS+0.9M NaCl.

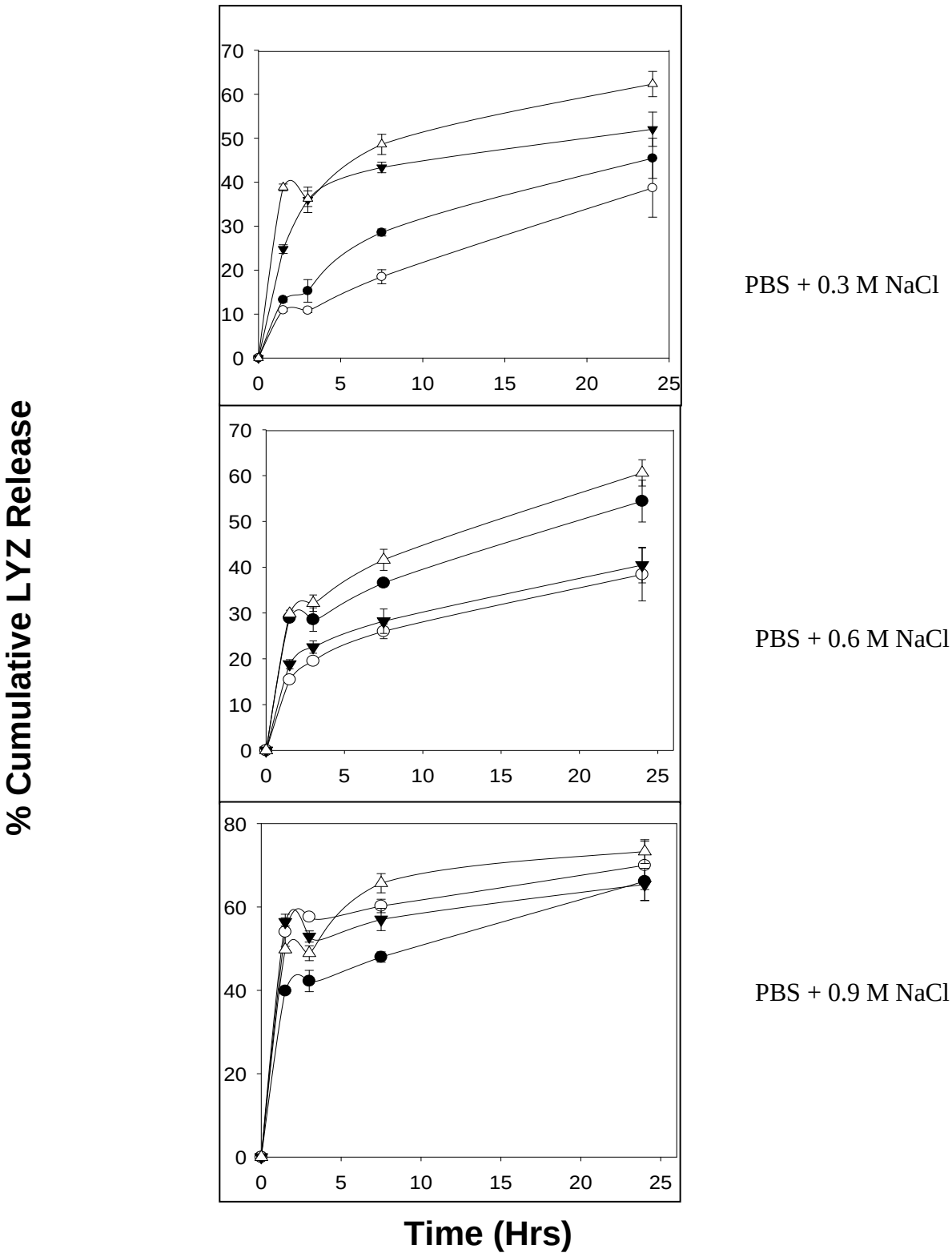

Figure 2-3: LYZ release profiles in 1ml of release media (pH 7.4) at 37 °C from HDS-LYZ complexes formed at BP:LYZ of 0.33 (-●-), 0.14 (-○-), 0.11 (-▼-) and 0.07 (-Δ-) quantified by UV at 282 nm. The values are expressed as mean ± SE; n=3.

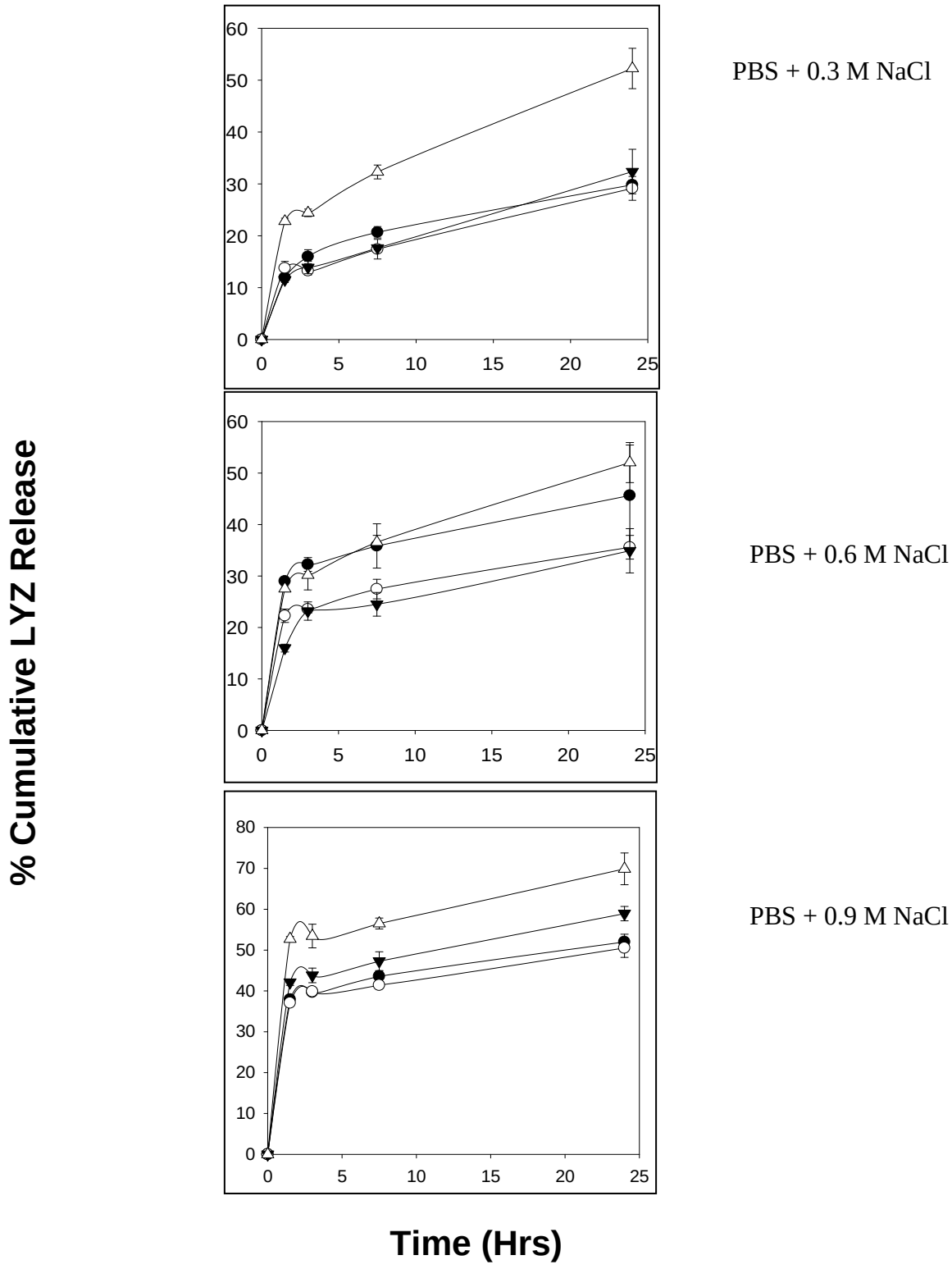

Figure 2-4: LYZ release profiles in 1ml of release media (pH 7.4) at 37 °C from LDS-LYZ complexes formed at BP:LYZ of 0.33 (-●-), 0.14 (-○-), 0.11 (-▼-) and 0.07 (-Δ-) quantified by UV at 282 nm. The values are expressed as mean ± SE; n=3.

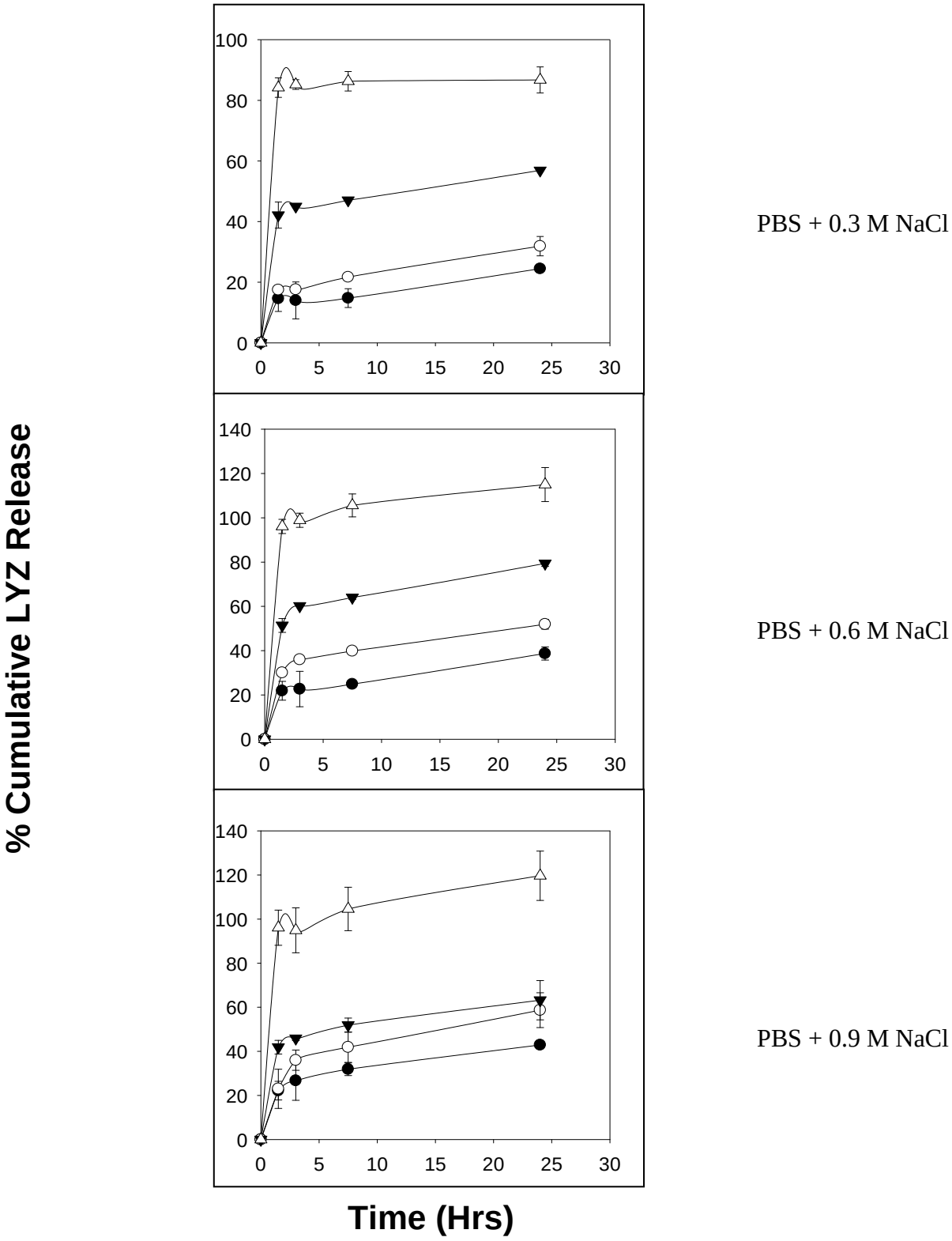

Figure 2-5: LYZ release profiles in 1ml of release media (pH 7.4) at 37 °C from HP-LYZ complexes formed at BP:LYZ of 0.33 (-●-), 0.14 (-○-), 0.11 (-▼-) and 0.07 (-Δ-) quantified by UV at 282 nm. The values are expressed as mean ± SE; n=3.

Overall, the difference in release kinetics of complexes formed at different mass ratios (BP:LYZ) was observed to decrease as the ionic strength of the release media increased, suggesting that ionic strength is playing a vital role in unraveling the complex and releasing the LYZ. Also, ionic strength greatly reduces the effect to of initial BP:LYZ (w/w) ratio in determining release kinetics of LYZ. Blanch *et al* have shown that LYZ solubility at constant ionic strength and pH is constant, and its solubility is approximately proportional to the initial LYZ concentration [21].

2.4.2.4 Activity of Released LYZ

To investigate the suitability of using BPs to sequester and bind LYZ in PLGA matrix, it was essential to ensure that the bound LYZ is active upon being released form LYZ. The activity of LYZ released form BP-LYZ complexes (Figure 2-6) formed at BP:LYZ of 0.3 and 0.1 was investigated (Figure 2-7).

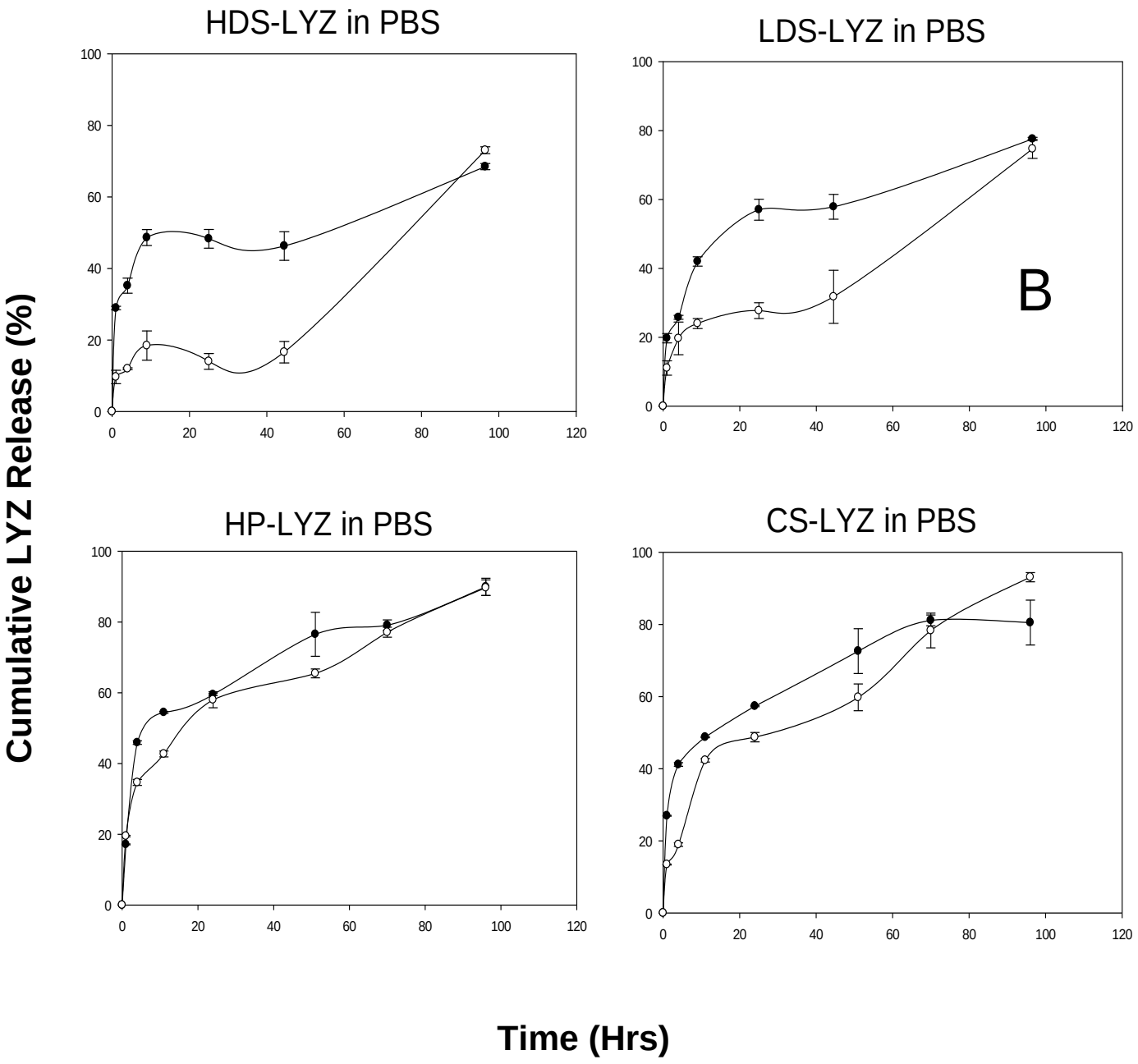

Figure 2-6 : LYZ release profiles in 1ml PBS (pH 7.4) at 37 °C quantified by UV at 280 nm (A-D). The values are expressed as mean ± SD, n=3. 0.14 BP:LYZ (─○─) and 0.3 and BP:LYZ(─●─) 0.1.

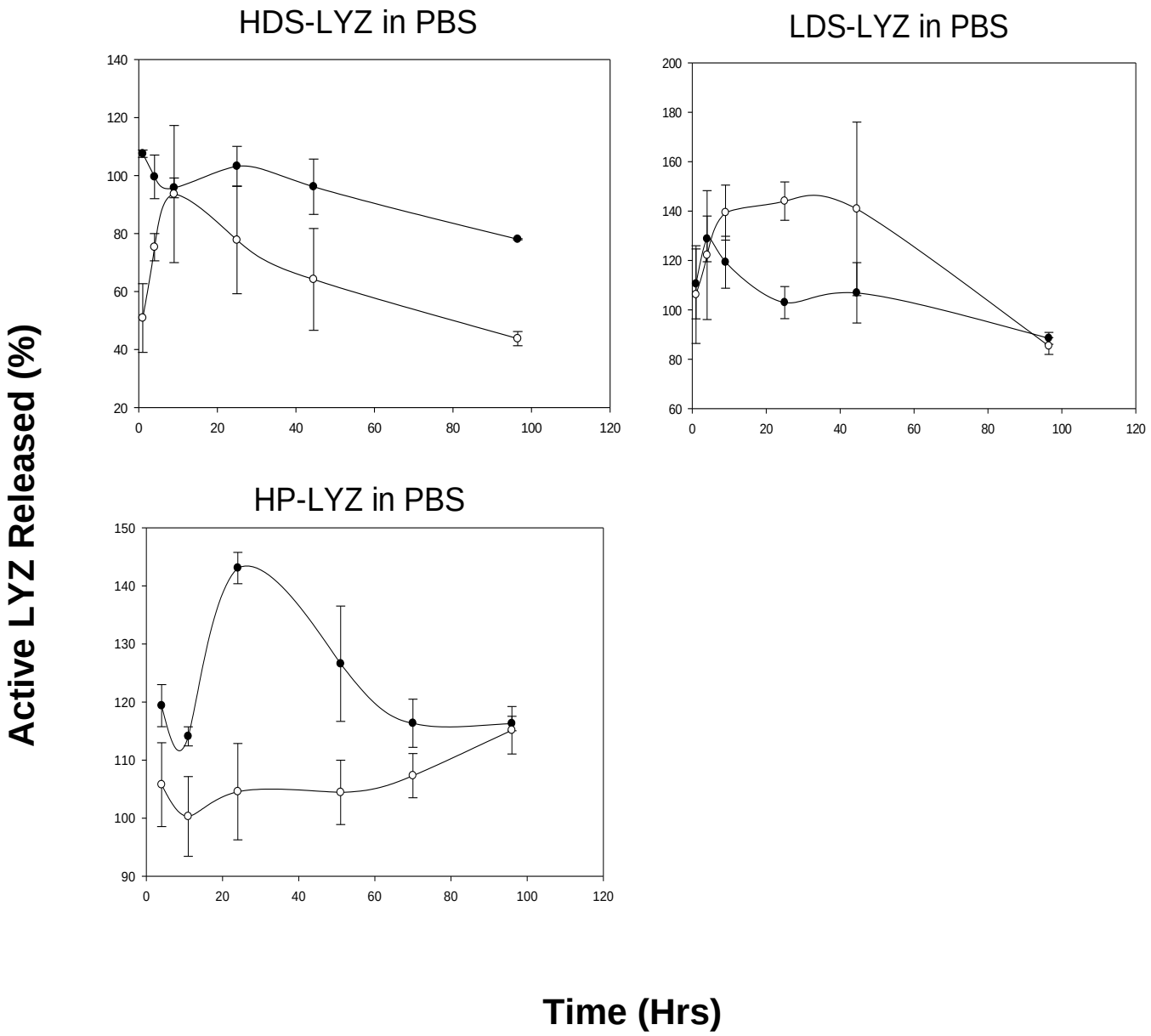

Figure 2-7 : LYZ activity quantified by Enzchek® lysozyme assay. The values are expressed as mean ± SD, n=3. 0.14 BP:LYZ (─○─) and 0.3 and BP:LYZ(─●─) 0.1.

Release kinetics of LYZ from the complex was similar to as reported in the above section (Figure 2-2). Complexes formed at a BP:LYZ ratio (w/w) of 0.3 were found to release LYZ faster than complexes formed at a ratio of 0.1, in case of HDS and LDS (Figure

2-5). In contrast, the CS and HP complexes formed at different mass ratios had similar LYZ release kinetics over 100 h. Activity data for CS-LYZ are not reported as the CS in release media was found to interfere with the LYZ activity used.

HDS-LYZ complexes were seen to release ~ 65 % of the bound LYZ. The activity of the released LYZ was quantified. The LYZ released from the HDS:LYZ complex formed at 0.3 mass ratio, was found to have lower activity when compared to complex formed at 0.1, over 100 hrs. A large amount of LYZ released from HDS-LYZ complexes formed at 0.3 mass ratios, was noted to have poor activity during the initial release period and after 40-100 h. In contrast, LDS complexes formed at mass ratio of 0.3 were found to have higher activity than the complex formed at the mass ratio of 0.1. In addition, LYZ released from LDS complexes were seen to have higher activity than from HDS complexes. It is not feasible to make further comparisons due to the errors associated with LYZ quantification and activity assessment.

HP-LYZ complexes were observed to release LYZ with excellent activity over 100 h. The overall activity of the LYZ released was much higher than that form HDS-LYZ complexes over 100 hrs. HP:LYZ complexes formed at 0.1 mass ratio were found to release highly active LYZ (> 100 %). This could be due to poor sensitivity of the quantification of LYZ via UV or due to HP interference during the LYZ activity assay. Overall, the data suggests that LDS and HP would be good candidates for incorporating in PLGA matrix, as the LYZ bound to these BP's would be highly active upon subsequent release.

2.5 Conclusions

The BP binding data suggests that LYZ can be very efficiently (> 90 %) bound to HDS, LDS and HP at suitable w/w ratios. BP-LYZ complexes prepared at different BP:LYZ (w/w) were evaluated to check for suitability of the release kinetics of the released LYZ. Role of electrostatic interactions in complex formation was ascertained by the effect of ionic strength on release kinetics of bound LYZ. HP-LYZ complexes were identified to have high burst release. LDS-LYZ and HP-LYZ complexes were found to release highly active LYZ (> 90 %) over 100 h.

These data suggest that suitably selected BPs could potentially be incorporated in PLGA matrix to bind and sequester LYZ via the biomimetic approach. The feasibility of this approach is investigated in the following chapters.

2.6 References

1. Taipale, J. and J. Keski-Oja, *Growth factors in the extracellular matrix.* The FASEB journal, 1997. **11**(1): p. 51-59.
2. Jones, L.S., B. Yazzie, and C.R. Middaugh, *Polyanions and the Proteome.* Molecular & Cellular Proteomics, 2004. **3**(8): p. 746-769.
3. Gandhi, N.S. and R.L. Mancera, *The Structure of Glycosaminoglycans and their Interactions with Proteins.* Chemical Biology & Drug Design, 2008. **72**(6): p. 455-482.
4. Lai, P.-H., et al., *Acellular biological tissues containing inherent glycosaminoglycans for loading basic fibroblast growth factor promote angiogenesis and tissue regeneration.* Tissue Engineering, 2006. **12**(9): p. 2499-2508.
5. Raman, R., V. Sasisekharan, and R. Sasisekharan, *Structural Insights into Biological Roles of Protein-Glycosaminoglycan Interactions.* Chemistry & Biology, 2005. **12**(3): p. 267-277.
6. Pike, D.B., et al., *Heparin-regulated release of growth factors in vitro and angiogenic response in vivo to implanted hyaluronan hydrogels containing VEGF and bFGF.* Biomaterials, 2006. **27**(30): p. 5242-5251.
7. Riley, C.M., et al., *Stimulation of in vivo angiogenesis using dual growth factor-loaded crosslinked glycosaminoglycan hydrogels.* Biomaterials, 2006. **27**(35): p. 5935-5943.
8. Fromm, J.R., et al., *Pattern and Spacing of Basic Amino Acids in Heparin Binding Sites.* Archives of Biochemistry and Biophysics, 1997. **343**(1): p. 92-100.
9. Goerges, A.L. and M.A. Nugent, *pH Regulates Vascular Endothelial Growth Factor Binding to Fibronectin: A Mechnism for control of Extracellular Matrix Storage and Release.* Journal of Bioloical Chemistry, 2004. **279**(3): p. 2307-2315.
10. Goerges, A.L. and M.A. Nugent, *Regulation of Vascular Endothelial Growth Factor Binding and Activity by Extracellular pH.* Journal of Biological Chemistry, 2003. **278**(21): p. 19518-19525.
11. *Polysaccharides : Structural Diversity and Functional Versatility*, ed. S. Dumitriu. 2005, Hoboken: CRC Press.
12. Johnson, O.L., et al., *A month-long effect from a single injection of microencapsulated human growth hormone.* Nature Medicine, 1996. **2**(7): p. 795-9.
13. Lee, H.J., et al., *In vivo characterization of sustained-release formulations of human growth hormone.* The Journal of Pharmacology and Experimental Therapeutics, 1997. **281**(3): p. 1431-9.
14. Lee, J.Y. and A.P. Spicer, *Hyaluronan: a multifunctional, megaDalton, stealth molecule.* Current Opinion in Cell Biology, 2000. **12**(5): p. 581-586.
15. Pardue, E., S. Ibrahim, and A. Ramamurthi, *Role of hyaluronan in angiogenesis and its utility to angiogenic tissue engineering.* Organogenesis, 2008. **4**(4): p. 203-214.

16. Toole, B.P., *Hyaluronan: from extracellular glue to pericellular cue.* Nature Reviews Cancer, 2004. **4**(7): p. 528-39.
17. Distler, O., et al., *The molecular control of angiogenesis.* International Reviews of Immunology, 2002. **21**(1): p. 33-49.
18. Mehvar, R., *Dextrans for targeted and sustained delivery of therapeutic and imaging agents.* Journal of Controlled Release, 2000. **69**(1): p. 1-25.
19. Cooper, C.L., et al., *Polyelectrolyte–protein complexes.* Current opinion in colloid & interface science, 2005. **10**(1–2): p. 52-78.
20. Steitz, R., W. Jaeger, and R.v. Klitzing, *Influence of Charge Density and Ionic Strength on the Multilayer Formation of Strong Polyelectrolytes.* Langmuir, 2001. **17**(15): p. 4471-4474.
21. Shih, Y.C., J.M. Prausnitz, and H.W. Blanch, *Some characteristics of protein precipitation by salts.* Biotechnol Bioeng, 1992. **40**(10): p. 1155-64.

CHAPTER 3 Development of Hyaluronic-PLGA Formulations

3.1 Abstract

Poly (DL)-lactic-co-glycolic acid (PLGA) microspheres have been widely used for delivery of a large number of therapeutic agents. To overcome issues with protein stability, a self-encapsulation paradigm based on passive loading was recently developed. Here we investigate an effort to improve the paradigm via a biomimetic approach to improve loading from dilute protein solutions using hyaluronic acid (HA). HA-PLGA microspheres (20–63 μm) were prepared by a double water–oil–water emulsion method with a range of HA content, trehalose, and $MgCO_3$ to control microclimate pH and to create percolating pores for protein. Hyaluronic acid (HA)-PLGA microsphere formulations were developed with HA of 66, 357 and 1010 kDa M_w. Biomimetic active self-encapsulation (ASE) of lysozyme (LYZ) was accomplished by incubating blank HA-PLGA microspheres in low concentration protein solutions at ~ 24 °C, for 48 h. Pore closure was induced at 42.5 °C under mild agitation for 42 h. In the absence of $MgCO_3$, LYZ loading was found to increase with HA M_w and content. This effect on LYZ loading was dampened by the addition of $MgCO_3$ to HA-PLGA microspheres. Release kinetics of LYZ from HA-PLGA microspheres was evaluated in 1 ml PBS at 37 °C (pH 7.4), with complete media replacement. No significant differences were observed in release kinetics

of LYZ from HA-PLGA microspheres with a range of HA M_w and content, with ~ 37 - 48 % of encapsulated LYZ released over 28 days. Based on poor LYZ loading (< 2 % w/w of LYZ) and undesirable release kinetics, HA-PLGA microspheres were determined to be not suitable for developing a biomimetic approach to protein encapsulation.

3.2 Introduction

PLGA microspheres have been widely used for delivery of pharmaceutically active peptides, proteins and other bio-macromolecules [1-3]. A wide variety of techniques have been developed to overcome the major issues associated with the delivery of biotherapeutics using PLGA [4, 5]. These challenges include; instability caused by the manufacturing process, instability during encapsulation/loading of biomacromolecule and instability during in-vivo release [6]. A large number of operation parameters and choice of materials govern the size, shape, pore structure, surface morphology, encapsulation, and release characteristics of microspheres prepared with PLGA [7-10].

A common misconception is that the release kinetics from PLGA are undesirable and do not provide continuous zero-order type release. On the contrary, it has been known for more than 30 years that, by incorporating a low molecular weight PLGA into the polymer matrix, a continuous release of polypeptides is observed without an induction time before polymer mass loss (should the polypeptide remain soluble) [11]. There are also PLGA products that release highly water-soluble peptides without a significant burst release

[12]. Another perception about PLGA is that proteins are unstable when encapsulated in PLGAs. This has become a more persistent issue, and one that is complicated by the analytical difficulties associated with analysis of proteins in the release media and in the polymer. The major issue with the commercial adoption of PLGA products could primarily be associated to issues related with the scaling up of lab-scale processes to an industrial level.

Recently, after discovering the remarkable ability of small pores on the surface of PLGA to close spontaneously in water and overcome issues with large initial burst release [13], our group has devised a paradigm to microencapsulate large molecules in water by self-assembly of polymer chains to heal defects [14, 15]. It involves first preparing drug-free microspheres, in which a percolating pore network is created. Then, porous self-encapsulating (SE) microspheres are placed in an aqueous solution containing the drug for encapsulation under mild agitation at a temperature below the hydrated polymer (T_g). This incubation allows the entry of the drug deep within the polymer matrix. The polymer is then healed by raising the temperature > T_g, which leads to closing of the pores at the surface of the polymer and separation of pores within the polymer matrix. The surface pore closure thus encapsulates the drug in the polymer for controlled release [16].

This approach can be done either passively [15], or actively [17], e.g., by placing a "trapping agent" as an excipient in the polymer matrix that traps the drug as it enters the polymer. The passive SE approach is limited in terms of the encapsulation efficiency.

However, the ASE (active self-encapsulation) strategy with $Al(OH)_3$ adjuvant has achieved >97% efficiency of loading and (with 1-2% w/w antigen load) high immunoreactivity of the tetanus toxoid [17]. Moreover, the ASE microspheres could be sterilized by gamma-irradiation before successful encapsulation and release with little change in microsphere performance [18]. In this chapter, we discuss the feasibility of using hyaluronic acid (HA) to bring about ASE via the biomimetic approach in self-encapsulating PLGA microspheres.

3.3 Materials and Methods

3.3.1 Materials

PLGA with an inherent viscosity (i.v.) of 0.57 dLg^{-1} (50:50, PLGA DL LOW IV, lot # A11-071, lauryl ester end group, 51 kDa) was purchased from Lakeshore Biomaterials (Birmingham, Alabama). Sodium hyaluronate (HA) powders were obtained as a gift from Lifecore Biomedical (MN, USA). Lysozyme (chicken egg white) and magnesium carbonate were purchased from Sigma-Aldrich. All other reagents, common solvents, and supplies were obtained from Sigma-Aldrich, unless otherwise specified.

3.3.2 Preparation of HA-PLGA Microspheres

Porous active self-microencapsulating (SM) microspheres with BP for protein absorption in the PLGA pores, $MgCO_3$ as a pH modulator and porosigen [19], and trehalose [20] to similarly enhance the percolating pore structure of the microspheres, were prepared by double water-oil-water (W/O/W) emulsion. The first emulsion was created by homogenizing 1 ml of 250 mg/ml PLGA and $MgCO_3$ in CH_2Cl_2 with an inner water phase of varying amount of BPs, at 18000 rpm for 60s over an ice bath, using the Tempest IQ^2 (Virtis, USA). Two ml of 5% PVA solution was added to the resultant emulsion and the second emulsion was created by vortexing at 10000 rpm for 60s. The w/o/w emulsion was added to 100 ml of 0.5% PVA solution, and allowed to harden at room temperature for 3 h. Hardened microspheres (20-63 μm) were collected using sieves, washed with double-distilled water and immediately lyophilized.

3.3.3 Scanning Electron Microscopy

Scanning electron microcopy (SEM) images were obtained using a Hitachi S3200N scanning electron microscope (Hitachi, Japan). Briefly, lyophilized microspheres were fixed on double-sided adhesive carbon tape. Samples were coated with a thin layer of gold (~ 5 nm) under vacuum and images were taken at 10-15 kV excitation voltage. EDAX® software was used to obtain the final image.

3.3.4 Active Self Encapsulation of LYZ by HA-PLGA Microspheres

ASE is a two-step process consisting of a loading phase followed by pore closure. Studies were carried out to determine the lowest temperature and duration at which a majority of surface pores closed while encapsulating the maximum amount of protein from the loading solution. Biomimetic ASE of protein was achieved by incubating blank HA-PLGA microspheres in protein solution for 48 h at 24 °C. LYZ loading solutions were prepared in 10 mM phosphate buffer (pH 7).

Pore closure was induced at 42.5 ºC under mild agitation for 42 h. These parameters were determined by quantifying effect of temperature and duration of pore closure on LYZ loading *(discussed in next chapter).* After pore closure, HA-PLGA microspheres were removed from the loading solution, washed with double-distilled water, and immediately lyophilized. To freeze-dry, microspheres were flash frozen in liquid nitrogen and lyophilized using a FreeZone 2.5 (Labconco, USA) at < 0.080 mbar and - 42 °C, for 24 h. SEM images were taken to check if a majority of surface pores had closed.

3.3.5 Determination of loading and encapsulation efficiency

Loading of HA-PLGA microspheres was determined by a) protein content in loading solution after ASE, as described below and b) direct hydrolysis of ASE HA-PLGA microspheres followed by amino acid analysis (AAA), also as described below. Percentage w/w loading was quantified as $\left(\frac{\text{mass of protein encapsulated in micropsheres}}{\text{total mass of microspheres in loading solution}}\right) \times 100$. Percentage encapsulation efficiency was calculated as $\left(\frac{\text{mass of protein encapsulated in micropsheres}}{\text{total mass of protein in loading solution}}\right) \times 100$.

3.3.6 LYZ Quantification

3.3.6.1 Size Exclusion (SE) Chromatography

SE chromatography was performed using high performance liquid chromatography (HPLC) (Waters, USA). The mobile phase consisted of 0.1 M sodium phosphate with 0.3 M sodium sulfate at pH 6.7 at the rate of 0.8 ml/min for SE-HPLC. Samples and standards were injected onto TSKgel G2000SWxl (Tosoh Bioscience, USA) on HPLC systems. Protein detection by UV was done at 214 and 282 nm. Retention times of roughly 11 min were obtained for LYZ during SE-HPLC.

3.3.6.2 Amino Acid Analysis

Amino Acid Analysis (AAA) was performed to determine the total content of LYZ loaded in HA-PLGA microspheres (~ 5 mg), soluble protein solutions and standards were weighed into clear glass ampules in a total volume of 1.5 ml 6 N HC1. Ampules were sealed under light vacuum, and incubated at 110 °C for 24 h. Following incubation, each vial was completely emptied into microcentrifuge tubes, and the solution was evaporated under vacuum at room temperature. One ml of 1.0 M sodium bicarbonate buffer (pH 9.5) was added to each tube to neutralize the remaining acid. For individual amino acid analysis, a weighed amount of 350 µl of hydrolyzed protein solution and 350 µl of o-phthaldialdehyde reagent solution were mixed and immediately injected onto a C18 (Waters, USA) column fitted with a guard column [21, 22]. Each sample had a run time of 50 min, with a mobile phase at 1.4 ml/min of A) methanol-water (65:35) and B) methanol-THF-50 mM phosphoric acid (titrated to pH 7.5 with 10 N NaOH (20:20:960). The run started with 40% A for 0.5 min, 17 min gradient to 50% A, 15 min gradient to 100% A, a 5 min isocratic elution with 100% A, 7.5 min linear gradient to 40% A, and isocratic 40% A for 5 min. The fluorescence (excitation at 350 nm; emission at 455 nm) detection was used for quantification. Protein and standards were quantified using the average of the 3 individual amino acids alanine, phenylalanine, and lysine [15].

3.3.7 Evaluating Release Kinetics

The release kinetics of LYZ was determined by incubating LYZ loaded HA-PLGA microspheres at 37 ºC in the specified volume of PBS or PBST (PBS with 0.02% Tween

80) with complete replacement of release media. The amount of protein released was assayed by size-exclusion (SE) chromatography, as described above.

3.4 Results and Discussion

In the following sections, the development of HA-PLGA microsphere formulation is discussed. Factors governing biomimetic active self-encapsulation of LYZ and the subsequent release of the encapsulated LYZ were investigated.

3.4.1 Development of HA-PLGA Microsphere Formulations

Excipients were included in the organic/water phase to control pore structure and emulsion parameters in order to obtain a percolating pore network. The percolating pore network is required for allowing the biomacromolecule in the loading solution to enter deep within the microsphere during ASE, and diffuse out during subsequent controlled release. On the other hand, the pores should not be too large as they could lead to incomplete self-healing and/or poor loading efficiency, and high burst release. Polyvinyl alcohol (PVA) was used as surfactant, and its role was to stabilize the emulsions and allow for dispersion of one phase into another immiscible phase [8]. A good emulsion avoids coalescence and agglomeration, leading to small and regular sized microspheres with a small size distribution.

Increasing concentration or M_w of PLGA increases the viscosity of the continuous phase. The viscosity of the continuous phase is known to be exponentially related to the size of the microspheres obtained from the emulsion [23]. Higher PLGA M_w and concentration is also known to improve encapsulation efficiency and size of microspheres, but is also associated with slower drug release [24]. The quantity of the dispersed phase (or inner water phase) is known to be associated with irregular microsphere pore structure and poor drug encapsulation [25]. Use of higher agitation rate is known to create emulsions which yield smaller microspheres with a small size distribution [26]. Porosigens are also used to produce pores within the microspheres; which increase the rate of polymer degradation and subsequent drug release.

Table 3-1 : Representative list of formulation variables explored for obtaining well-formed HA-PLGA microspheres[1].

PLGA	HA		Trehalose	Heparin	Inner Phase	First Emulsion		Second Emulsion	
(mg)	M_w(kDa)	%(w/w)	% (w/w)	(mg)	(µl)	(Rpm)	Time(s)	(Rpm)	Time(s)
321.4	1010	3.4	2.2	0	400	18000	90	10000	60
315.2	1010	6.2	0.66	0	400	18000	90	10000	60
318.8	1010	3.8	0.73	6.5	400	18000	90	10000	60
326.1	1010	7.1	1.1	5.2	400	18000	90	10000	60
249.2	357	9.8	3.3	12	250	18000	120	10000	60
251.5	357	9.5	3.3	12	250	18000	120	10000	60
267.8	1010	8.7	3.8	0	300	18000	75	10000	60
280.1	1010	8.8	3.8	0	300	18000	75	15000	90
275.2	1010	10.1	1.9	6	150	15000	60	15000	90
261.4	1010	10.7	2.0	6	150	15000	60	15000	90

[1] Microspheres were prepared with w/o/w double emulsion system with 1 ml of continuous phase. Two ml of 5 % PVA solution was added to the first emulation obtained from inner phase and continuous phase to obtain the second emulsion.

3.4.1.1 Effect of HA M_w and content

From the very beginning of the development process, viscosity of HA solutions was a major issue. It was crucial to ensure accurate volumes of HA solutions were being pipetted, especially for high M_w or high concentration HA solutions. Viscosity was expected to cause problems with creating good emulsions and well formed microspheres. Initial attempts to obtain well-formed microspheres were carried out using the high Mw HA (357 and 1010 kDa), as parameters developed for these could be easily applied to lower M_w HA formulations (Table 3-1).

SEM images were used to check if microspheres obtained were well formed and had a visibly uniform pore structure. As anticipated, a major issue with the formulation of the HA-PLGA microspheres was the viscosity of the HA solution constituting the inner water phase. Increasing viscosity associated with higher M_w and w/w content of HA in the microspheres led to poorly formed primary emulsions, which in turn, led to deformed microspheres with non-uniform pore structure (Figure 3-1). In some cases, very viscous inner water phase solutions with HA led to poor/unstable primary emulsions. In other cases, we failed to obtain well-formed microspheres. More work would be needed to understand the role played by viscosity of inner phase and its effect on the quality of

emulsions, and subsequent microsphere formation, if microspheres with high M_w and/or content of HA are desired.

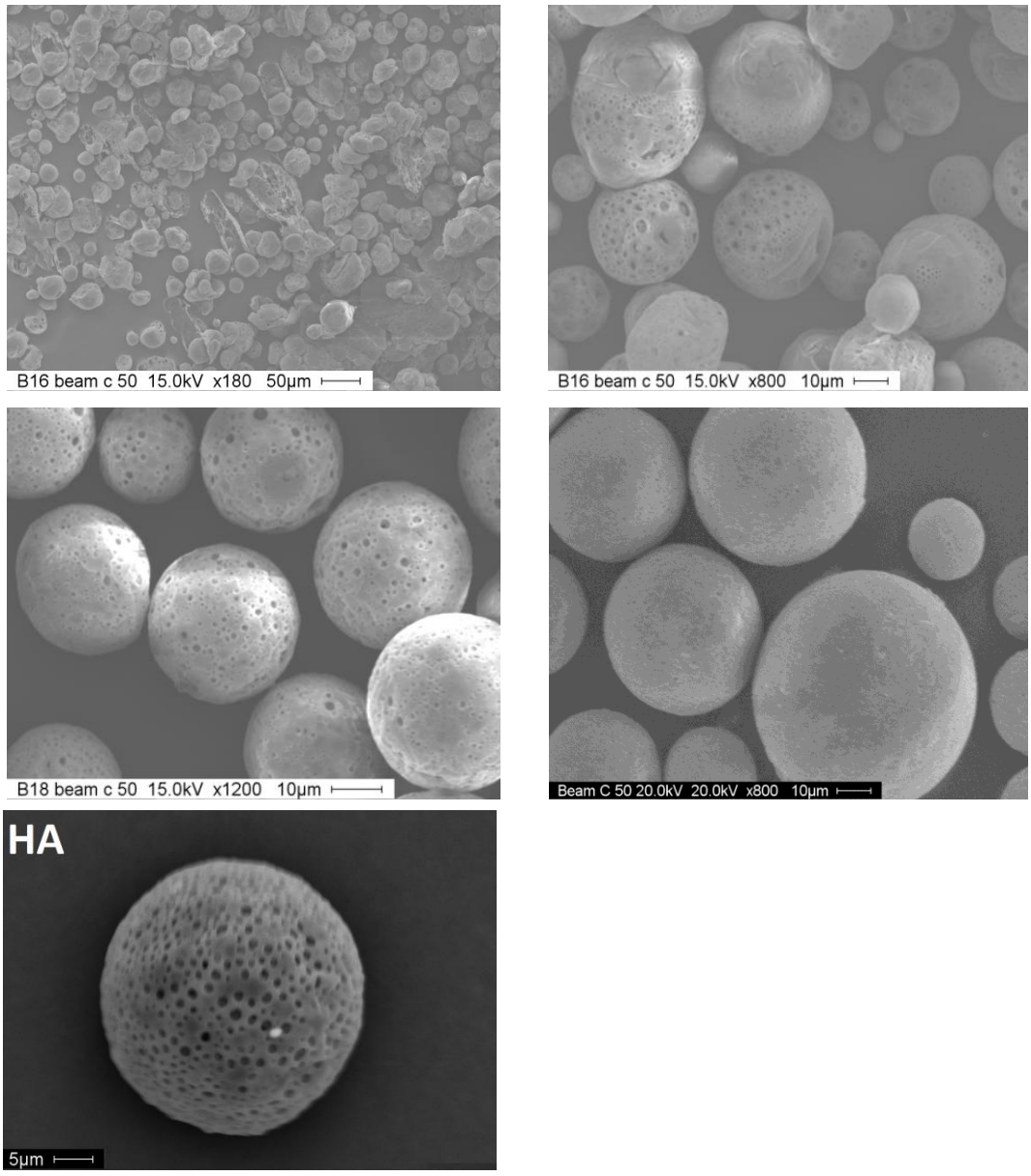

Figure 3-1 : Representative SEM images of HA-PLGA microspheres. Top (left to right): Failed batch of micropsheres due to poor quality of emulsion, and poorly-formed HA-PLGA micropsheres (4 % 1010 kDA). Middle (left to right): HA-PLGA micropsheres non-uniform surface pore (10 % 357 kDA). Bottom : Well formed HA-PLGA micropshere.

Upon analyzing SEM images of the microspheres of a wide variety of formulations, it was decided to use 250 mg/ml PLGA and 200 µl of inner phase volume for formulating ASE HA-PLGA microspheres. First and second emulsions were obtained at 18,000 rpm for 60 sec and 10,000 rpm for 60 sec, respectively. Higher speeds were used to ensure that small primary emulsions were created with the viscous BP containing inner water phase. To study the effect of M_w and % (w/w) content of HA on loading and release, attempts were made to obtain well formed HA microspheres with a range of M_w and HA content. HA of M_w of 66, 356 and 1010 kDa were used to formulate 2, 4, 8 and 13 % w/w HA-PLGA microspheres. We were able to obtain well-formed HA-PLGA microspheres with 66 kDa HA at 2 - 13 % w/w. In contrast, for 1010 and 357 kDa HA, we observed well-formed microspheres only for 2%, and 2 and 4 % w/w HA, respectively.

3.4.1.2 Effect of Trehalose and $MgCO_3$

As noted, pore network in PLGA microspheres is usually obtained by incorporating simple osmotic agents like a small sugar (e.g., trehalose) or alternative porosigen (e.g., $MgCO_3$). The selected excipients also act as protein stabilizers for the successful development of protein encapsulating biomimetic BP-PLGA microspheres.

To obtain stable lyophilized protein formulations, stabilizers are required to protect the protein during the freezing, drying and subsequent storage of the formulation [20]. Trehalose has been shown to be an ideal lyoprotectant, as it protects the protein during freezing and prevents unfolding during dehydration, due to its ability to form hydrogen bonds with the protein [20]. Bernstein *et al.* [27] showed that when poorly soluble bases (e.g., $MgCO_3$, $Mg(OH)_2$, $ZnCO_3$) are added to PLGAs of moderate M_w, instead of observing a lag phase, continuous release is observed. It is hypothesized that the base reacts with acids produced upon hydrolysis to form salts, which in turn, generates osmotic pressure and new pores for release of large molecules. Removal of acid from polymer phase reduces acid-catalyzed hydrolysis, slowing the PLGA degradation rate [28]. The inclusion of these acids induces significantly higher water uptake into the polymer matrix [29]. For this project, $MgCO_3$ is used. It reacts with acidic residues in the polymer to form salts and/or gaseous CO_2, helping to protect the encapsulated proteins from an acidic microenvironment. Our research group has used several poorly soluble bases to attenuate the microclimate pH in the polymer [28, 29].

Trehalose and $MgCO_3$ were added to the HA-PLGA microsphere formulations developed, in the previous section. Formulations containing the porisigens were seen to have a visibly improved pore structure, as observed by SEM. We expect this improvement to increase protein encapsulation and lead to good continuous release profiles upon subsequent release.

3.4.2 Active Self Encapsulation of LYZ by HA-PLGA Microparticles

HA-PLGA microspheres were prepared with 66 (4 and 12 % w/w), 356 (2 and 4 % w/w) and 1010 (2% w/w) kDa HA. These microspheres (~20 mg) were loaded in 0.5 ml of 1 mg/ml LYZ solution and the results are reported (Table 3-2).

3.4.2.1 Effect of HA M_w

As shown in the table, active encapsulation of LYZ increased with increasing $M_{w.}$ A similar trend was seen with increasing HA content in the HA-PLGA microspheres. Higher M_w HA was expected to improve LYZ loading of HA-PLGA microspheres, as the longer HA polymer chains were expected to be retained in the PLGA pores to a higher extent along with the bound LYZ. By contrast, the lower M_w HA was expected to diffuse out of HA-PLGA during the loading process. More work is needed to better understand the role of molecular chain length, viscosity, and polymer dynamics on protein binding and retention.

Table 3-2: Self-microencapsulation capacity and efficiency of optimal ASE HA-PLGA microspheres loaded from 0.5 ml of 1 mg/ml LYZ loading solution in 10 mM sodium phosphate (pH 7)[2] .

HA		$MgCO_3$	LYZ Loading		
M_w	%(w/w)	%(w/w)	% (w/w)[a]	% (w/w)[b]	% Efficiency [a]
66	4	0	0.34 ± 0.01	0.33 ± 0.11	18 ± 1
66	12	0	1.37 ± 0.07	1.5 ± 0.30	68 ± 2
357	2	0	0.42 ± 0.01	0.41 ± 0.07	21 ± 0.4
357	4	0	1.34 ± 0.01	1.33 ± 0.07	71 ± 5
1010	2	0	1.61 ± 0.02	1.57 ± 0.21	73 ± 7
66	4	3	0.73 ± 0.05	NA	37 ± 1
66	12	3	0.73 ± 0.03	NA	36 ± 2
357	2	3	0.83 ± 0.09	NA	41 ± 4
357	4	3	0.90 ± 0.07	NA	44 ± 1

[2] Theoretical content of trehalose was ~3 % w/w in the formulations. Data reported as mean ± SE, *n* = 7 for (a) SE and (b) AAA, respectively; total microsphere mass in loading solution was ~20 mg.

1010	2	3	0.78 ± 0.06	NA	38 ± 1

3.4.2.2 Effect of % w/w HA

Increased HA content would provide a larger amount and surface area of HA for LYZ binding, which should theoretically increase the LYZ loading. In addition, the hygroscopicity of larger amount of HA could potentially lead to a higher uptake of loading solution into the microsphere. We also hypnotized that increased HA content would lead to larger and more viscous HA-LYZ complexes inside the microspheres, which would be retained for a longer time inside the microsphere, as they slowly diffuse out of the pores and into the release media.

Such an effect of the HA content was observed, but was less pronounced than expected (Table 3-2). Here, it is assumed that incorporation of higher content of HA in the HA-PLGA microsphere did not significantly alter the pore structure.

3.4.2.3 Effect of $MgCO_3$

Upon the addition of 3% w/w $MgCO_3$, the effect of varying M_w and HA content on the active self-encapsulation of LYZ was greatly reduced (Table 3-2). This trend could be due to the increased osmotic pressure created by presence of $MgCO_3$, which could counteract the effect of higher M_w and HA content. In addition, the improved pore structure brought about by the addition of $MgCO_3$ led to visibly larger pores on the

surface of the microspheres. This could potentially lead to poor retention of the encapsulated LYZ inside the microspheres, as LYZ could leach out into the loading solution through the improved pore structure and larger surface pores.

No clear trend was seen upon comparing LYZ loading of similar formulations, with and without $MgCO_3$. In some cases addition of $MgCO_3$ to formulations led to an increase in LYZ encapsulation (66 kDA at 4% w/w, 357 kDa at 2 % w/w) as quantified by SE, whereas in others a decrease was seen (66 kDa at 12% w/w, 357 kDa at 4% w/w). The difference in the loading of LYZ by AAA and SE-HPLC could be possibly due to the high water uptake and gel-forming nature of the HA. The uptake of the protein solution by the HA-PLGA microspheres could lead to a decrease in the loading solution volume and thus underestimate the loss of protein from solution, as measured by the SE-HPLC.

3.4.3 Release Kinetics of HA-PLGA Microspheres

As noted above, the size and solubility of HA-LYZ complex was hypothesized to govern the amount of free LYZ available to percolate through the microsphere pore structure and ultimately diffuse out into the release media. Higher M_w HA was expected to slow the release of LYZ, as LYZ bound to higher M_w HA would be expected to facilitate retention in the PLGA matrix. Similarly, higher w/w content of HA would also retain LYZ inside the microspheres for a longer time. The hypotheses were tested by evaluating the release kinetics of LYZ from a range of HA-PLGA microspheres with trehalose and $MgCO_3$ in 1 ml PBS (pH 7.4), at 37 °C.

3.4.3.1 Effect of HA content

On comparing release kinetics of HA-PLGA microspheres prepared with 66 kDa, no significant differences were seen between formulations developed with 4% and 12% (w/w), as both formulations were seen to release ~ 44 % of encapsulated LYZ over 28 days (Figure 3-2). In contrast, small difference was seen with microspheres prepared with 357 kDa HA. HA-PLGA microspheres with 2 % (w/w HA) released ~ 48 % of the LYZ, whereas formulations with 4 % (w/w HA) released ~ 36 %.

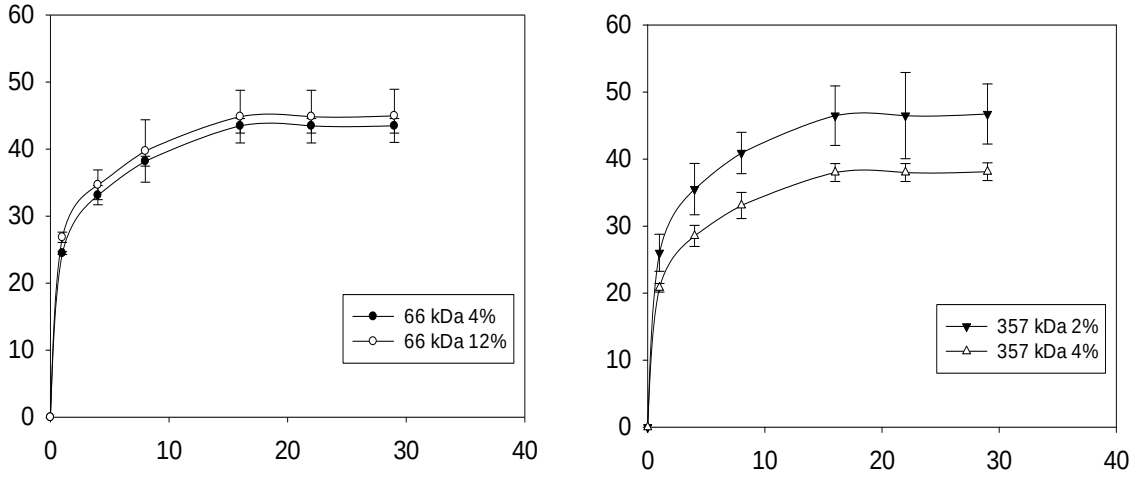

Figure 3-2 : LYZ release profiles in 1 ml PBS (pH 7.4) at 37 °C quantified by SE-HPLC at 282 nm. ASE HA-PLGA microspheres were loaded from 1 mg/ml LYZ in 10 mM phosphate buffer (pH 7). The values are expressed as mean ± SE; n=3; total microsphere mass in release media is ≈18 mg.

3.4.3.2 Effect of HA M_w

Upon comparing, 4 % (w/w) of 66 and 357 kDa HA, the former released ~ 44 % LYZ while the later released ~ 38 % (Figure 3-3). In contrast both 357 and 1010 kDa HA-PLGA formulations with 2 % HA (w/w) release ~ 46 % of the encapsulated LYZ.

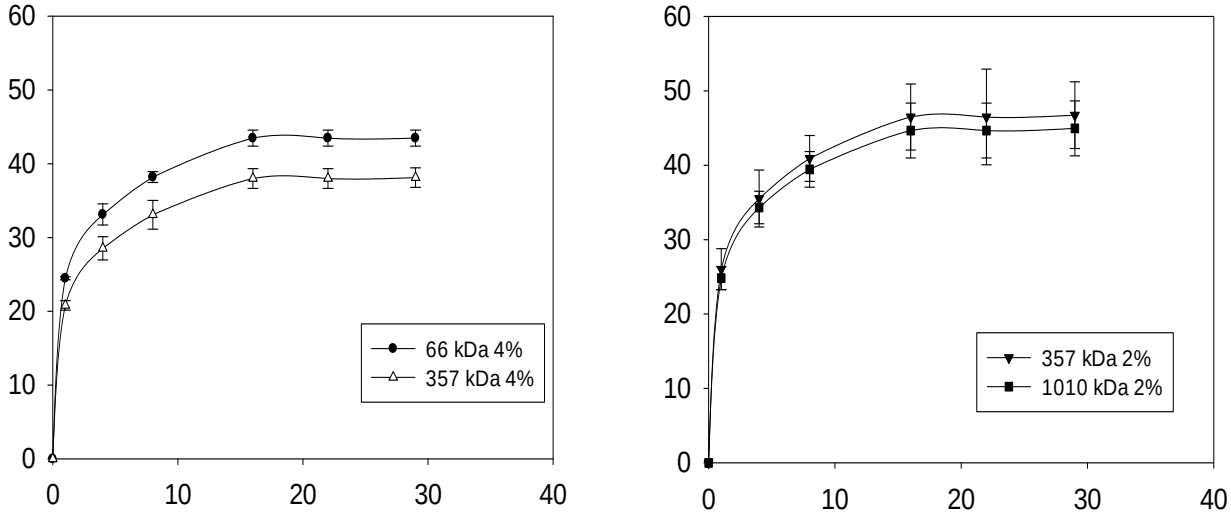

Figure 3-3 : LYZ release profiles in 1 ml PBS (pH 7.4) at 37 °C quantified by SE-HPLC at 282 nm. ASE HA-PLGA microspheres were loaded from 1 mg/ml LYZ in 10 mM phosphate buffer (pH 7). The values are expressed as mean ± SE; n=3; total microsphere mass in release media is ≈ 18 mg.

Overall, all HA-PLGA formulations released ~ 37-48 % of the encapsulated LYZ over 16 days and the release plateaued beyond that time (Figure 3-4). The plateauing of LYZ release beyond day 14 was noticeable across all HA-PLGA formulations. This is a major concern as the desired release profile is of a slow continuous release over 45-60 days.

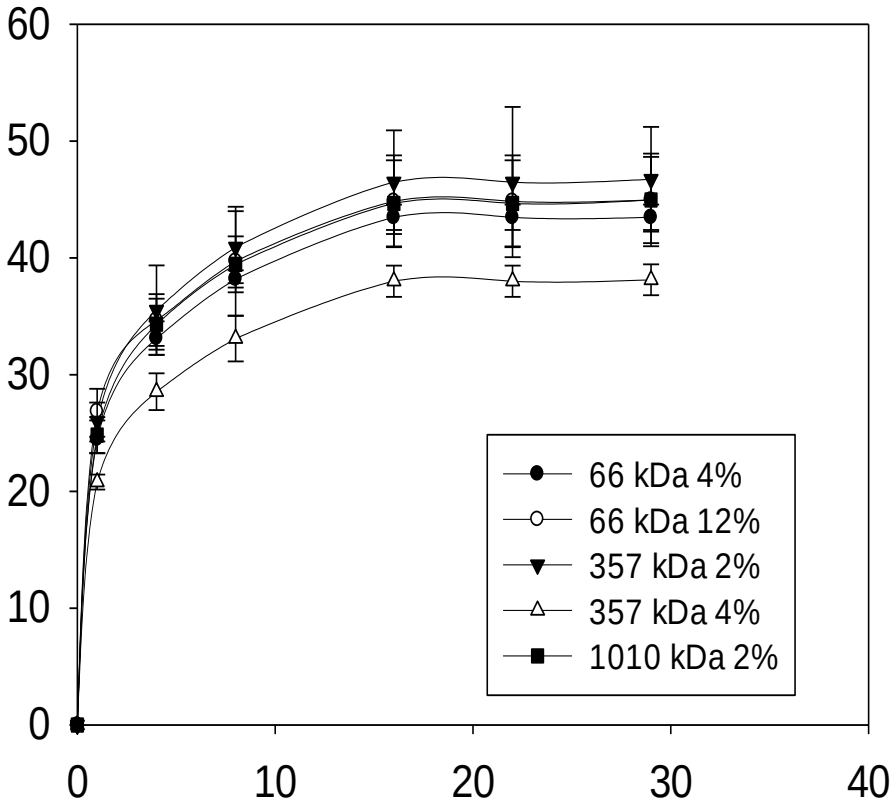

Figure 3-4 : LYZ release profiles in 1 ml PBS (pH 7.4) at 37 °C quantified by SE-HPLC at 282 nm. ASE HA-PLGA microspheres were loaded from 1 mg/ml LYZ in 10 mM phosphate buffer (pH 7). The values are expressed as mean ± SE; n=3; total microsphere mass in release mass in release media is ≈ 18 mg.

3.5 Conclusions

In this chapter, we determined formulation parameters for developing well-formed HA-PLGA microspheres with 66, 357 and 1010 kDa HA. $MgCO_3$ and trehalose were included as porosigens to improve protein stability and pore structure.

Biomimetic self-encapsulation of LYZ was quantified by measuring loss of protein from loading solution and amino acid analysis. Increased LYZ loading was observed for

formulations with higher HA M_w and content, but this effect was greatly suppressed when $MgCO_3$ was incorporated in the formulations. Release kinetics of LYZ was found not to alter significantly with HA M_w and content. The LYZ release was found to plateau around day 14 of release with a large amount of LYZ being retained inside the microspheres.

Our data suggested that HA-PLGA microspheres are not suitable for obtaining high protein loading (>2% w/w of LYZ) and had poor release kinetics. Thus, we decided to investigate sulfated BP-PLGA microsphere formulations for biomimetic ASE, as discussed in the next chapter.

3.6 References

1. Okada, H. and H. Toguchi, *Biodegradable microspheres in drug delivery.* Crit Rev Ther Drug Carrier Syst, 1995. **12**(1): p. 1-99.
2. Brown, L.R., *Commercial challenges of protein drug delivery.* Expert Opinion on Drug Delivery, 2005. **2**(1): p. 29-42.
3. Schwendeman, S.P., *Recent advances in the stabilization of proteins encapsulated in injectable PLGA delivery systems.* Critical Reviews in Therapeutic Drug Carrier Systems, 2002. **19**(1): p. 73-98.
4. Jain, R., *The manufacturing techniques of various drug loaded biodegradable poly (lactide-co-glycolide)(PLGA) devices.* Biomaterials, 2000. **21**(23): p. 2475-90.
5. Grund, S., M. Bauer, and D. Fischer, *Polymers in Drug Delivery—State of the Art and Future Trends.* Advanced Engineering Materials, 2011. **13**(3): p. B61-B87.
6. Fu, K., A.M. Klibanov, and R. Langer, *Protein stability in controlled-release systems.* Nature Biotechnology, 2000. **18**(1): p. 24-5.
7. Yeo, Y. and K. Park, *Control of encapsulation efficiency and initial burst in polymeric microparticle systems.* Archives of Pharmacal Research, 2004. **27**(1): p. 1-12.
8. Li, M., O. Rouaud, and D. Poncelet, *Microencapsulation by solvent evaporation: State of the art for process engineering approaches.* International Journal of Pharmaceutics, 2008. **363**(1–2): p. 26-39.
9. Jiang, G., et al., *Assessment of protein release kinetics, stability and protein polymer interaction of lysozyme encapsulated poly(d,l-lactide-co-glycolide) microspheres.* Journal of Controlled Release, 2002. **79**(1–3): p. 137-145.
10. Brunner, A., K. Mader, and A. Gopferich, *pH and osmotic pressure inside biodegradable microspheres during erosion.* Pharm Res, 1999. **16**(6): p. 847-53.
11. Hutchinson, F.G., *Continuous release pharmaceutical compositions; EP 0058481*, USPTO, Editor 1982: USA.
12. Fineman, M., et al., *Pharmacokinetics and Pharmacodynamics of Exenatide Extended-Release After Single and Multiple Dosing.* Clinical Pharmacokinetics, 2011. **50**(1): p. 65-74.
13. Wang, J., B.M. Wang, and S.P. Schwendeman, *Characterization of the initial burst release of a model peptide from poly(D,L-lactide-co-glycolide) microspheres.* J Control Release, 2002. **82**(2-3): p. 289-307.
14. Schwendeman, S.P., S.E. Reinhold, and J. Kang, *Immersing and soaking insoluble pore containing polymer into encapsulating solution containing active ingredient then initiating pore closing rearrangement by adjusting temperature and/or pH; US8017155 B2*, USPTO, Editor 2011.
15. Reinhold, S.E., et al., *Self-Healing Microencapsulation of Biomacromolecules without Organic Solvents.* Angewandte Chemie International Edition, 2012. **51**(43): p. 10800-10803.

16. Reinhold, S., *Self-healing polymers microencapsulate biomacromolecules without organic solvents*, 2009, University of Michigan.
17. Desai, K.G.H. *Active Self-microencapsulating PLGA Microspheres for Controlled Release of Vaccine Antigens: A New Paradigm for Low-cost, Safe, and Effective Antigen Delivery*. in *Controlled Release Society*. 2010.
18. Desai, K.G.H., S. Kadous, and S.P. Schwendeman, *Gamma Irradiation of Active Self-Healing PLGA Microspheres for Efficient Aqueous Encapsulation of Vaccine Antigens.* Pharmaceutical Research, 2013. **30**(7): p. 1768-1778.
19. Wu, F. and T. Jin, *Polymer-based sustained-release dosage forms for protein drugs, challenges, and recent advances.* AAPS PharmSciTech, 2008. **9**(4): p. 1218-1229.
20. Carpenter, J.F., et al., *Rational Design of Stable Lyophilized Protein Formulations: Some Practical Advice.* Pharmaceutical Research, 1997. **14**(8): p. 969-975.
21. Lindroth, P., A. Hamberger, and M. Sandberg, *Liquid Chromatographic Determination of Amino Acids After Precolumn Fluorescence Derivatization*, in *Amino Acids*, A. Boulton, G. Baker, and J. Wood, Editors. 1986, Humana Press. p. 97-116.
22. Lindroth, P. and K. Mopper, *High performance liquid chromatographic determination of subpicomole amounts of amino acids by precolumn fluorescence derivatization with o-phthaldialdehyde.* Analytical Chemistry, 1979. **51**(11): p. 1667-1674.
23. André-Abrant, A., J.-L. Taverdet, and J. Jay, *Microencapsulation par évaporation de solvant.* European Polymer Journal, 2001. **37**(5): p. 955-963.
24. C.-Y. Yang, S.-Y.T., R. C.-C. Tsiang, *An enhanced process for encapsulating aspirin in ethyl cellulose microcapsules by solvent evaporation in an O/W emulsion.* Journal of Microencapsulation, 2000. **17**(3): p. 269-277.
25. Witschi, C. and E. Doelker, *Influence of the microencapsulation method and peptide loading on poly(lactic acid) and poly(lactic-co-glycolic acid) degradation during in vitro testing.* Journal of Controlled Release, 1998. **51**(2–3): p. 327-341.
26. Gabor, F., et al., *Ketoprofen-poly(D,L-lactic-co-glycolic acid) microspheres: influence of manufacturing parameters and type of polymer on the release characteristics.* J Microencapsul, 1999. **16**(1): p. 1-12.
27. Howard Bernstein, Y.Z., M. Amin Khan, Mark A. Tracy, *Modulated release from biocompatible polymers; US 6,749,866*, USPTO, Editor 2004: USA.
28. Zhu, G. and S.P. Schwendeman, *Stabilization of proteins encapsulated in cylindrical poly(lactide-co-glycolide) implants: mechanism of stabilization by basic additives.* Pharm Res, 2000. **17**(3): p. 351-7.
29. Zhu, G.Z., S.R. Mallery, and S.P. Schwendeman, *Stabilization of proteins encapsulated in injectable poly (lactide-co-glycolide).* Nature Biotechnology, 2000. **18**(1): p. 52-57.

CHAPTER 4 Development of Sulfated BP-PLGA Formulations

4.1 Abstract

The purpose of this study was to evaluate the biomimetic active self-encapsulation of proteins by sulfated biopolymer (BP)-PLGA microspheres. Sulfated BPs [high molecular weight dextran sulfate (HDS), low molecular weight dextran sulfate (LDS), chondroitin sulfate (CS), heparin (HP)] were used to formulate BP-PLGA microspheres (20–63 μm). Microspheres were prepared by a double water–oil–water emulsion method with a range of BP content, trehalose, and $MgCO_3$ to control microclimate pH and to create percolating pores for protein. Biomimetic active self-encapsulation (ASE) of proteins [LYZ, vascular endothelial growth factor165 (VEGF) and fibroblast growth factor (FgF-20)] was accomplished by incubating blank BP-PLGA microspheres in low concentration protein solutions at ~ 24 °C, for 48 h. Pore closure was induced at 42.5 °C, under mild agitation for 42 h. Formulation parameters of BP-PLGA microspheres and loading conditions were optimized for protein loading. Sulfated BP-PLGA microspheres were capable of loading LYZ (~2-7 % w/w), VEGF (~ 4% w/w), and FgF-20 (~2% w/w) with high efficiency. Protein loading was found to be dependent on the loading solution concentration, with higher protein loading obtained at higher loading solution concentration within the range investigated. Loading also increased with content of

sulfated BP in microspheres. Release kinetics of proteins was evaluated *in-vitro* with complete release media replacement. The pH of the release media was not significantly affected by the presence of BPs amongst the microsphere degradation products. Rate and extent of release were found to depend upon volume of release (with non-sink conditions observed < 5ml release volume for ~18mg loaded BP-PLGA microspheres), ionic strength of release media and loading solution concentration. HDS-PLGA formulations were identified as having ideal loading and release characteristics. These optimal microspheres released ~ 73-80 % of the encapsulated LYZ over 60 days, with > 90 % of protein being enzymatically active. Nearly 72% of immunoreactive VEGF was similarly released over 42 days, without significant losses in heparin binding affinity in the release medium.

4.2 Introduction

The ability to impart sustained drug levels in the blood or target tissue for 1-3 months following a single injection is a holy grail for numerous drug companies for delivery of their bio-macromolecular drugs. PLGA microspheres have long demonstrated an ability to deliver therapeutic agents from weeks to months in commercial products. This long duration has not being attained by non-PLGA biodegradable systems for commercial use. Hence, most non-PLGA based systems do not have commercial precedence and lack the so-called “real world biomaterial” status.

Long-acting-release products (LARs) not only improve lifestyle by minimizing exposure to the needle, but also generally improve patient outcomes by improving patient compliance and reducing peak-and-valley blood levels [1]. The noninvasive and peptide/protein modification strategies have typically been limited to weekly dosing. For example, the ability to extend peptide and protein half-lives in blood, usually by modification of the peptide/protein molecule, has been accomplished by PEGylation [2], protein fusion (e.g., to albumin or Fc region of the antibody) [3, 4], and lipidation [5].

A number of protein and peptide drugs could provide greater therapeutic benefit if the plasma concentration could be maintained for an extended period. In addition, other products could benefit from sustained delivery of systemic dose such as blood coagulation factors, metabolic peptides, monoclonal antibodies and antibody fragments, enzymes, and cytokines. Delivery of growth factors holds great promise for regenerative medicine for treatment of peripheral vascular and ischemic heart diseases [6-8]. However, systemic administration of growth factors has led to mixed clinical outcomes. Polymer depots can maintain systemic levels of therapeutic drug, allowing for delivery of drugs for local/site-specific activity. However, in order to accomplish 1-3 month controlled release, typically large doses have to be initially encapsulated in the polymer.

In this chapter, we discuss the feasibility of our biomimetic approach to load large amounts of proteins efficiently, to develop LAR products using sulfated BPs. Our paradigm would allow us to overcome some of the major instability issues associated with encapsulating proteins in PLGA [9-11]. Using BPs in the PLGA matrix to bind and

stabilize proteins would allow proteins to be protected during loading and release, as upon binding and immobilization, proteins are protected from physical and chemical instability caused by exposure to PLGA and other destabilizing factors [11, 12].

4.3 Materials and Methods

4.3.1 Materials

PLGA with an inherent viscosity (i.v.) of 0.57 dLg $^{-1}$ (50:50, PLGA DL LOW IV, lot # A11-071, lauryl ester end group, 51 kDa) was purchased from Lakeshore Biomaterials (Birmingham, Alabama). High molecular weight (~ 500 kDa) dextran sulfate (HDS), low molecular weight (~15.5 kDa) dextran sulfate (LDS), chondroitin sulfate (~ 63 kDa, shark cartilage) (CS), porcine heparin (~18 kDa) (HP) sodium salts were purchased from Sigma-Aldrich. Chitosan (~ 61 kDa) was also from Sigma-Aldrich. VEGF165 were obtained as a gift from Genentech. Lysozyme (chicken egg white) and magnesium carbonate were purchased from Sigma-Aldrich. FgF-20 was obtained from the National Cancer Institute-Biometric Research Branch (NCI-BRB) preclinical repository. Human VEGF standard ELISA development kit was purchased from Peprotech (NJ, USA). Cyanine-5 labelled lysozyme and FITC-dextran were bought from Nanocs (NY, USA). All other reagents, common solvents, and supplies were obtained from Sigma-Aldrich, unless otherwise specified.

4.3.2 Preparation of Sulfated BP-PLGA Microspheres

Porous active self-microencapsulating (SM) microspheres with BP for protein absorption in the PLGA pores, $MgCO_3$ as a pH modulator and porosigen [13], and trehalose [14] to similarly enhance the percolating pore structure of the microspheres, were prepared by double water-oil-water (W/O/W) emulsion. The first emulsion was created by homogenizing 1 ml of 250 mg/ml PLGA and $MgCO_3$ in CH_2Cl_2 with an inner water phase of varying amount of BPs, at 18000 rpm for 60s over an ice bath, using the Tempest IQ^2 (Virtis, USA). Two ml of 5% PVA solution was added to the resultant emulsion and the second emulsion was created by vortexing at 10000 rpm for 60s. The w/o/w emulsion was added to 100 ml of 0.5% PVA solution, and allowed to harden at room temperature for 3 h. Hardened microspheres (20-63 μm) were collected using sieves, washed with double-distilled water and immediately lyophilized.

4.3.2.1 HDS(FITC)-PLGA Microspheres

HDS-PLGA microspheres were prepared as described above.

4.3.3 HDS-PLGA Microspheres with $ZnCO_3$

HDS-PLGA microspheres were prepared as described above, with $ZnCO_3$ used instead of $MgCO_3$.

4.3.4 Scanning Electron Microscopy

Scanning electron microcopy (SEM) images were obtained using a Hitachi S3200N scanning electron microscope (Hitachi, Japan). Briefly, lyophilized microspheres were fixed on double-sided adhesive carbon tape. Samples were coated with a thin layer of gold (~ 5 nm) under vacuum and images were taken at 10-15 kV excitation voltage. EDAX® software was used to obtain the final image.

4.3.5 Active Self Encapsulation of LYZ, FgF-20 and VEGF by BP-PLGA Microspheres

ASE is a two-step process consisting of a loading phase followed by pore closure. Studies were carried out to determine the lowest temperature and duration at which a majority of surface pores closed while encapsulating the maximum amount of protein from the loading solution. Biomimetic ASE of protein was achieved by incubating blank BP-PLGA microspheres in protein solution for 48 h at 24 °C. LYZ loading solutions were prepared in 10 mM phosphate buffer (pH 7) and FgF-20 loading solutions were prepared in 0.5 M arginine, 0.05 M sodium phosphate and 0.08% polysorbate 20 (pH 7). VEGF loading solutions were prepared in 5 mM succinate buffer, 275 mM trehalose and 0.01% polysorbate 20 (pH 5).

Pore closure was induced at 42.5 ºC under mild agitation for 42 h. These parameters were determined by quantifying effect of temperature and duration of pore closure on LYZ loading. After pore closure, BP-PLGA microspheres were removed from the loading solution, washed with double-distilled water, and immediately lyophilized. To freeze-dry, microspheres were flash frozen in liquid nitrogen and lyophilized using a FreeZone 2.5 (Labconco, USA) at < 0.080 mbar and - 42 °C, for 24 h. SEM images were taken to check if a majority of surface pores had closed.

4.3.6 Determination of loading and encapsulation efficiency

Loading of BP-PLGA microspheres was determined protein content in loading solution after ASE, as described in the following section. Percentage w/w loading was quantified as $\left(\frac{\text{mass of protein encapsulated in micropsheres}}{\text{total mass of microspheres in loading solution}}\right) \times 100$. Percentage encapsulation efficiency was calculated as $\left(\frac{\text{mass of protein encapsulated in micropsheres}}{\text{total mass of protein in loading solution}}\right) \times 100$.

4.3.7 Protein Quantification

4.3.7.1 Size Exclusion (SE) Chromatography

SE chromatography was performed using high performance liquid chromatography (HPLC) and ultra performance chromatography (UPLC) systems (Waters, USA). The

mobile phase consisted of 0.1 M sodium phosphate with 0.3 M sodium sulfate at pH 6.7 at the rate of 0.8 ml/min and 0.4 ml/min for SE-HPLC and SE-UPLC, respectively. Samples and standards were injected onto TSKgel G2000SWxl (Tosoh Bioscience, USA) and Acquity BEH200 (Waters, USA) on HPLC and UPLC systems, respectively. Protein detection by UV was done at 214 and 282 nm. Retention times of roughly 11 and 5 min were obtained for LYZ during SE-HPLC and SE-UPLC, respectively. FgF-20 and VEGF both had retention times of roughly 5 min during SE-UPLC. The UPLC was preferentially used in quantifying protein release kinetics in 5 ml release media, as it had higher sensitivity when compared to SE-HPLC for the conditions studied.

4.3.7.2 UV Spectroscopy

Quantification of protein was carried out with Synergy 2 microplate reader (Biotek, USA) at 214 and 282 nm with appropriate standards and controls, using 96 well plates (Corning, USA).

4.3.7.3 Coomassie Plus protein assay

Quantification was carried out using appropriate standards and controls at 595 nm using the microplate reader, as per protocol provided by manufacturer (Coomassie Plus, Pierce). The assay was used to quantify VEGF loading along with SE-UPLC.

4.3.7.4 VEGF enzyme linked immunosorbent assay

VEGF enzyme linked immunosorbent assay (ELISA) was carried out as per the manufacturer's protocol. Briefly, 96 well microplates were incubated overnight with 100 µl of 0.5 µg/ml capture antibody in PBS at room temperature. After washing with PBS containing 0.05% Tween 20, 100 µl of standards and samples in diluent (PBS with 0.05% Tween 20 and 0.1% BSA) were added in triplicate and incubated for 2 h at room temperature. After washing, 100 µl of 0.25µg/ml biotinylated secondary antibody in diluent was added to each well and allowed to incubate for 2 h at room temperature. After another wash, 100 µl of diluted (1:2000) avidin-HPR conjugate was incubated in each well for 30 min. After a final wash, 100 µl of ABTS substrate was added to each well for detection. Activity was determined after 25 min by monitoring plate optical density at 405 nm with wavelength correction set at 650 nm and fitting the data using the Gen5 software (Biotek, USA).

4.3.7.5 Heparin-affinity chromatography

Heparin-affinity chromatography was performed using an Alliance HPLC system (Waters, USA). Each sample had a run time of 15 min, with a mobile phase at 1.0 ml/min of A) 50 mM phosphate buffer (pH 7) and B) 50 mM phosphate buffer with 3M NaCl (pH 7). Samples and standards were injected onto POROS® Heparin 50 µm column (Applied Biosystems®, USA). The run started with 100% A for 5 min, 2 min gradient to 0% A, 5 min gradient to 100% A, and an isocratic 100% A for 3 min. Heparin binding

VEGF was detected by UV at 214 and 282 nm with a retention time of ~ 10 min. The large BSA peak from the release media samples was baseline separated from the VEGF peak and had a retention time of ~ 3.5 min. Percentage heparin binding VEGF was quantified as $\left(\frac{\text{mass of heparin binding VEGF}}{\text{mass of immunoreactive VEGF}}\right) \times 100$.

4.3.8 Biomimetic ASE of LYZ(CY5) by HDS(FITC)-PLGA Microspheres

Biomimetic ASE Cy5 LYZ was brought about as described above.

4.3.9 Confocal Microscopy

HDS-PLGA microspheres were prepared as described in section 2.4. The microspheres were loaded from Cyanine-5 (Cy5) labeled LYZ at 1 mg/ml concentration in 10 mM phosphate buffer (pH 7), as described above for unlabelled LYZ. After ASE, the microspheres were washed and lyophilized. Volumetric images of HDS-PLGA microspheres encapsulating Cy5-LYZ were generated by taking images at different focal lengths with a step size of 2 μm (Nikon A1R/A1 confocal microscope). NIS-Elements® software was used to combine these images into volumetric images.

4.3.10 Evaluating Release Kinetics

The release kinetics of LYZ was determined by incubating loaded BP-PLGA microspheres at 37 ºC in the specified volume of PBS or PBST (PBS with 0.02% Tween 80) with complete replacement of release media. The amount of protein released was assayed by size-exclusion (SE) chromatography, as described below. The activity of released LYZ was quantified by Enzchek®, described below. Release kinetics of VEGF was determined in PBST+10 mg/mL BSA, also with complete media replacement at each time point by ELISA, as described below.

4.3.11 Measurement of pH

The pH of the release media was measured by Orion model 290 pH meter (Thermo Scientific, USA), as per the protocol provided by the manufacturer. Measurements of samples were taken in triplicate.

4.4 Results and Discussion

In the following sections, the development of BP-PLGA microspheres is discussed. Parameters governing the biomimetic loading of proteins were investigated. The role of the type of BP, content of BP in PLGA, and concentration of loading solution on ASE of protein were investigated. Factors governing protein release kinetics from the BP-PLGA

microspheres were also investigated. The effect of BP type, BP content, volume of release, and ionic strength of release media on release kinetics, was studied.

4.4.1 Optimization of Biomimetic ASE parameters for encapsulation of LYZ by BP- PLGA microspheres

Biomimetic ASE is a two-step process, consisting of a loading phase followed by pore closure. Studies were carried out to determine the lowest temperature and duration at which a majority of surface pores closed, while encapsulating the maximum amount of protein from the loading solution.

Initial attempts to determine loading temperature and duration were carried out with PLGA microspheres formulated with HDS, HA (66 kDa), CH (soluble chitosan) and blank microspheres. Pore closure should be carried out at a high enough temperature to ensure that the PLGA polymer chains could mobilize to allow for "self-healing" of the microsphere surface, but not at high enough temperature and duration to damage the protein. SEM images and LYZ loading was determined to check for pore closure and quantify loading at different time points of the pore closure study.

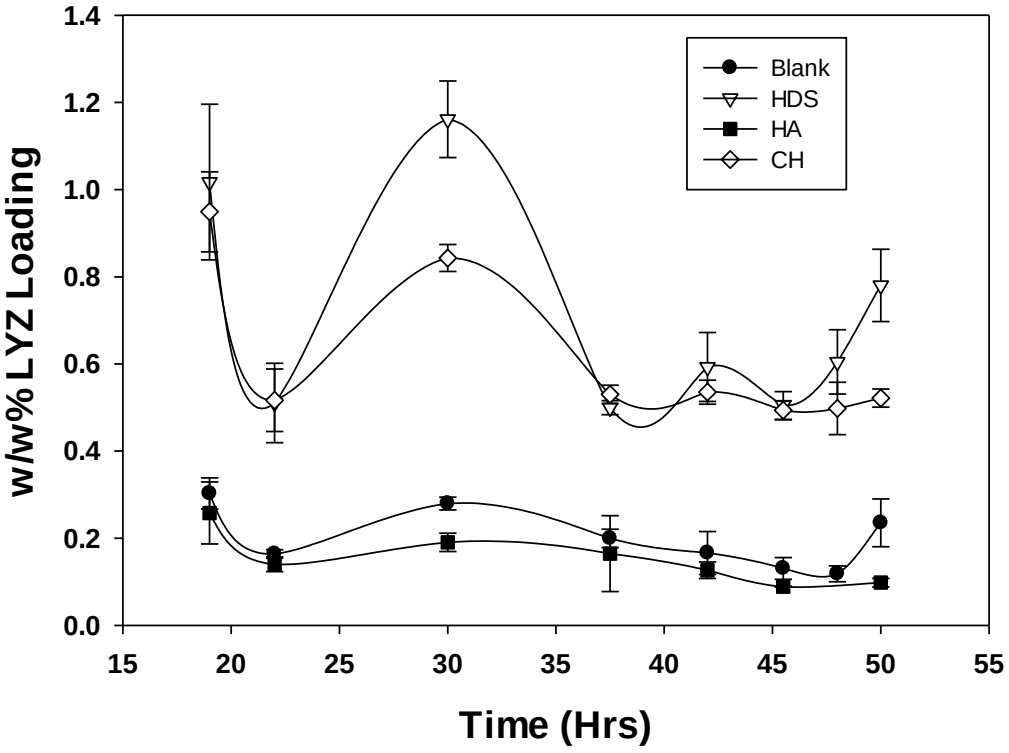

Figure 4-1 : Theoretical content of $MgCO_3$ and trehalose was ~3 % w/w in the formulations. LYZ loading was quantified by SE-HPLC. Pore closure was carried out at 42.5° C. Data reported as mean ± SE, n = 3.

BP-PLGA microspheres were loaded with 0.5 ml of 0.25 mg/ml LYZ in 10 mM phosphate buffer (pH 7) at 24 °C. Pore closure was carried out at 42.5 °C, as previously reported [15]. LYZ loading for the time points of study were quantified as shown (Figure 4-1). Across all formulations studied, the highest loading was observed at 30 h of pore closure, but the SEM images of the microsphere surface were noted to have large surface pores. LYZ loading at 19 h and 50 h was also higher compared to some of time points.HDS and SC formulations had some of the higher LYZ loading whereas HA and blank microspheres consistently had some of the lowest LYZ loading during the entire pore closure study. The images obtained showed that a majority of the surface pores on

the BP-PLGA microspheres were closed beyond 42 h (data not shown). Based on these images, it was decided to carry out pore closure for 42 hr for all BP-PLGA microspheres.

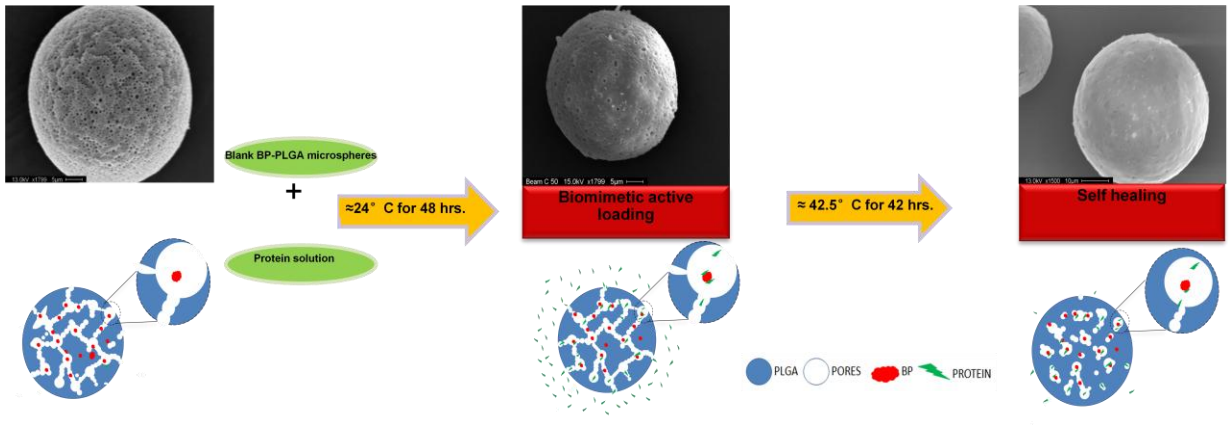

Figure 4-2 : Schematic of the biomimetic active self encapsulation of proteins by BP-PLGA

4.4.2 Effect of BP-PLGA microspheres on release media pH

To evaluate the feasibility of using BP-PLGA microspheres, we wanted to study the effect of BP containing PLGA formulations on the pH of the release media. This was brought about by carrying out a release study of unloaded HDS-PLGA, SC-PLGA, HA-PLGA, and blank PLGA microspheres (~ 20 mg) in 1ml PBS (pH 7) at 37 °C, with complete media replacement. The pH profile of the release media was monitored over 28 days (Figure 4-3).

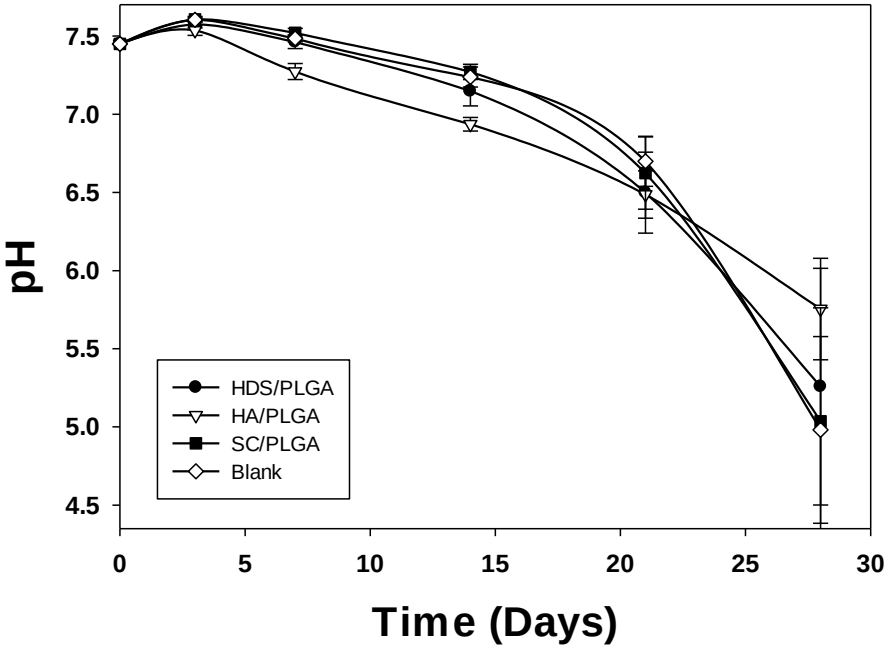

Figure 4-3 : pH profile of 1ml of PBS release media (pH 7.4) with BP-PLGA microspheres (~ 20 mg) in at 37 °C. Data reported as mean ± SE, n = 4.

Across all formulations, the pH of the release media was found to drop below pH 7.4. On day 7 and 14, HA-PLGA microspheres were found to have the lowest pH amongst all formulations investigated. As expected the acidic nature of HA does bring about a reduction in the pH of HA-PLGA over 15 days, as compared to other formulations. At day 21 and 28, there were no significant differences in pH profiles, suggesting that the pH was primarily determined by PLGA degradation products accumulated in the release media and not significantly altered by any residual BP. As expected, the poor solubility of CH lead to SC-PLGA and PLGA formulations having similar pH profiles. It is important to note that no major difference in pH was seen for all other formulations

(including PLGA microspheres without any BP), suggesting that the pH of release media is not significantly affected by the addition of BP over 28 days.

4.4.3 BP-PLGA Microsphere Formulations

BP-PLGA microspheres were prepared with HDS, LDS, CS, and HP, based on parameters used for formulating optimum HA-PLGA microspheres. The viscosity of the inner water phase obtained using these BP's was much lower, as compared to HA. Thus, it was possible to produce BP-PLGA formulation with high BP (% w/w) content.

To investigate the effect of BP content (% w/w) on formulations, HDS-PLGA and CS-PLGA microspheres were produced with ~ 2, 5, and 12 % w/w. As anticipated and established with HA formulations, addition of larger amounts of BP in the inner water phase impacted the uniformity of pore structure and the morphology of the microspheres, as observed by SEM. In case of HDS, the microspheres did not appear to differ much as its content increased, but for CS formulations with 12% were noted to have non-uniform pore structures.

4.4.4 Active Self Encapsulation of LYZ by BP-PLGA

4.4.4.1 Effect of BP content

To study the influence of BP content in formulations on LYZ encapsulation, CS-PLGA and HDS-PLGA microspheres were loaded from 10 mM phosphate solutions of LYZ (Table 4-1).

Table 4-1: Biomimetic self-microencapsulation capacity and efficiency of CS-PLGA and HDS-PLGA microspheres[3].

	BP	**LYZ Loading**	
	% (w/w)	**%(w/w)**	**% Loading Efficiency**
HDS	2	2.0 ± 0.04	100.0 ± 0.8
HDS	5.1	2.1 ± 0.08	100.0 ± 0.3
HDS	12.6	2.1 ± 0.02	100.0 ± .9
CS	2	1.8 ± 0.01	83 ± 0.8
CS	5.1	1.4 ± 0.01	68 ± 0.7
CS	12.6	2.0 ± 0.07	93 ± 2.4

[3] Microspheres were loaded from 0.5 ml of 1 mg/ml LYZ solutions in 10 mM phosphate buffer (pH 7)Theoretical content of $MgCO_3$ and trehalose was ~3 % w/w in the formulations. Data reported as mean ± SE, n = 3; total microsphere mass in loading solution was ~20 mg.

Across all HDS-PLGA formulations, almost all of the LYZ was encapsulated from the loading solution. In contrast, CS-PLGA microspheres were observed to have higher LYZ loading at 2 and 12 % (w/w), than at 5% CS. This suggests that even though it might be feasible to improve loading capacity of BP-PLGA microspheres by increasing BP content, there does not exist a simple linear relationship between % BP (w/w) and encapsulation of LYZ, in the range of formulations investigated. It is important to note that the formulations with high BP content had non-uniform pore structures, thus making them not ideal for further development.

As HDS formulations had absorbed all the LYZ in the previous study, it was decided to load ~10 mg of HDS-PLGA (2, 5.1 and 12.6 %w/w HDS) microspheres from 1 ml of 3 mg/ml and 0.5 ml of 6 mg/ml LYZ loading solutions (Table 4-2). A smaller amount of microspheres (~ 10 mg), were loaded with an excess of LYZ (3 mg), to also investigate the role of loading solution concentration at the same time. Loading was found to be higher at 6 mg/ml than at 3 mg/ml. The theoretical amount of LYZ bound to 1 mg of HDS increased with loading concentration. The data indicates that the maximum ASE capacity of HDS-PLGA microspheres increases with loading concentration of LYZ. Higher self-encapsulation was also seen with increasing HDS content, when loaded with an identical LYZ concentration. Overall, the low loading and encapsulation efficiency could be attributed to the HDS-PLGA having exceeded the protein binding capacity, as a smaller mass of microspheres was loaded with higher amount of protein.

Table 4-2: Self-microencapsulation capacity and efficiency of a small amount of ASE HDS-PLGA microspheres loaded with excess of LYZ from 10mM phosphate buffer (pH 7)[4].

HDS	Loading Solution		LYZ Encapsulation		LYZ bound
(% w/w)	Vol.(ml)	Conc.(mg/ml)	(% w/w)	Efficiency (%)	(mg/mg HDS)
2	1	3	1.3 ± 0.1	4.5 ± 0.1	0.66 ± 0.01
5.1	1	3	3.4 ± 0.4	13.5 ± 0.4	0.67 ± 0.03
12.6	1	3	3.4 ± 0.3	13.1 ± 0.2	0.28 ± 0.02
2	0.5	6	4.1 ± 0.01	13.7 ± 0.1	2.03 ± 0.04
5.1	0.5	6	6.2 ± 0.3	20.9 ± 0.5	1.26 ± 0.02
12.6	0.5	6	8.1 ± 0.2	27.1 ± 0.3	0.67 ± 0.03

[4] Theoretical content of $MgCO_3$ and trehalose was ~3 % w/w in the formulations. LYZ binding capacity was calculated using theoretical amount of HDS and LYZ in the loading solution. Data reported as mean ± SE, $n = 3$; total microsphere mass in loading solution was ~10 mg

4.4.4.2 Effect of LYZ Loading Concentration

Based on the binding curves (chapter 2) and formulation issues associated with high BP content as discussed above, 4% w/w BP-PLGA microspheres were identified to be suitable for > 2 % (w/w) protein loading. Approximately 20 mg of BP-PLGA were loaded from 0.5, 1, and 1.5 mg/ml LYZ solutions (Table 4-3). BP-PLGA ASE microspheres exhibited an excellent active protein loading capabilities and efficiencies. LDS formulations had the lowest loading efficiencies (and corresponding LYZ loading) among the BPs tested. This was in contrast to the binding ratio data from chapter 2, which had suggested that LDS might bring about high LYZ loading across a wide range of LDS:LYZ ratios. HDS, CS, and HP formulations had greater than 90% efficiency across all loading concentrations investigated. Most of the LYZ partitioned into the BP containing PLGA pores when LYZ concentration in the loading solution increased from 0.5 mg/ml to 1 mg/ml and 1.5 mg/ml (Table 4-3). This high loading capacity (~ 7 wt %) and efficiency (94-96%) was achieved at a lower BP:LYZ ratio in the loading solution. The loading was found to increase with the concentration of the loading solution in the range investigated; an excellent linear relationship was observed (Figure 4-4). Thus, the loading solution concentration could be used to obtain ASE formulations with desired protein content. It is important not to draw conclusions regarding the exact BP:LYZ ratio for high efficiency loading, as the data does not quantify the BP:LYZ in the internal pores of BP-PLGA microspheres.

Table 4-3: Self-microencapsulation capacity and efficiency of optimal ASE BP-PLGA microspheres loaded from 1 ml LYZ solutions in 10 mM phosphate buffer (pH 7) [5].

BP	Loading Solution Conc. (mg/ml)	LYZ Encapsulation (% w/w)	LYZ Encapsulation Efficiency (%)
HDS	0.5	2.2 ± 0.1	90 ± 0.1
HDS	1	4.6 ± 0.1	95 ± 0.2
HDS	1.5	7.0 ± 0.1	97 ± 0.1
LDS	0.5	1.5 ± 0.1	63 ± 2
LDS	1	4.1 ± 0.1	83 ± 2
LDS	1.5	6.8 ± 0.2	91 ± 1
CS	0.5	2.1 ± 0.1	89 ± 0.1
CS	1	4.5 ± 0.1	95 ± 0.3
CS	1.5	7.4 ± 0.1	97 ± 0.2
HP	0.5	2.2 ± 0.1	90 ± 0.3
HP	1	4.7 ± 0.2	94 ± 1
HP	1.5	7.3 ± 0.1	97 ± 0.1

[5] Theoretical content of $MgCO_3$, trehalose and BP was ~3, 3 and 4 % w/w in the formulations, respectively. Data reported as mean ± SE, n = 3; total microsphere mass in loading solution was ~20 mg.

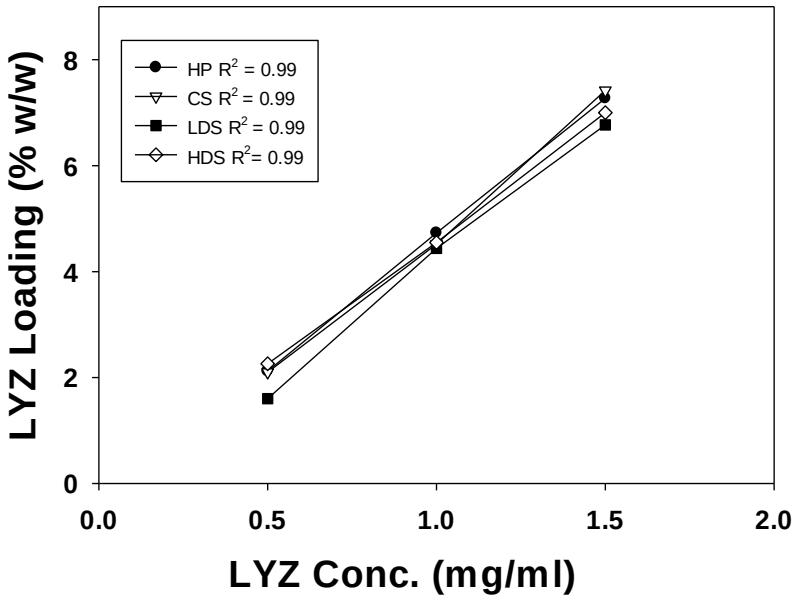

Figure 4-4 : A fit of the % w/w LYZ loading of optimal ASE BP-PLGA microspheres as a function of the LYZ loading concentration. Theoretical content of BPs, trehalose and $MgCO_3$ was ~ 4, 3 and 3 %w/w, respectively, in the formulations.

4.4.5 Distribution of Biomimetically ASE Cy5-LYZ in HDS(FITC)-PLGA microspheres

To visualize the distribution of BP and biomimetically encapsulated protein, we used FITC-HDS and Cy5-LYZ. In theory, the FITC-HDS would be uniformly distributed in the microspheres during the double emulsion manufacturing process. The evenly distributed BP would allow for uniform binding and loading of protein, which could allow for a slow and uniform controlled release.

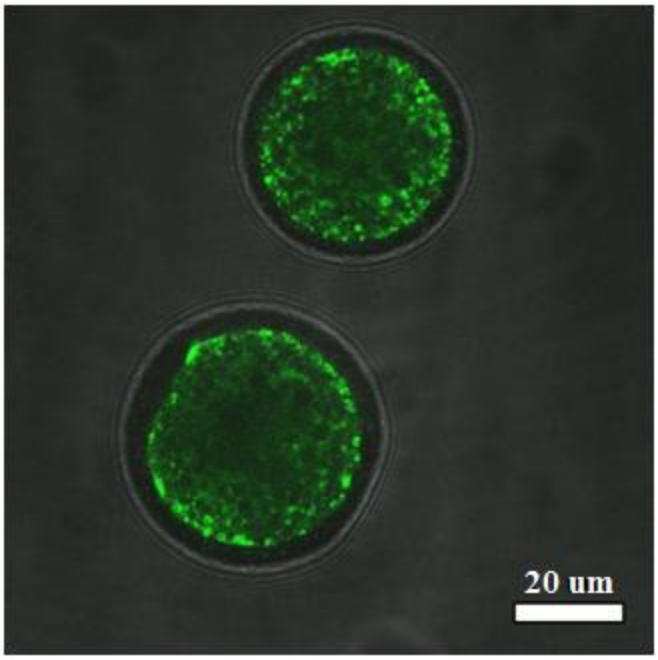

Figure 4-5 : Distribution of HDS(FITC) in microspheres.

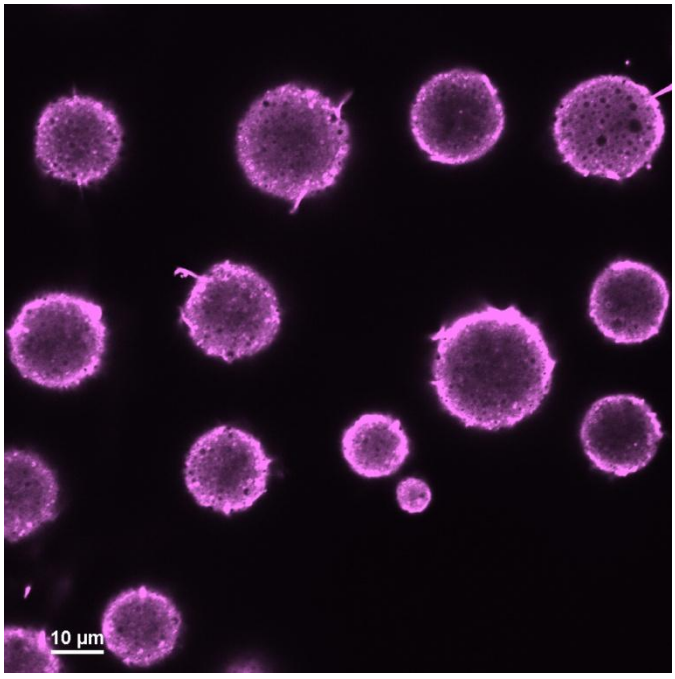

Figure 4-6 : Distribution of ASE Cy5-LYZ in HDS-PLGA microspheres loaded from 1ml of 1mg/ml Cy5-LYZ in 10 mM phosphate solution (pH 7).

Upon imaging the lyophilized FITC HDS-PLGA microspheres, FITC-HDS was unevenly distributed in the microspheres (Figure 4-5). It was pre-dominantly localized in the outer regions of the microspheres; the inner pores contained comparatively lower amounts. Similarly, larger amounts of Cy5-LYZ were found on the outer surface and regions of the biomimetically loaded ASE microspheres (Figure 4-6). Attempts to quantify the degree of overlap between FITC-HDS and Cy5-LYZ were limited due to issues associated with the use of FITC.

Volumetric images were generated by combining multiple images obtained at different focal lengths. The image shows that LYZ was able to enter the porous microsphere extensively, with greater distribution in the outer areas of the particle (Figure 4-7). This was expected, as during the loading process LYZ was diffusing into the microsphere from the liquid-microsphere interface, via the surface pores. Red domains indicate areas of high LYZ concentration near the surface of the HDS-PLGA microsphere. Ideally, uniform distribution of LYZ in the microsphere would allow for a long acting release formulation with slow continuous release, without a large burst release. This suggests that improving the distribution of the biomimetically ASE Cy5-LYZ could potentially improve first-order type release kinetics, as described below.

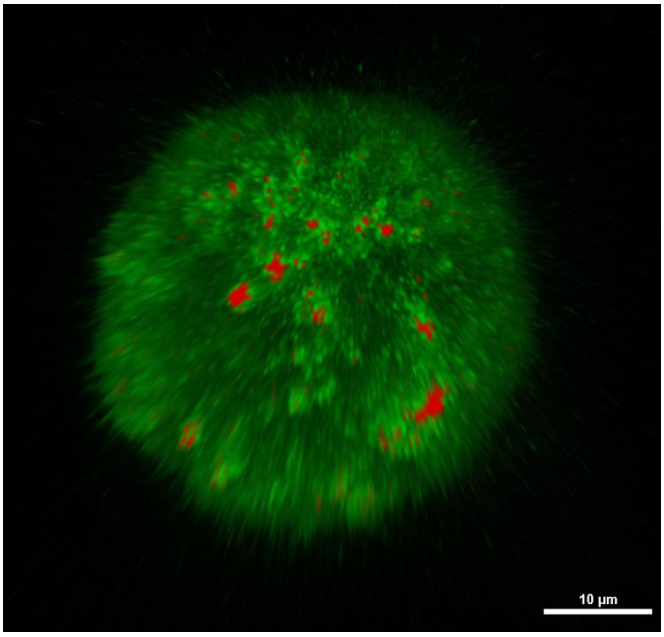

Figure 4-7 : Distribution of ASE Cy5-LYZ in HDS-PLGA microsphere. Volumetric image was obtained by combining images taken at different heights. Red regions indicate regions of very high concentration of Cy5-LYZ.

4.4.6 Release Kinetics of LYZ from BP-PLGA Microspheres

The release kinetics of biomimetically encapsulated LYZ from sulfated BP-PLGA microspheres was initially investigated in 1 ml PBS at pH 7.4 (Figure 4-8). PBS was used to avoid initial complications associated with LYZ quantification, due to overlap of Tween 80 and LYZ peaks during SE-HPLC analysis.

4.4.6.1 Effect of LYZ Loading Concentration

Across all formulations, the cumulative release plateaued at around day 7 and increased after 28 days of release (Figure 4-8). The first stage of this two-phase release would be expected to be driven by diffusion of the LYZ, which was either poorly encapsulated or released from the microsphere prior to healing of newly formed pores created during drying or initial hydration of the microspheres. After this initial phase, continuous release could be sustained by the presence of the $MgCO_3$ excipient, which reacts with the degradation products to create osmotic pressure and new pores in the polymer matrix. The kinetics is also likely governed by the BP-LYZ interactions and the movement of complexes and soluble LYZ, through the pore network.

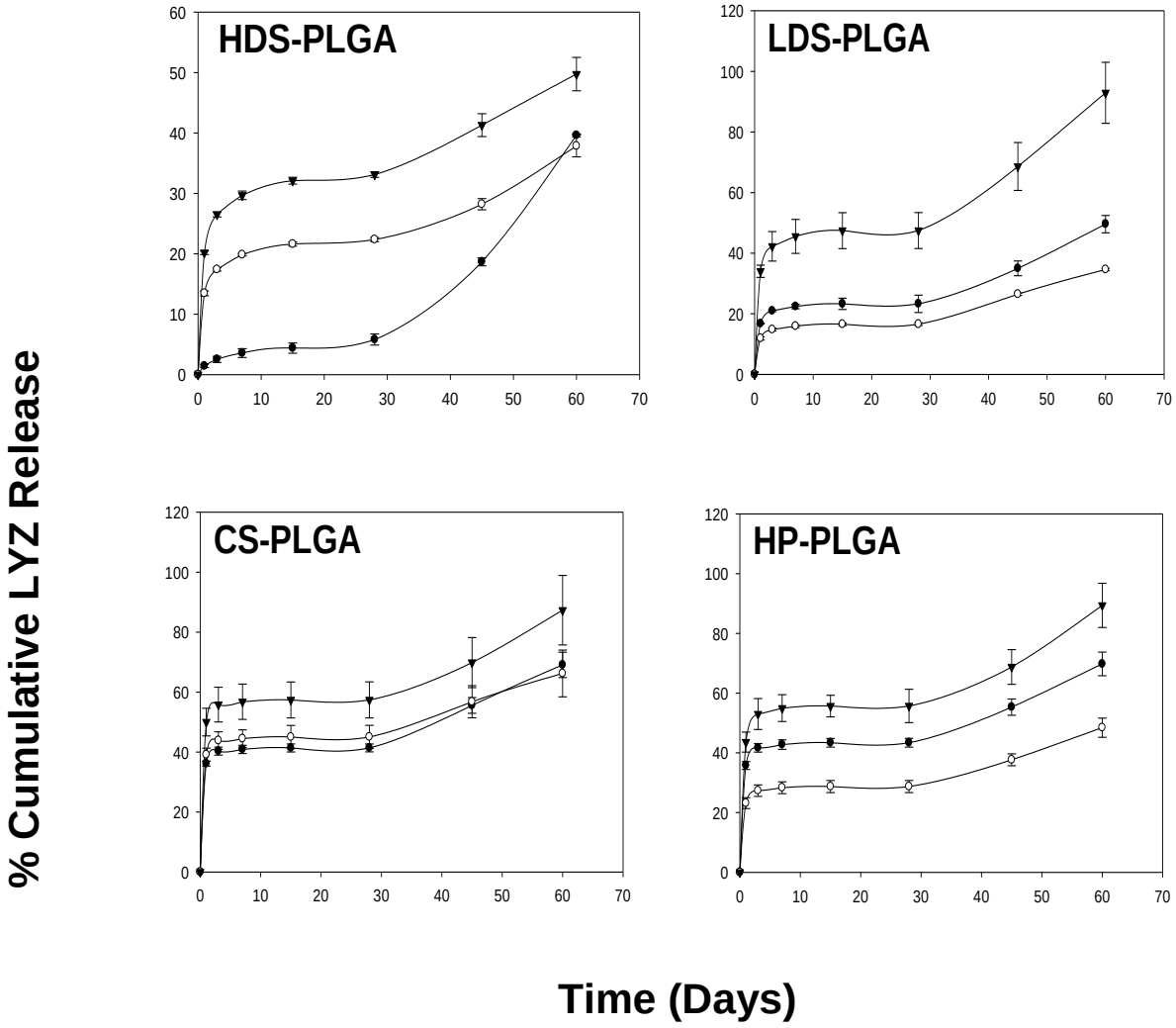

Figure 4-8 : LYZ release profiles in 1 ml PBS (pH 7.4) at 37 °C quantified by SE-HPLC at 282 nm. ASE BP-PLGA microspheres were loaded from LYZ in 10 mM phosphate buffer at concentrations of 0.5(—●—), 1(—○—) and 1.5(—▼—) mg/ml. The values are expressed as mean ± SD n=3; total microsphere mass in release media was ~ 18 mg.

BP-PLGA microspheres loaded with 1.5 mg/ml LYZ had the highest rate of release and extent (≈ 80%) of the self-encapsulated LYZ for all BP-PLGA microspheres, except HDS-PLGA. Overall, HDS-PLGA microspheres had some of the lowest burst release, as well as rate and extent of long-term release. They were noted to release ~ 35-45 % of the

encapsulated LYZ. Whereas, LDS-PLGA formulations exhibited a higher rate and extent of release when compared to HDS loaded at 1.5 mg/ml LYZ. LDS-PLGA formulations loaded from 0.5 and 1 mg/ml LZY solutions released ~ 28-40 % LYZ. CS-PLGA formulations had the highest burst release (> 40 %) across the sulfated BP-PLGA microspheres investigated. They were observed to release ~ 60-80 % of the encapsulated LYZ over 60 days. HP-PLGA formulations were also observed to have very high burst release, and released ~ 60-80 % of the LYZ.

4.4.6.2 Effect of Ionic Strength

To evaluate the role of BP-LYZ interactions on release kinetics, the ionic strength of the release media was varied. *In-vitro* release of LYZ loaded BP-PLGA microspheres were quantified in 1ml of PBS+0.3 M NaCl and PBS+0.6 M NaCl. Due to the electrostatic component of the BP-Protein interaction, the rate and extent of LYZ released was expected to increase with ionic strength of the release media. This was verified, as the rate and extent of LYZ release was found to increase across all ASE formulations, with increasing ionic strength. This suggests that the ionic interaction played an important role in determining the protein release. The solubility of lysozyme has been shown to slightly increase with increasing NaCl concentration, which is in the middle of the Hofmeister series [16]. Thus, it is unlikely that the progressively increasing amount of lysozyme release with the NaCl concentration was due to a salting-in effect exerted to lysozyme solubility within the microspheres. It is also noted that the increase of the salt

concentration in the medium slowed down polymer degradation [17]. Park *et al.* have shown that LYZ *in-vitro* release kinetics are influenced by presence of NaCl, suggesting that the NaCl disrupts the ionic interactions between PLGA and protein [18]. Lee *et al.* have also reported similar effects of ionic strength on release of BSA and histone [19]. Thus, it is highly probable that the faster lysozyme release due to NaCl for BP-PLGA microspheres cannot be only attributed to the disruption of ionic interaction between lysozyme and PLGA, but also due to unraveling of BP-LYZ complexes, as previously shown (Figure 2-3,Figure 2-4 and Figure 2-5).

Upon examining [LYZ released/mass of BP-PLGA microspheres] versus time, the amount and rate of LYZ release increased with ionic strength across all ASE formulations. No significant differences were seen in the rate of release amongst the LDS-PLGA, HP-PLGA and CS-PLGA microspheres loaded with different concentrations of LYZ in PBS, PBS+0.3M NaCl and PBS+0.6M NaCl. In PBS, clear differences were seen in the rate of LYZ released amongst the HDS-PLGA microspheres loaded with different LYZ concentrations (Figure 4-9). The rate decreases with the decreasing LYZ loading solution concentration, suggesting that the HDS:LYZ ratio during loading is indeed an important variable governing LYZ release kinetics.

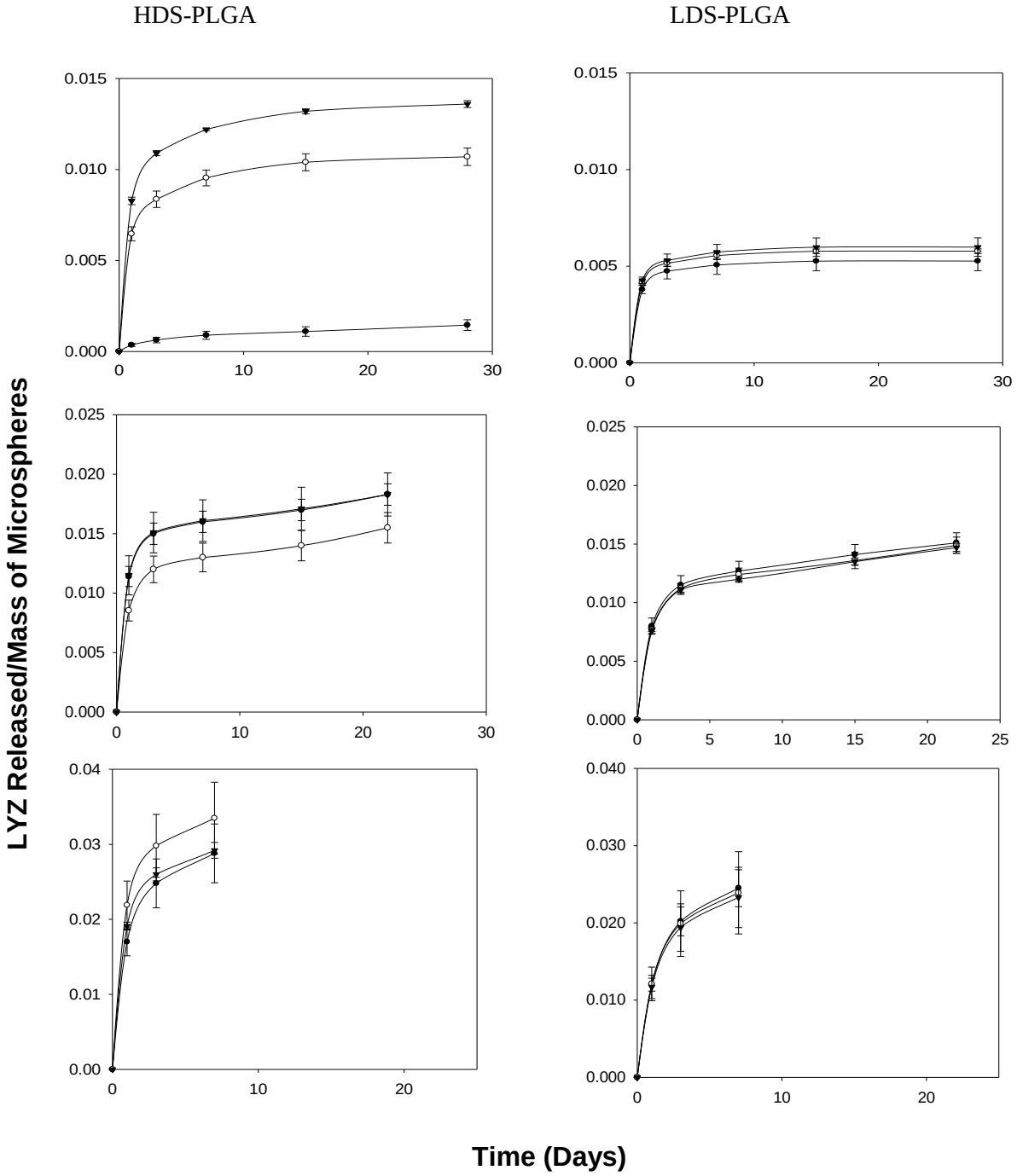

Figure 4-9 : Representative plots showing the effect of ionic strength on LYZ release in 1 ml PBS (pH 7.4) at 37 °C. Trends similar to LDS-PLGA were observed for CS-PLGA and HP-PLGA. LYZ quantified by SE-HPLC at 282 nm. ASE BP-PLGA microspheres were loaded from 10 mM Phosphate (pH 7) LYZ loading solutions with conc. of 0.5(─●─), 1(─○─) and 1.5(─▼─) mg/ml. The values are expressed as mean ± SE; n = 3; total microsphere mass in release media was ≈ 18 mg. (Top row): Release in PBS. (Middle row) Release in PBS + 0.3M NaCl. (Bottom row) Release in PBS + 0.6 M NaCl.

4.4.6.3 Effect of Release Volume

To study the effect of volume on kinetics of release, LDS-PLGA microspheres loaded with ≈ 2% w/w LYZ solution were incubated in PBS at pH 7.4 over a range of volumes (0.5 – 20 ml), with the LYZ release being quantified by SE-UPLC. The rate and extent of LYZ release from LDS-PLGA was found to increase as the volume of release was increased from 0.5 ml to 5ml (Figure 4-10). LYZ release from LDS-PLGA microspheres over 60 days was ~ 40, 68, and 85 % for 1 ml, 3 ml and 5 ml, respectively. LYZ release in 10, 15, and 20 ml was also quantified up to 3 days, beyond which the LYZ concentration in the release media could not be detected by SE-UPLC. Upon comparing the LYZ release in 5, 10, 15 and 20 ml, no significant differences were seen. This suggests that sink conditions were attained at and above 5 ml of PBS for ≈ 18 mg of LYZ loaded LDS-PLGA microspheres. This effect of volume should be considered while estimating release kinetics during *in-vitro* experiments

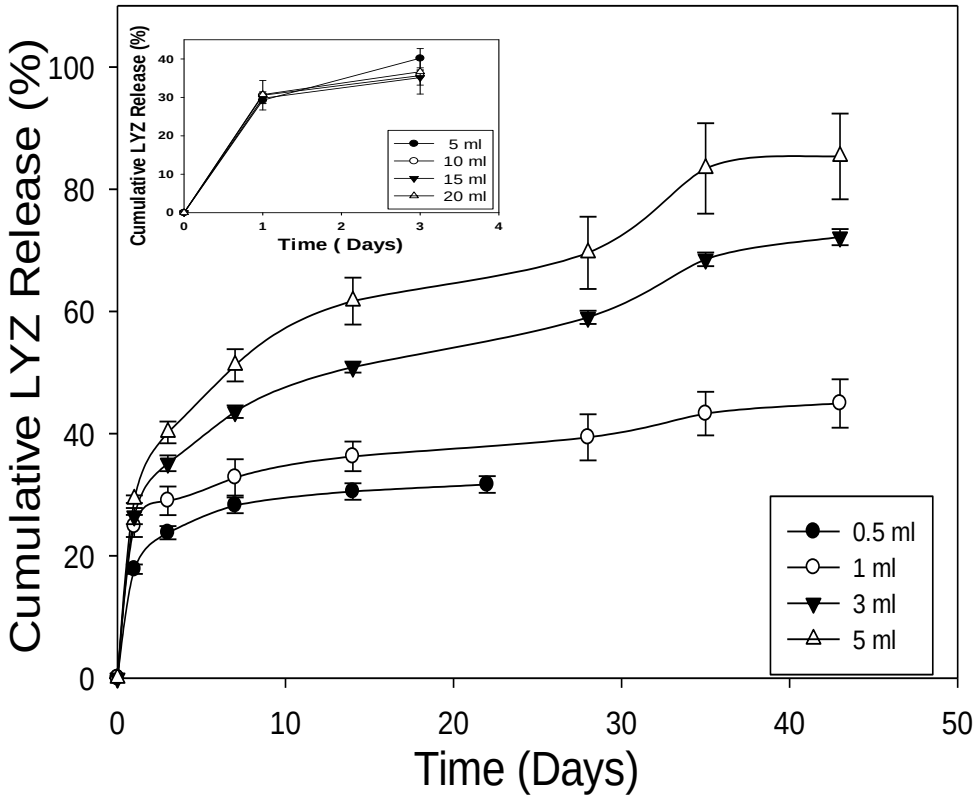

Figure 4-10 : LYZ release profiles from LDS-PLGA microspheres in PBS (pH 7.4) at 37 °C, quantified by SE-UPLC at 282 nm, as a function of release media volume. Microspheres were loaded from 1 mg/ml LYZ in 10 mM phosphate buffer (pH 7). The values are expressed as mean ± SE; n=3; microsphere mass in release media was ~ 18 mg. Insert - Release in high volume was not feasible beyond 3 days due to poor quantification of protein at very low concentration via SE-UPLC.

This effect of volume on release kinetics has not been reported in the literature, to the best of our knowledge. We initially hypothesized the effect could possible due to the solubility of BP-LYZ complexes inside the PLGA microspheres. This dissolution of the complex would be expected to increase as the volume is increased, allowing the free LYZ to leach out of the microspheres, as the volume is increased upto the level of sink conditions.

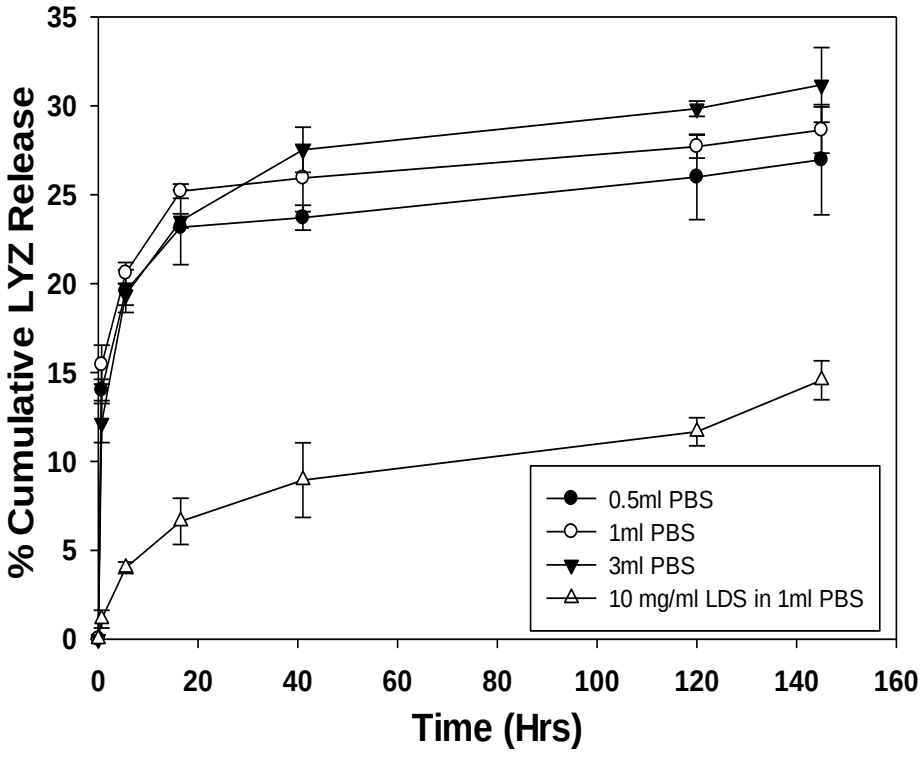

Figure 4-11 : LYZ release profiles from LDS-LYZ complexes in PBS (pH 7.4) at 37 °C, quantified by SE-UPLC at 282 nm, as a function of release media volume. The values are expressed as m as mean ± SE; n=3; mass of complexes in release media was ~ 4 mg.

To check the validity of the hypothesis, release kinetics of LDS-LYZ complexes were investigated at 0.5 ml, 1 ml, and 3 ml (Figure 4-11). The complexes were seen to release ~ 30 % of the LYZ over 140 h. Contrary to our hypothesis, no significant differences were seen in the release kinetics of LYZ amongst the 3 volume investigated. In addition, to investigate the effect of free LDS on release kinetics, LYZ release studied in PBS + 10 mg/ml LDS. As expected, LDS slowed down the release of LYZ, possible due to its ability to bind and precipitate LYZ from solution. LYZ release in PBS + LDS was only ~ 12 %, in comparison to nearly ~ 30 % in PBS.

4.4.6.4 Release Kinetics of LYZ in Optimized Release Media Volume

From our data, we identified HDS-PLGA formulations to be ideal for evaluating controlled release formulations as they consistently have amongst the highest loading (and encapsulation efficiency) and the lowest burst release of all formulations investigated. The HDS-LYZ complexes also had shown excellent release characteristics to be used for developing long-acting-release formulations (Figure 2-2). The data further suggests that the rate of release could be adjusted by changing the HDS:protein ratio during ASE. In addition, the high M_w of HDS should minimize any potential leaching and complications during ASE of proteins.

Based upon the release data above, ~ 18 mg of HDS-PLGA (loaded with 1 ml and 1.5 mg/ml LYZ) formulations were incubated in 5 ml PBST to evaluate LYZ release kinetics and activity of released LYZ (Figure 4-12). It was not feasible to use a higher release volume as released LYZ concentrations would be too low to be quantified using SE-UPLC beyond 3 days of release. HDS-PLGA formulations loaded with 1.5 mg/ml were found to have good release kinetics with ~ 60% released over 21 days. The remaining protein was gradually released over the period monitored, leading to ~ 73-80% of encapsulated protein being released over 55 days. The average activity of the released LYZ was found be > 90 % during the entire course of release experiment.

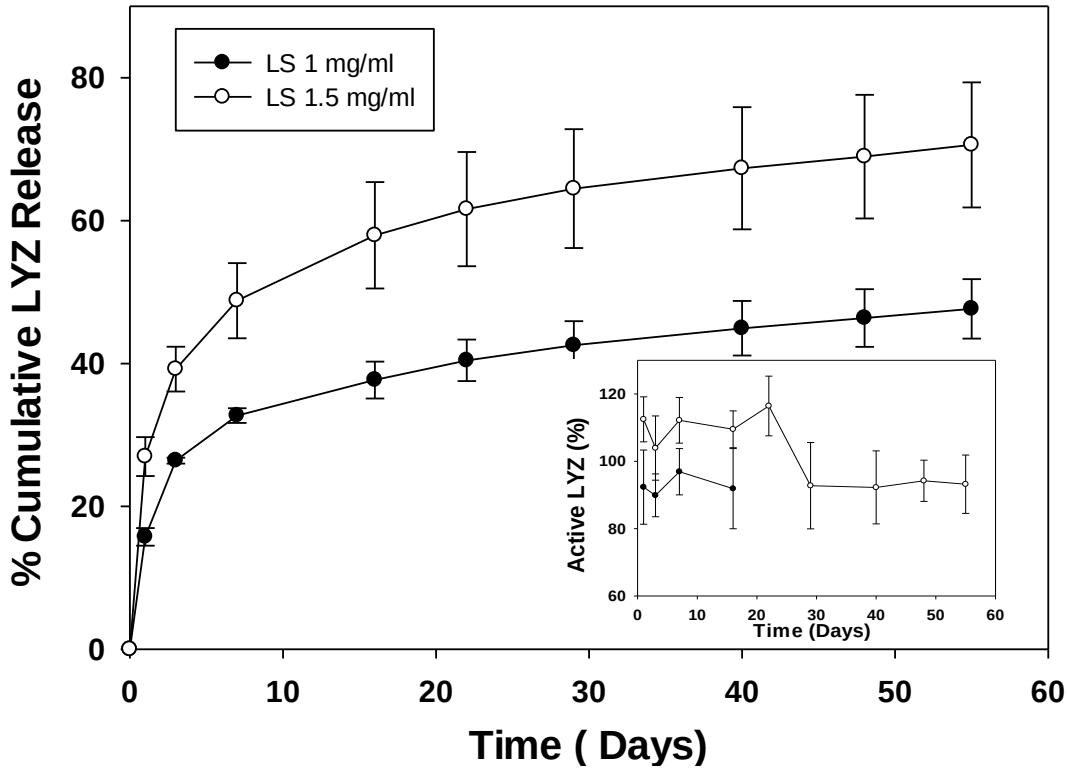

Figure 4-12 : LYZ release profiles in PBST (PBS with 0.02% Tween 80) quantified by SE-UPLC at 282 nm. ASE HDS-PLGA microspheres were loaded from 1.5 mg/ml LYZ in 10 mM phosphate buffer (pH 7). The values are expressed as mean ± SE; n = 3; microsphere mass in solution was ~ 18 mg.

Whereas, the formulations loaded with 1 mg/ml LYZ were found to have comparatively slower LYZ release kinetics. Over 21 days, ~ 38 % of the encapsulated LYZ was released after which the release slowed down to release ~ 48 % of the LYZ in 55 days. The average activity of the released LYZ was ~ 90 % over 14 days. The data clearly demonstrates the role of loading solution concentration in governing LYZ release kinetics of LYZ form HDS-PPLGA microspheres, with higher concentration leading to faster release kinetics.

4.4.7 Active Self Encapsulation of growth factors by BP-PLGA

Based upon the success of encapsulating LYZ in sulfated BP-PLGA microspheres via ASE, the feasibility of the biomimetic paradigm was verified by the encapsulation of recombinant human FgF-20 and VEGF165 (Table 4-4). Loading efficiencies of >80% with ~2% (w/w) were obtained for FgF-20, across all the BP formulations analyzed. These results are very encouraging as encapsulation was achieved in presence of 0.5 M Arg in loading solution to overcome solubility and stability issues associated with FgF-20. Upon biomimetic ASE of VEGF by HDS-PLGA microspheres, ~ 4% (w/w) loading was obtained with nearly 75% efficiency. This was achieved in presence of 275 mM trehalose, to improve stability of the VEGF during the loading and incubation.

Table 4-4: Biomimetic ASE of growth factors in BP-PLGA microspheres[6]

BP	Loading Solution	Loading (% w/w)	Encapsulation Efficiency (%)
HDS	0.5 mg/ml FgF-20	2.3 + 0.1	87 + 1
LDS	0.5 mg/ml FgF-20	2.1 ± 0.1	84 ± 1
CS	0.5 mg/ml FgF-20	1.9 ± 0.2	85 ± 2
HP	0.5 mg/ml FgF-20	2.1 ± 0.1	81 ± 1
HDS	1 mg/ml VEGF	4.1 ± 0.4	73 ± 6

[6] Theoretical content of $MgCO_3$, trehalose and BP was ~3, 3 and 4 % w/w in the formulations, respectively. ASE of FgF-20 was from 1ml of 0.5 mg/ml FGF-20 loading solution (0.5M arginine, 0.05 M sodium phosphate and 0.08% polysorbate). ASE of VEGF in HDS-PLGA microspheres was from 1ml of 1 mg/ml VEGF loading solution (5 mM succinate buffer, 275 mM trehalose and 0.01% polysorbate 20). Mean ± SE, n = 3; total microsphere mass in loading solution was ~20 mg.

4.4.7.1 Release kinetics of VEGF from HDS-PLGA microspheres

The release kinetics of VEGF loaded HDS-PLGA was evaluated in 5 ml PBST + 1% BSA, with full media replacement (Figure 4-11). BSA was added in the release media to improve stability of released VEGF and prevent non-specific adsorption to the release vessel [20]. Over 42 days, nearly 72 % of encapsulated VEGF was released in an immunoactive form. The released VEGF retained its ability to bind to heparin (> 92 % relative to immunoreactive VEGF over 23 days), consistent with retaining a very high fraction of the growth factor's native structure during long-term release. The release kinetics were found to be slightly faster when compared to LYZ, which could have resulted from the presence of 275 mM trehalose and 10 mg/ml BSA in the external loading solution, which reasonably could affect the VEGF-HDS interaction. Release kinetics of FgF-20 was not characterized because of the lack of a suitable release assay for a viable release media.

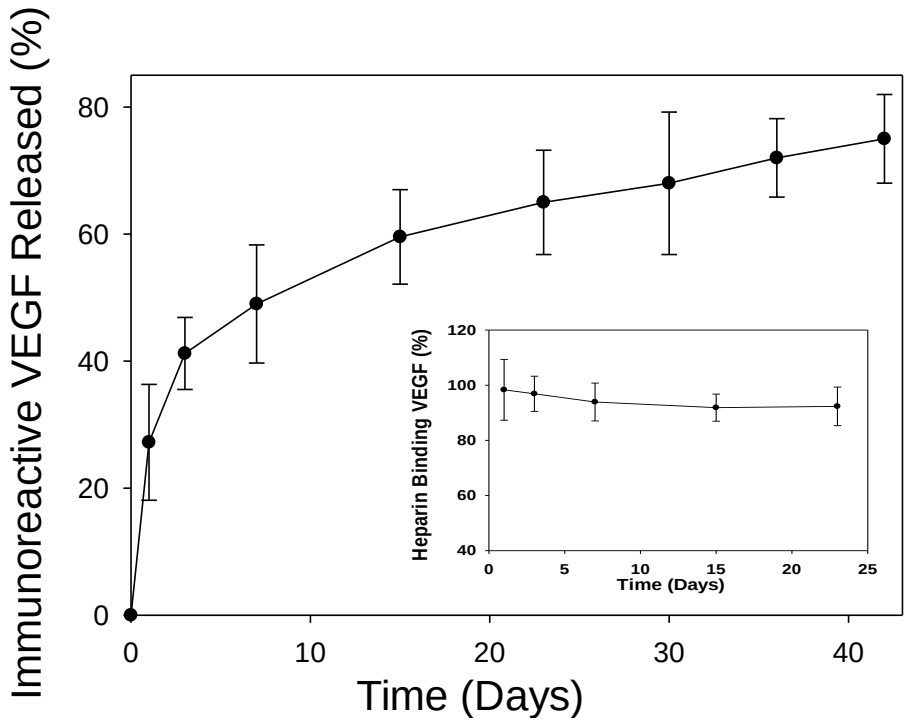

Figure 4-13 : VEGF release profile from HDS-PLGA microspheres in 5 ml PBST (pH 7.4 with 1% BSA), were quantified using ELISA. ASE HDS-PLGA microspheres were loaded from 1 ml of 1.0 mg/ml VEGF solution (5 mM succinate bufer, 275 mM trehalose and 0.01% polysorbate 20).

4.4.8 Efforts to improve LYZ release profile

In an effort to improve protein stability, our research group has tested a number of basic salts to control the pH and prevent aggregation of protein inside PLGA [21, 22]. During the process, the choice of base and content was also found to influence the release kinetics of the encapsulated protein. Increasing base content was found to be an effective means of increasing rate and total amount of release. Use of base with higher solubility was found to improve water uptake in the PLGA matrix, allowing for faster protein release. On comparing $Mg(OH)_2$, $MgCO_3$, $ZnCO_3$, and $Ca_3(PO_4)_2$; $Mg(OH)_2$ was found to perform poorly in PLGA microspheres due to its poor solubility whereas, $MgCO_3$ was

identified to be much better at controlling the microclimate [21]. $ZnCO_3$ and $Ca_3(PO_4)_2$ are comparatively weaker bases, which can potentially lead to higher non-covalent aggregates as compared to $Mg(OH)_2$ [22]. PLGA millicylinders with $ZnCO_3$ were found to have faster BSA release kinetics when compared to $Ca_3(PO_4)_2$. Thus, to improve the release characteristics of biomimetically ASE LYZ from HDS-PLGA microspheres, formulations with $ZnCO_3$ and $MgCO_3$ were evaluated. These microspheres were prepared with a new batch of polymer and were found to have different pore closing properties, than all formulations discussed above and in earlier chapters. Increasing the base content, as discussed above, could potentially allow for a better release profile with a slow continuous release and a less pronounced lag phase.

The microspheres were loaded with 1 mg/ml LYZ in phosphate buffer (pH 7) (Table 4-5). Microspheres with $MgCO_3$ encapsulated most of the LYZ from the solution; whereas formulation with higher $ZnCO_3$ content was more efficient at encapsulating LYZ. This could probably be related to the improved pore structure seen with higher base content.

Table 4-5: Biomimetic ASE of LYZ in HDS-PLGA microspheres[7]

BP	Base	LYZ Loading	
	(%w/w)	(% w/w)	Encapsulation
HDS	3.1 % $MgCO_3$	4.4 ± 0.1	99.6 ± 0.05
HDS	7.7 % $MgCO_3$	4.57 ± 0.3	99.7 ± 0.01
HDS	3.1 % $ZnCO_3$	4.14 ± 0.1	89.4 ± 0.8
HDS	8.3 % $ZnCO_3$	4.5 ± 0.2	99.9 ± 0.02

Release kinetics were evaulted in 5 ml PBST (pH 7.4) at 37 °C, with complete media repalcement (Figure 4-14). Over 24 days, formulations with $MgCO_3$ released ~ 14-16 % of the encapsulted LYZ. Slight differences in release profile could be observed with varying base content, but no significant conclusions can be drawn from the data. LYZ release profile from formulations with 3.1 and 8.3 % (w/w) $ZnCO_3$ were nearly identiocal over 24 days. Overall, formaultions with $MgCO_3$ were observed to have a faster rate and extent of release over the time period of the experiment.

[7] Theoretical content of trehalose and BP was ~ 3 and 4 % w/w in the formulations, respectively. HDS-PLGA microspheres were loaded from 1 mg/ml LYZ in 10 mM phosphate buffer (pH 7).Data reported as mean ± SE, *n* = 3; total microsphere mass in loading solution was ~25 mg.

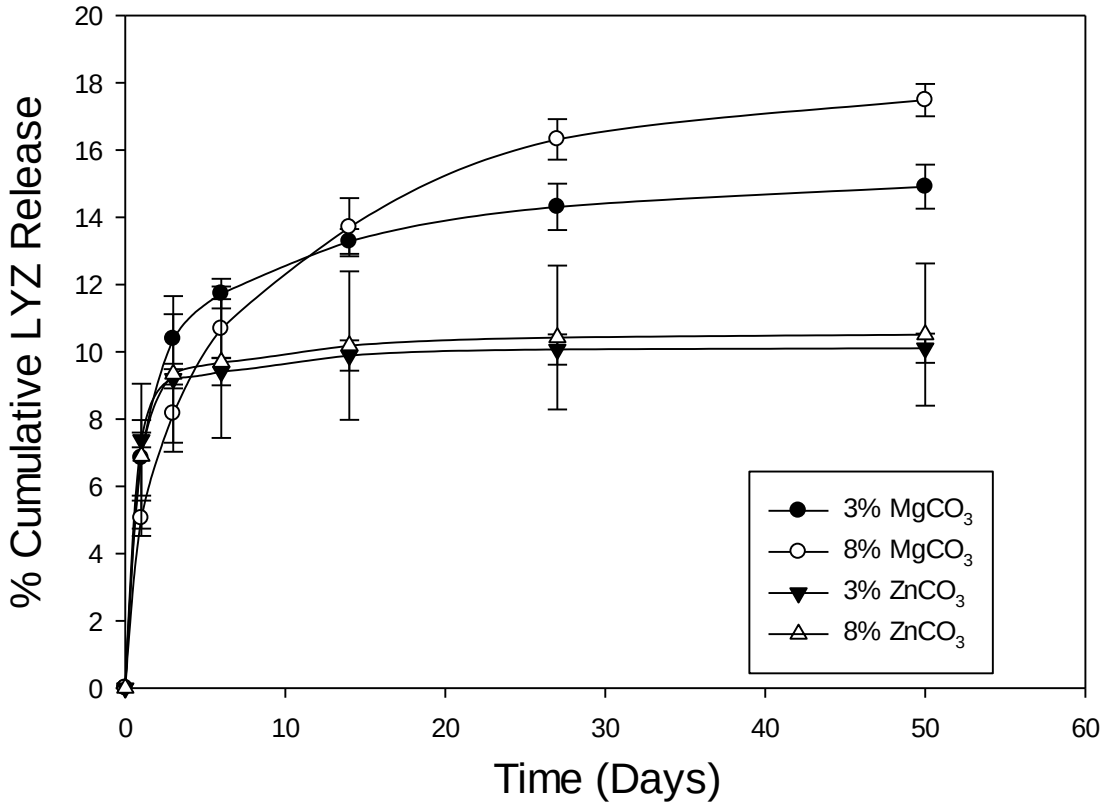

Figure 4-14 : LYZ release profiles in PBST (PBS with 0.02% Tween 80) quantified by SE-UPLC at 282 nm. ASE HDS-PLGA microspheres were loaded from 1ml of 1mg/ml LYZ in 10 mM phosphate buffer (pH 7). The values are expressed as mean ± SE; n = 3; microsphere mass in solution

The release kinetics of LYZ from HDS-PLGA microspheres made from the new batch of polymer was found to be slower than microspheres made with the older batch of PLGA. This highlights one of the major issues in the field, namely the change in properties of the polymer with every batch of PLGA.

4.5 Conclusions

The biomimetic paradigm provided excellent LYZ, VEGF165 and FgF-20 loading, encapsulation efficiency and potential for long-term release. ASE of LYZ could be achieved at ~ 7 % (w/w) with ~ 97 % encapsulation efficiency. This high efficiency of loading is remarkable for a loading mechanism primarily driven by diffusion. Subsequently, we were able to demonstrate excellent release profile and stability over 60 days, of the LYZ released form biomimetically ASE BP-PLGA microspheres.

The ~ 4 % w/w loading of VEGF achieved by ASE is significantly higher [23-25], than the literature where the VEGF was included in the first emulsion, during the preparation of PLGA particles. The encapsulation efficiency is also higher than reported in most cases [26-28]. This is significant as our methodology allows the protein to be loaded after the formation of the PLGA microparticle, protecting it from harsh conditions and processes associated with manufacturing. The release kinetics reported here are comparable to the literature with ≈ 70 % of immunoreactive VEGF released over 30 days with excellent stability and without significant losses to heparin binding affinity, making it a promising delivery system. LYZ release from PLGA has been studied extensively, and it is reported to suffer from stability issues when encapsulated with traditional paradigms [18, 29-31]. In our work, we were able to demonstrate high LYZ loading and encapsulation efficiency with excellent release profile and stability over 60 days. Thus, our data demonstrates the potential for using biomimetic ASE for developing long-acting-release products for protein delivery.

4.6 References

1. Buse, J.B., et al., *DURATION-1: Exenatide Once Weekly Produces Sustained Glycemic Control and Weight Loss Over 52 Weeks.* Diabetes Care, 2010. **33**(6): p. 1255-1261.
2. Harris, J.M. and R.B. Chess, *Effect of pegylation on pharmaceuticals.* Nat Rev Drug Discov, 2003. **2**(3): p. 214-221.
3. GSK, *GSK receives US approval for once-weekly type 2 diabetes treatment, Tanzeum™ (albiglutide)*, 2014, GSK: London UK
4. Jiang, X.R., et al., *Advances in the assessment and control of the effector functions of therapeutic antibodies.* Nature Reviews Drug Discovery, 2011. **10**(2): p. 101-110.
5. *Victoza(R) [package insert].Novo Nordisk.* . [cited 2014 5/10/2104].
6. Golub, J.S., et al., *Sustained VEGF delivery via PLGA nanoparticles promotes vascular growth*. Vol. 298. 2010. H1959-H1965.
7. Yoon, Y.-s., et al., *Therapeutic myocardial angiogenesis with vascular endothelial growth factors.* Molecular and Cellular Biochemistry, 2005. **264**(1): p. 63-74.
8. Banfi, A., P. Fueglistaler, and R. Gianni-Barrera, *The Maturation of Vessels – A Limitation to Forced Neovascularization?* 2007. p. 139-158.
9. Allison, S.D., *Analysis of initial burst in PLGA microparticles.* Expert Opin Drug Deliv, 2008. **5**(6): p. 615-28.
10. Schwendeman, S.P., *Recent advances in the stabilization of proteins encapsulated in injectable PLGA delivery systems.* Critical Reviews in Therapeutic Drug Carrier Systems, 2002. **19**(1): p. 73-98.
11. Schwendeman, S.P., et al., *Injectable controlled release depots for large molecules.* Journal of Controlled Release, 2014. **190**(0): p. 240-253.
12. Schwendeman SP, C.M., Brandon MR, Klibanov A, Langer R., *Stability of proteins and their delivery from biodegradable polymer microspheres.*, in *Microparticulate systems for the delivery of proteins and vaccines*, B.H. Cohen S, Editor. 1996: New York. p. 1-49.
13. Wu, F. and T. Jin, *Polymer-based sustained-release dosage forms for protein drugs, challenges, and recent advances.* AAPS PharmSciTech, 2008. **9**(4): p. 1218-1229.
14. Carpenter, J.F., et al., *Rational Design of Stable Lyophilized Protein Formulations: Some Practical Advice.* Pharmaceutical Research, 1997. **14**(8): p. 969-975.
15. Reinhold, S., *Self-healing polymers microencapsulate biomacromolecules without organic solvents*, 2009, University of Michigan.
16. Arakawa, T. and S.N. Timasheff, *Theory of protein solubility*, in *Methods in Enzymology*, C.H.W.H.S.N.T. Harold W. Wyckoff, Editor. 1985, Academic Press. p. 49-77.

17. Makino, K., H. Ohshima, and T. Kondo, *Mechanism of hydrolytic degradation of poly(L-lactide) microcapsules: effects of pH, ionic strength and buffer concentration.* Journal of Microencapsulation, 1986. **3**(3): p. 203-212.
18. Park, T.G., H. Yong Lee, and Y. Sung Nam, *A new preparation method for protein loaded poly(d,l-lactic-co-glycolic acid) microspheres and protein release mechanism study.* Journal of Controlled Release, 1998. **55**(2–3): p. 181-191.
19. Lee, M., et al., *Modulation of protein delivery from modular polymer scaffolds.* Biomaterials, 2007. **28**(10): p. 1862-1870.
20. Zhang, L., *Controlled Release of Angiogenic Growth Factors from Poly(Lactic-Co-Glycolic Acid) Implants for Therapeutic Angiogenesis*. 2009.
21. Zhu, G., S.R. Mallery, and S.P. Schwendeman, *Stabilization of proteins encapsulated in injectable poly (lactide- co-glycolide).* Nat Biotech, 2000. **18**(1): p. 52-57.
22. Zhu, G. and S. Schwendeman, *Stabilization of Proteins Encapsulated in Cylindrical Poly(lactide-co-glycolide) Implants: Mechanism of Stabilization by Basic Additives.* Pharmaceutical Research, 2000. **17**(3): p. 351-357.
23. Ferreira, L.S., et al., *Bioactive hydrogel scaffolds for controllable vascular differentiation of human embryonic stem cells.* Biomaterials, 2007. **28**(17): p. 2706-2717.
24. Formiga, F.R., et al., *Sustained release of VEGF through PLGA microparticles improves vasculogenesis and tissue remodeling in an acute myocardial ischemia–reperfusion model.* Journal of Controlled Release, 2010. **147**(1): p. 30-37.
25. Borselli, C., et al., *Bioactivation of collagen matrices through sustained VEGF release from PLGA microspheres.* Journal of Biomedical Materials Research Part A, 2010. **92A**(1): p. 94-102.
26. Karal-Yılmaz, O., et al., *Preparation and in vitro characterization of vascular endothelial growth factor (VEGF)-loaded poly(D,L-lactic-co-glycolic acid) microspheres using a double emulsion/solvent evaporation technique.* Journal of Microencapsulation, 2011. **28**(1): p. 46-54.
27. Ennett, A.B., D. Kaigler, and D.J. Mooney, *Temporally regulated delivery of VEGF in vitro and in vivo.* Journal of Biomedical Materials Research Part A, 2006. **79A**(1): p. 176-184.
28. King, T.W. and C.W. Patrick, *Development and in vitro characterization of vascular endothelial growth factor (VEGF)-loaded poly(DL-lactic-co-glycolic acid)/poly(ethylene glycol) microspheres using a solid encapsulation/single emulsion/solvent extraction technique.* Journal of Biomedical Materials Research, 2000. **51**(3): p. 383-390.
29. Jiang, G., et al., *Assessment of protein release kinetics, stability and protein polymer interaction of lysozyme encapsulated poly(d,l-lactide-co-glycolide) microspheres.* Journal of Controlled Release, 2002. **79**(1–3): p. 137-145.
30. van de Weert, M., et al., *The effect of a water/organic solvent interface on the structural stability of lysozyme.* Journal of Controlled Release, 2000. **68**(3): p. 351-359.

31. Diwan, M. and T.G. Park, *Pegylation enhances protein stability during encapsulation in PLGA microspheres.* Journal of Controlled Release, 2001. **73**(2–3): p. 233-244.

CHAPTER 5 PROTEIN-BIOPOLYMER INTERACTIONS

5.1 Abstract

Aggregation and stability of biologics are two of the major hurdles impeding development of injectable protein formulations. In this chapter, we explored the potential of using biopolymers [high molecular weight dextran sulfate (HDS), low molecular weight dextran sulfate (LDS), chondroitin sulfate (CS), and heparin (HP)] as stabilizing agents for the development of pharmaceutical formulations of proteins [lysozyme (LYZ), human growth hormone (hgH), vascular endothelial growth factor165 (VEGF) and fibroblast growth factor (FgF-20)]. Using circular dichroism, isothermal titration calorimetry, differential scanning calorimetry, and intrinsic fluorescence, we compared the protein-biopolymer interactions to commonly used polyions like phytic acid (PA) and sucrose octasulfate (SO). LYZ-BP interactions were found to be enthalpically driven, with a Gibbs free energy of ~ 30-40 kJ/mol. BPs were found to change the secondary structure of LYZ. Thermal melts of LYZ were also analyzed in the presence of BPs. BPs were also observed to reduce the apparent T_m of LYZ and hgH in solution. Thus, the data suggests that suitably selected BP could potentially be used to formulate proteins, which tend to aggregate and self-associate.

5.2 Introduction

Biologics are rapidly emerging as a major class of drug products with expected sales of nearly $200 billion by 2017, representing 19-20% of total market value [1]. Proteins, antibodies and vaccines account for a total sales of ~ $108 billion in 2012, with 29 blockbusters amongst their ranks [1, 2]. In addition, increasing healthcare costs make it essential to develop inexpensive yet robust formulations, especially with the expected growth of biosimilars in the near future. A number of challenges associated with formulation development need to be addressed for this to happen. Stability and aggregation of biologics in solution is one of the major challenges being faced during production and storage of injectable biologics [3, 4]. Aggregation causes not only loss of therapeutic dose, but also leads to potentially adverse immunogenic reactions [5-7].

Numerous studies have indicated that both specific and non-specific elements govern interactions between polyions and proteins. The interaction of surface proteoglycans to growth factors have been extensively reviewed in the literature [8, 9]. Angiogenic growth factors are engaged in multiple interactions in the extracellular environment and on the extra-cellular surface of cells. They bind to a variety of free or immobilized proteins, polysaccharides, and complex lipids present in the extracellular milieu and these interactions may affect their stability, integrity, bioavailability and diffusion [10]. They are found in body fluids as circulating complexes or immobilized in the extra-cellular matrix (ECM) and in the sub-endothelial lamina of micro-and macrovasculature [8]. The ECM is largely composed of complex polysaccharides, with glycosaminoglycans (GAGs)

being one of the major classes of polysaccharides. They are known to bind and regulate a number of distinct proteins, including chemokines, cytokines, growth factors, morphogens, adhesion molecules and enzymes [8, 9, 11].

In the previous chapters, we have discussed the use of BP for stabilizing and protecting proteins embedded in PLGA matrix. In this chapter, we sought to understand the nature of interactions between the BPs and proteins. The thermodynamics of the interactions were investigated using a variety of analytical techniques; we explored the potential of using BPs as stabilizing agents for the development of pharmaceutical formulations of bio-macromolecules. Using multiple analytical techniques, in addition to elucidating the nature of interactions, we have attempted to develop a rationale for selecting polyions for developing pharmaceutical formulations of proteins. We compared the interactions of BPs to commonly used polyions like phytic acid and sucrose octasulafate [12-14]. The availability and ease of use made lysozyme (LYZ) the ideal candidate to study the interactions with BP using a number of techniques. Its interactions were studied using circular dichroism (CD), isothermal titration calorimetry (ITC), differential scanning calorimetry (DSC), and intrinsic fluorescence (IF). The cost, availability, and buffer composition limited the use of these techniques for human growth hormone (hgH), vascular endothelial growth hormone (VEGF) and fibroblast growth factor 20 (FgF-20).

5.3 Materials and Methods

5.3.1 Materials

High molecular weight (~ 500 kDa) dextran sulfate (HDS), low molecular weight (~15.5 kDa) dextran sulfate (LDS), chondroitin sulfate (~ 63 kDa, shark cartilage) (CS), porcine heparin (~18 kDa) (HP), Phytic Acid (PY) sodium salts were purchased from Sigma-Aldrich. Suscrose octasulfate (SO) was bought from Toronto Research Chemicals (Canada). Lysozyme (chicken egg white) was also purchased from Sigma-Aldrich. FgF-20 was obtained from the NCI-BRB Preclinical Repository. VEGF and hgH were obtained as gifts from Genentech (CA, USA). All other reagents, common solvents and supplies were obtained from Sigma-Aldrich, unless otherwise specified.

5.3.2 Circular Dichroism and Fluorescence Spectroscopy

CD and fluorescent measurements were made using the JASCO 815 spectrophotometer (JASCO, USA) equipped with peltier temperature controller. CD spectra were collected from 190 to 270 nm at the speed of 50 nm/min, resolution of 0.1 nm and a DIT of 1 sec. Thermal melts were obtained at 5C intervals from 20-85°C, with a heating rate of 15°C/hr and a 5 min equilibration time. Five cycles of spectra were collected and reported as average.

Fluorescent measurements were obtained over 305-440 nm via excitation of Trp residues at 295nm with a resolution of 1 nm. Five cycles of spectra were collected and reported as average.

5.3.3 Differential Scanning Calorimetry

Thermographs were collected with the TA Instruments (USA) nano series differential scanning calorimeter. Data was collected from 20 – 95 ºC at a scan rate of 1 ºC /min under a pressure of 42 psi. Appropriate controls were also scanned, and these thermographs were subtracted from sample melts before data analysis using NanoAnalyse.

5.3.4 Isothermal Titration Calorimetry

Calorimetric titrations were performed with TA Instruments (USA) nano series isothermal titration calorimeter. 400 µl of protein solution was titrated against 50 µl of BP solution at the specified temperature with the stirrer set at 250 rpm. The reference cell contained 400 µl of purified water, and all solutions were degassed prior to use. Appropriate heats of dilution were also obtained using controls, and were subtracted from sample data. The corrected data were analyzed using TA's NanoAnalsye software and were fit to an independent set of multiple biding sites. Samples were run in triplicates.

5.4 Results and Discussion

5.4.1 Protein Stabilization by Excipients

Protein stability is a major issue with development of biopharmaceuticals, but the free energy of the native protein conformation is only 5-20 kJ/mol more stable than the denatured biologically inactive form [15]. A wide range of excipients have been developed to stabilize and protect the native state of the protein for pharmaceutical development [3, 16-19].

Electrostatic interactions, van der Waals forces, hydrogen bond, and hydrophobic interaction are the major interactions governing protein structure and amino acid interactions. Electrostatic interactions occur between charged atoms or molecules, which depends on environmental pH, and ionic strength. Van der Waals interactions consist of interactions between two permanent dipoles, permanent and induced dipoles, and two induced dipoles. Hydrogen bonds are strong dipole-dipole interactions, which arise due to electrostatic attraction between polar molecules when hydrogen is bound to a strong electronegative atoms. It plays a crucial role in determining protein structure and is reported to be 2-10 kcal/mole [20]. Hydrophobic interactions are created by the minimization of contact between non-polar and polar species. It is known to bring about preferential hydration of proteins. It is a major determinant of protein structure and stability.

Protein interactions with co-solvents have been widely studied. A specific stabilizing ligand binds to the native and functional protein, thereby directly stabilizing it. It can also potentially bind to the denatured state to prevent aggregation. An osmolyte is usually a small molecule, which also preferably interacts with the native form over the unfolded form, thus increasing the unfolding energy [16, 21]. Arginine's role in protein stability is still not very clearly understood and a number of different mechanisms have been proposed. It is known to suppress aggregation by preferably binding to denatured state, decrease non-specific adsorption of proteins, stabilize proteins via hydrophobic interactions, etc [18, 21, 22]. Denaturants are known to change the secondary and tertiary structure of native proteins they bind to [16]. They are known to denature the protein via direct chemical attacks or strong changes at the protein-solution interfaces to bring about protein unfolding and precipitation.

5.4.2 Proteins and Biopolymers

As discussed in the previous chapters, specificity of GAG-protein interactions are driven by the ionic interactions between sulfate and carboxylate on GAG's and basic amino acids on the protein [8]. The three-dimensional conformations of the GAG and protein determine the exposed sulfate, carboxylate and amino acid groups [9]. Strong ionic interactions are expected between GAGs and proteins [8]. Clusters of positively charged basic amino acids on proteins form ion pairs with spatially defined negatively charged sulphate or carboxylate groups on heparin chains. Glycosaminoglycans interact with

residues that are prominently exposed on the surface of proteins. The main contribution to binding affinity comes from ionic interactions between the highly acidic sulphate groups and the basic side chains of arginine, lysine and, to a lesser extent, histidine [23]. The interactions of GAGs with proteins also involve a variety of different types of interactions, including van der Waals (VDW) forces, hydrogen bonds, and hydrophobic interactions with the carbohydrate backbone. It has also been observed that heparin-binding domains contain amino acids such as asparagine and glutamine, which are capable of hydrogen bonding. The affinity of heparin-binding proteins for heparin/HS was also enhanced due to the presence of polar residues with smaller side chains like serine and glycine.

Various growth factors bind to the ECM of target tissues by forming tight complexes with sulphated-glycosaminoglycans [24]. Variations of the fine structure of the GAG chains may allow cells to control their responses to individual growth factors and to change the specificity of their response to different members of the growth factor family. Reports indicate that GAG's mediate the activity of FGF-2 by inducing dimer formation and transient dimerization though specific interactions with FGF-2 and its receptor [25, 26]. No significant change in the structure of FGF-2 was observed upon binding. Sulphated-GAG's bind to different VEGF isoforms, exerting multifaceted effects. They contribute to VEGF accumulation in the ECM and acts as EC core-receptors for VEGF [27]. The effect of GAG's on VEGF165 would depend upon the size of the chains, high molecular weight chains increase VEGF binding to receptors while the lower molecular weight chains inhibit pro-angiogenic activity of VEGF165. VEGF is one of the most well

studied growth factor involved in EC migration, mitogenesis, sprouting, and tube formation [28]. Recombinant human vascular endothelial growth factor (rhVEGF) behaves similar to native VEGF in terms of its binding to heparin and its biological activity. RhVEGF is a homodimeric protein consisting of 165 amino acids per monomer with a molecular weight of 38.3 kDa and a pI of 8.5. The protein consists of 2 domains, a receptor-binding domain (residues 1-110) and a heparin-binding domain (residues 111-165) [29].

Heparin consists of repeating units of 1→4 linked pyranosyluronic acid and 2-amino-2-deoxyglucopyranose (glucosamine) residues [9]. The uronic acid residues typically consist of 90%L-idopyranosyluronic acid (L-iduronic acid) and 10% D-glucopyranosyluronic acid (D-glucuronic acid). It has been studied extensively due to its well understood functions in anti-coagulation and is known to be highly evolutionarily conserved with similar structures found in a broad range of vertebrate and invertebrate organisms [23].

5.4.3 Effect of BPs on Protein Structure

Circular Dichroism uses the differences in absorption of left versus right handed polarized light to determine structural element of proteins. The secondary structure of proteins can be analyzed in the far –UV region (190-250nm). If data from the entire range is not available, the reliability of structural quantification is questionable but the

compassions of spectra are not compromised. In contrast to far UV region, near CD region provides information about the columbic interactions between dipoles, structural information via relative polarity and hydrogen bonding characteristics of environment surrounding Trp, Phe, Tyr, and Cys residues [30].

Intrinsic fluorescence of protein is a very sensitive technique to study protein conformational transitions, subunit association, substrate binding, or denaturation [31, 32]. The relatively rare amino acids phenylalanine (Phe), tyrosine (Tyr) and tryphophan (Try) are all fluorescent. Phe has a very poor quantum yield, so its emission is rarely observed for proteins. The emission maximum of Trp is highly sensitive to local environment whereas Try maximas are insensitive to its local environment. Trp can be selectively excited at 295-300 nm and has been widely used to study the polarity of its environment. At 295 nm, Trp emission spectra reflect the average environment of the residues in the protein. Trp, in a completely non-polar environment has a blue shifted structure characteristic of indole in cyclohexane, while on being hydrogen bonded or exposed to water, its emission shifts to longer wavelengths.

5.4.3.1 Effect of BPs on LYZ Melt

LYZ thermal melts were used to analyze the change in structure in the presence of BP. The CD spectra of native LYZ has been reported to contained two minima at 208 nm and 222 nm, characteristic of a predominantly α-helical structure [33]. The 208 nm band is

known to correspond to π–π* transition of the α-helix and the 222 nm band due to *n*–π* transition for both the α-helix and random coil.

To estimate the ability of BPs to stabilize the LYZ, thermal melts were obtained at 42X (BP:LYZ). The spectra of the native LYZ shows a loss of the minima and the maxima at 190 nm, indicating a change in the native α-helical structure at 75 °C and above. This suggests that the native protein undergoes a structural transition due heat denaturation around 75 °C. In the presence of HDS, the minima were larger in 208-220 nm regions, suggesting that the α-helical content is larger and the LYZ undergoes a structural transition where helical content is lost, beyond 50 °C. The presence of LDS reduced the minima and brought about a larger transition in LYZ structure beyond 50°C. In presence of HP, the spectra were found to be similar to LDS, with a major denaturation event accompanied with a loss of helical content beyond 60°. A similar transition in the spectra of LYZ was seen in presence of PA, beyond 65 °C. Among all the BP, SO increased the minima in the 208-220 nm and maintained the structure of LYZ throughout the melt.

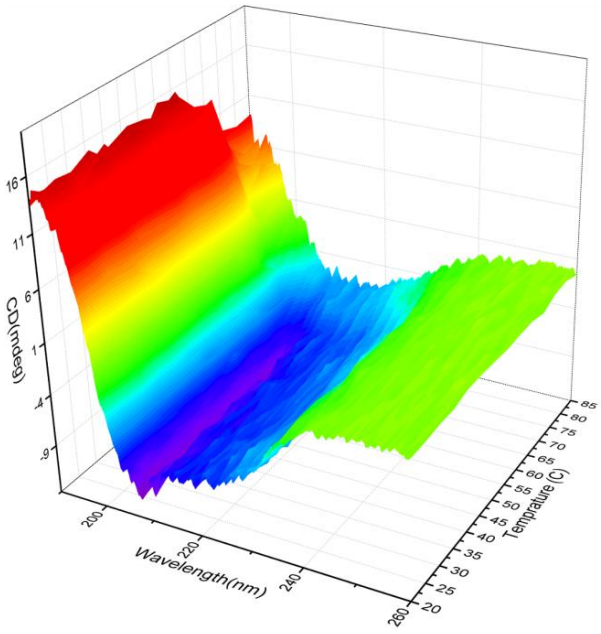
CD(mdeg)
16
11
6
1
-4
-9
Wavelength(nm)
200
220
240
260
Temprature (C)
20
25
30
35
40
45
50
55
60
65
70
75
80
85

(a)

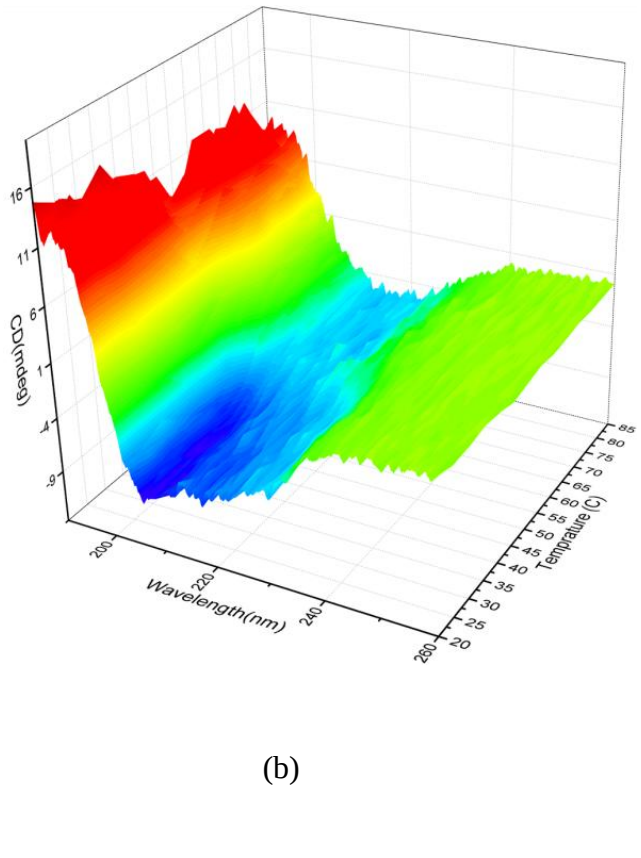
CD(mdeg)
16
11
6
1
-4
-9
Wavelength(nm)
200
220
240
260
Temprature (C)
20
25
30
35
40
45
50
55
60
65
70
75
80
85
-13.70
-10.35
-7.000
-3.650
-0.3000
3.050
6.400
9.750
13.10
16.45
19.80

(b)

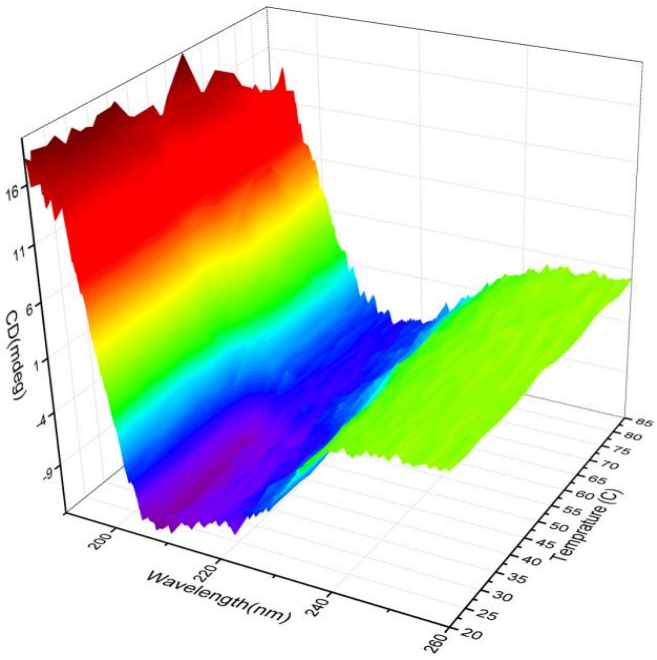
CD(mdeg)
16
11
6
1
-4
-9
Wavelength(nm)
200
220
240
260
Temprature (C)
20
25
30
35
40
45
50
55
60
65
70
75
80
85

(c)

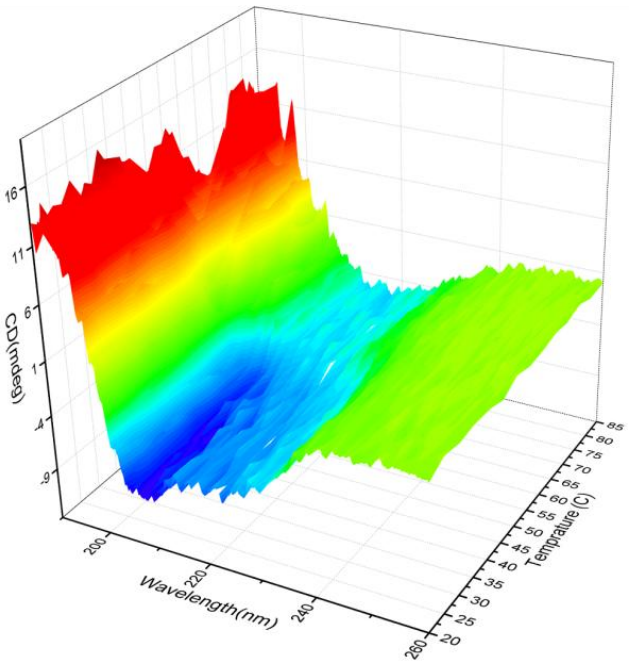
CD(mdeg)
16
11
6
1
-4
-9
Wavelength(nm)
200
220
240
260
Temprature (C)
20
25
30
35
40
45
50
55
60
65
70
75
80
85

(d)

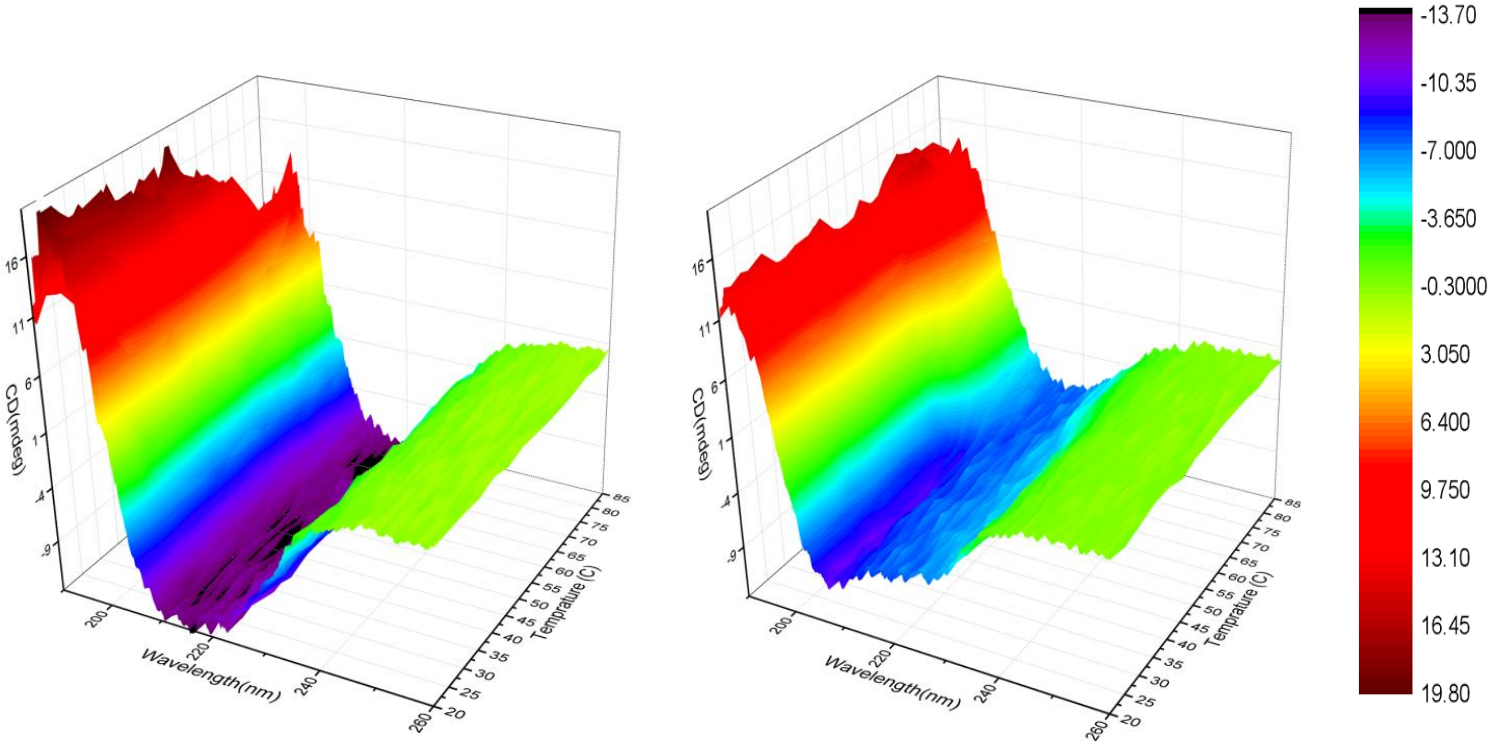

(e) (f)

Figure 5-1 : CD Spectra of (a) 0.12 mg/ml LYZ in 10 mM Phosp. Buff (b) 25X LDS (c) 25X HDS (d) 25X HP (e) 25X OS (f) 25X PA

5.4.3.2 Effect of BPs on LYZ structure

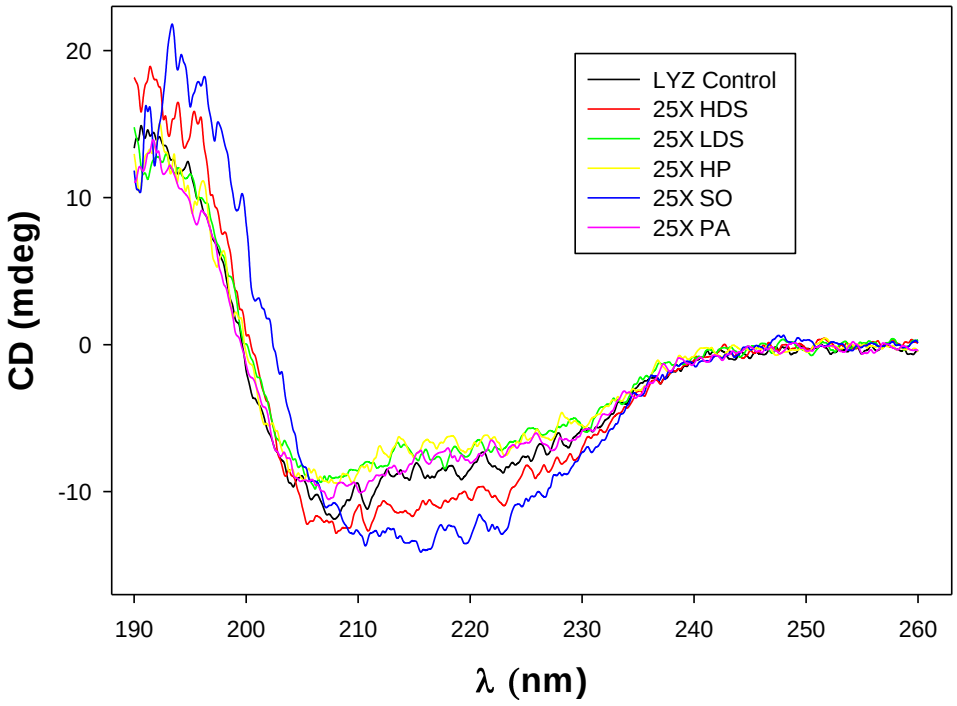

Figure 5-2 : Effect of BPs on 0.012 mg/ml LYZ in phosphate buffer (pH 7) with 25 times mass excess.

The effect of the BPs on the secondary structure of the LYZ was studied at 25 times mass excess by CD (Figure 5-2). HDS and SO were observed to increase the minimas in 208-222 nm region, suggesting that the λ content is increased. This could be attributed to the ability of larger BPs to lock LYZ into particular conformations via interactions with a larger number of charges on the molecular chain. Comparatively, smaller BPs were noted to have a smaller effect on the LYZ secondary structure.

The effect of the BPs was also studied at different mass excess to further study the change in LYZ structure (Figure 5-3). As expected, increasing amount of BP increases its ability to bring about the change in structure of LYZ as discussed above (Figure 5-2).

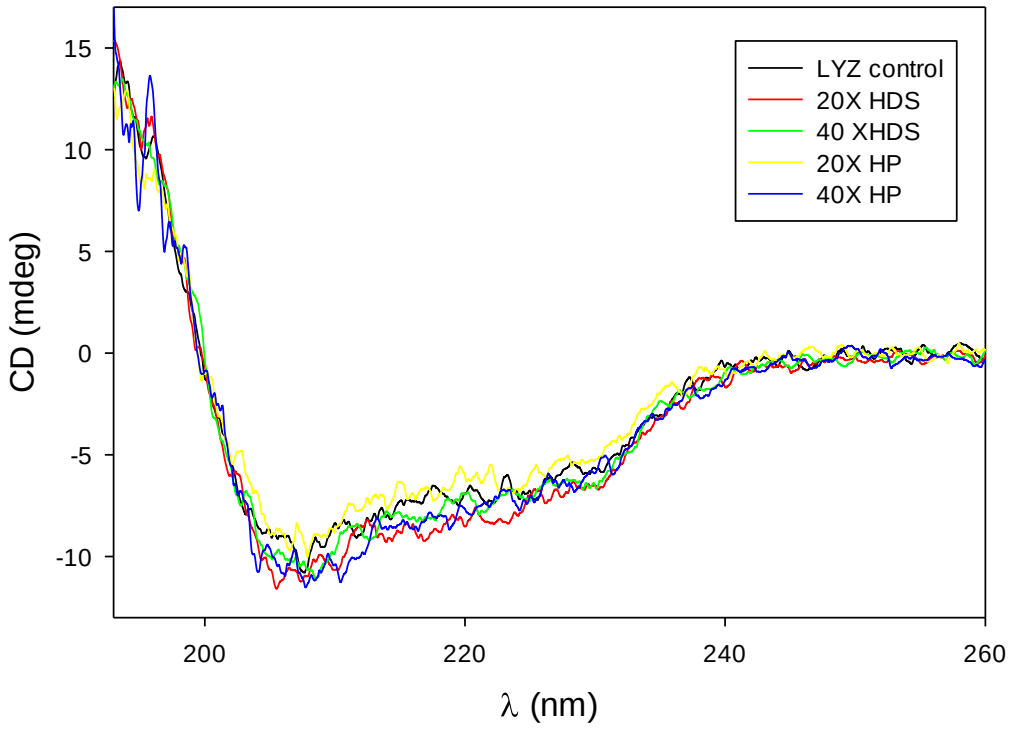

Figure 5-3 : Representative CD profiles of 0.012 mg/ml LYZ in phosphate buffer (pH 7) with 20 and 40 times mass excess BPs.

Similarly, the effect of BPs on the tertiary structure of LYZ was studied with intrinsic fluorescence (IF) (Figure 5-4). HDS is observed to bring about a red shift, suggesting hydrogen bonding and increase in polarity. HP brought about a slight blue shift, suggesting that the Trp residues are being exposed to a non-polar environment. Similar changes in polarity were seen with other BPs confirming the change in LYZ structure, as demonstrated by CD data.

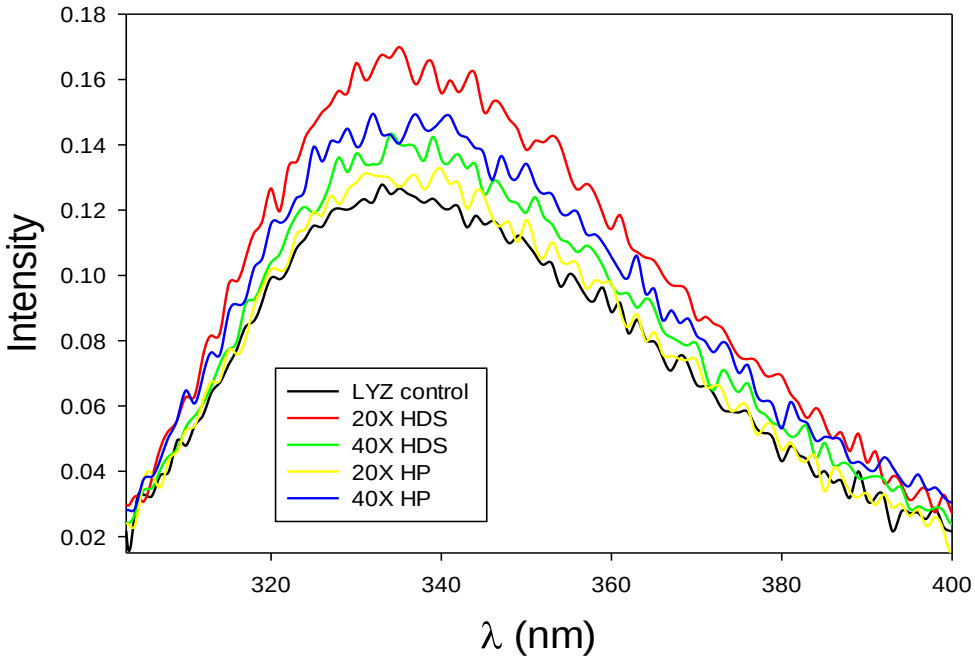

Figure 5-4 : Representative fluorescence intensity profiles of HDS and HP on 0.1 mg/ml LYZ in phosphate buffer (pH 7) with 20 and 40 times mass excess.

5.4.3.3 Effect of BPs on hgH structure

The effect of BPs on the secondary structure of hgH was studied at 25 times mass excess (Figure 5-5). In contrast to LYZ, BPs were not observed to bring about major changes except for CS, which is known to have interference in the CD signal below 200 nm.

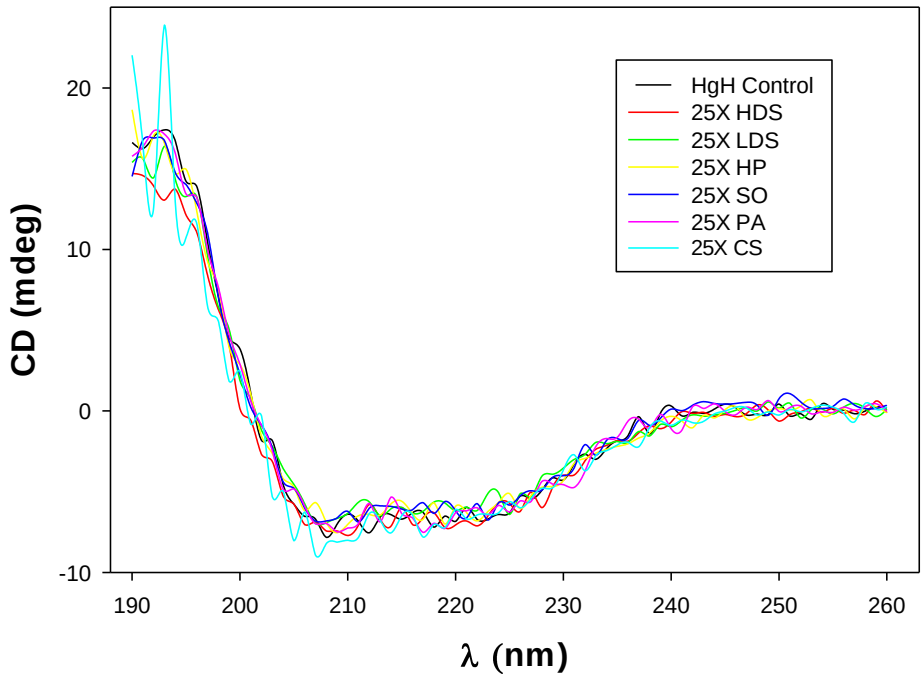

Figure 5-5 : Effect of BPs on 0.05 mg/ml hgH in bicarbonate buffer (pH 8) with 25 times mass excess by circular dichroism

5.4.4 Isothermal Titration Calorimetry

Thermodynamic analysis of protein-BP interactions were carried out using isothermal titration calorimetry (Table 5-1). Upon interaction, the change in enthalpy relates to the heat released or absorbed, whereas the change in entropy reflects the change in conformation as BP and protein combine to form a BP-protein complex.

Table 5-1: Thermodynamics of BP-LYZ interactions. ΔG and ΔS were calculated using ΔG = ΔH - TΔS.

Temp. (°C)	**BP**	**Ka(10^6) (1/M)**	**n**	**# LYZ bound to one BP**	**ΔH (kJ/mol)**	**ΔS*T (kJ/mol)**	**ΔG (kJ/mol)**
4	LDS	3.8 ± 0.2	0.13	~ 7	-499 ± 12	-465	-35
8	LDS	3.2 ± 0.4	0.13	~ 7	-423 ± 17	-389	-35
24	LDS	2.1 ± 0.5	0.12	~ 8	-488 ± 32	-452	-36
37	LDS	16.7 ± 0.6	0.11	~ 9	-365 ± 21	-322	-43
4	CS	7.3 ± 0.1	0.03	~ 30	-1159 ± 13	-1122	-35
8	CS	7.8 ± 0.2	0.03	~ 31	-1057 ± 21	-1020	-37
24	CS	23.5 ± 0.2	0.04	~ 29	-1052 ± 27	-1010	-42
37	CS	53.3 ± 4.5	0.03	~ 36	-1143 ± 38	-1097	-46
4	HP	3.5 ± 0.2	0.09	~ 12	-483 ± 29	-448	-35
8	HP	2.1 ± 0.4	0.08	~ 12	-474 ± 21	-440	-34
24	HP	5.2 ± 0.6	0.09	~ 11	-466 ± 37	-427	-38
37	HP	3.2 ± 0.9	0.94	~ 1	-41 ± 7	-2	-39

Enthalpy values calculated from ITC in macromolecular systems typically result from the formation and breakage of many different types of interactions. The individual

contributions may produce positive or negative enthalpy changes, thus severely complicating any attempt at further analysis of those values. The interactions were primarily found to be driven by enthalpy. Due to the strong electrostatic nature of interactions, the enthalpic changes were found to be large and negative. This is could be attributed to the electrostatic interactions involved in the binding. Larger polyions have been shown to have larger enthalpy [14, 16], possibly due to larger number of negative charges possessed by these ligands, which provide multiple binding sites through extended electrostatic interactions with the positive charges on the protein molecules. As expected, CS, which has a larger amount of charge and size, was found to be more exothermic, when compared to HP and LDS. Similar trend was reported for polyions interacting with growth hormones and parathyroid hormone [14, 34]. Enthalpic contributions were significantly less negative on a mole of charge basis. These adjusted enthalpies were similar for all ligands, consistent with major electrostatic contributions (Figure 5-6). This is contrasted, however, by the negative entropy values. The loss of entropy was expected, as the protein-BP complex would have lower degrees of freedom as they form a complex and due to the strong biding, as reflected by change in enthalpy. ΔS values were also found to be similar across the BPs and became less favorable as the size of BP increased. Dependence of enthalpy on temperature is related to hydrophobic interactions or solvation level. A decrease in ΔH at higher temperature indicates that hydrophobic bonds are formed and vice-versa (Figure 5-6).

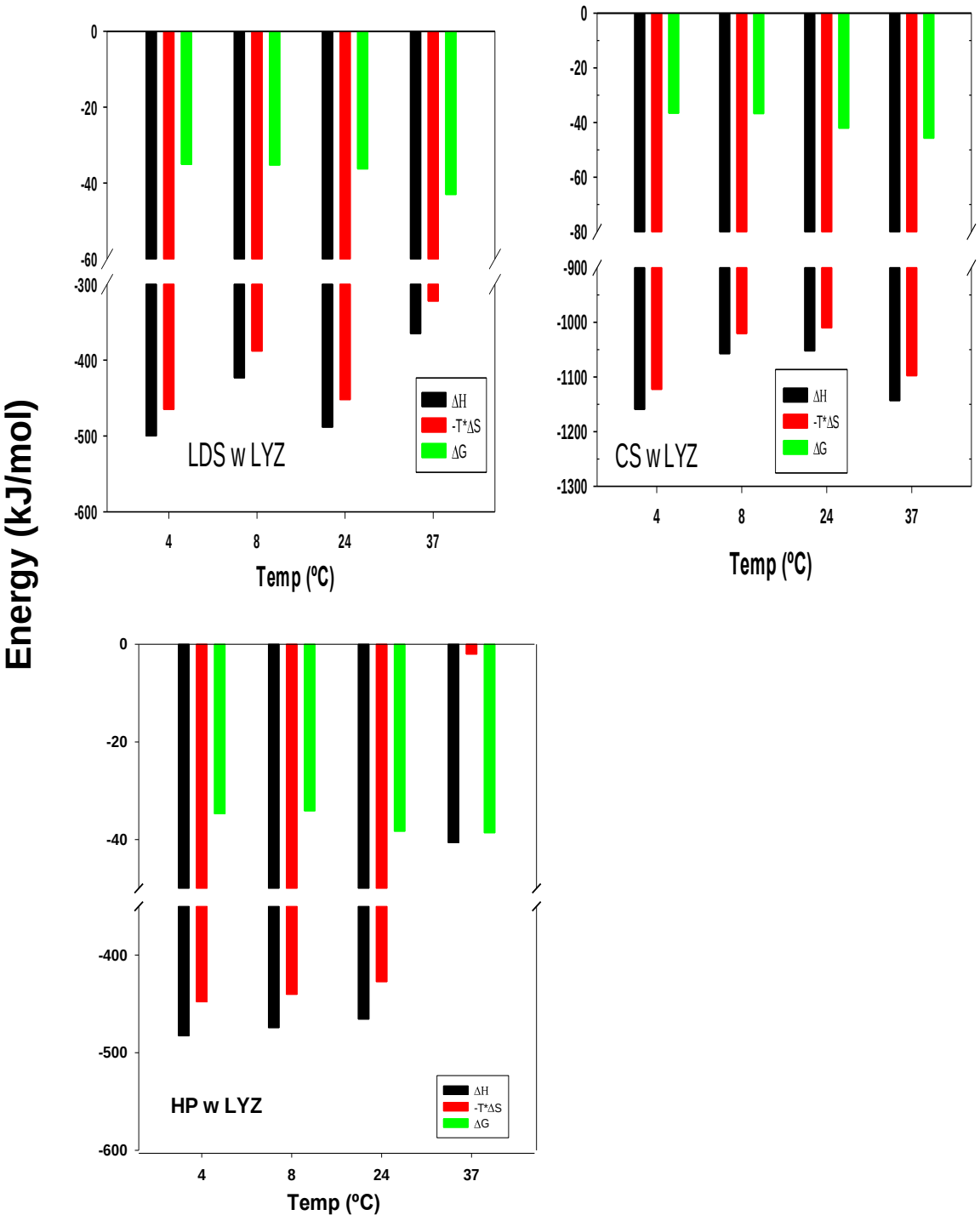

Figure 5-6 : Thermodynamics of BP-LYZ analyzed by ITC. The graphs represent the values of ΔG, ΔH, and -T*ΔS.

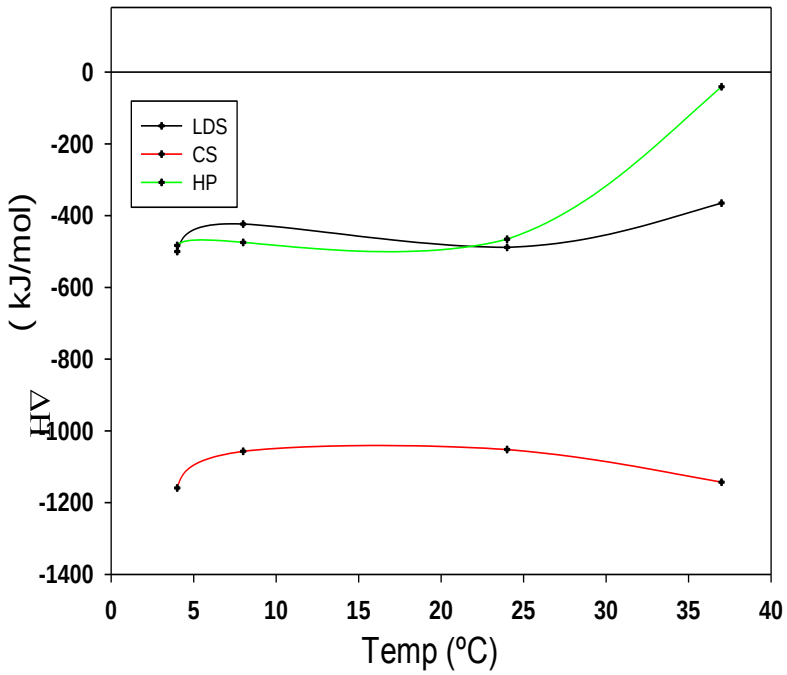

Figure 5-7 : Enthalpy Vs temperature plotted for CS-LYZ, HP-LYZ, and LDS-LYZ binding interactions.

The ΔG for the interactions were found to be negative for the BP's analyzed, indicating that the interactions are spontaneous and thermodynamically favored over the conditions investigated. The calculated Gibbs free energy were found to increase modestly with temperature, and were found to be similar to ones reported in the literature [14, 34]. Moderate to strong binding constants were observed for all interactions with Ka values in the micro-molar range

5.4.5 Differential Scanning Calorimetry

Biochemical reactions tend to have smaller heat effects associated with them, when compared to chemical reactions. DSC has been widely used to investigate formulation stability by investigating thermal stability of liquid pharmaceuticals [35]. DSC experiments typically provide ΔC_p (change in heat capacity), ΔH (change in enthalpy), and T_m (midpoint of thermal transition) for a reversible transition.

The effect of temperature on protein stability is complex, and proteins are known to aggregate and precipitate with an increase in temperature. The solvation process being spontaneous has negative free energy associated with it, leading to a highly negative ΔH ($\Delta G = \Delta H - T\Delta S$). Water molecules are known to orient around hydrophobic groups of protein in solution, and the change in entropy is negative. Thus, the ΔH of the aggregation/precipitation process will be positive and the Arrhenius equation will predicts that the process will accelerate with temperature [22].

Thermal unfolding of proteins is known to be irreversible primarily due to aggregation/precipitation, thus there is no equilibrium to calculate accurate thermodynamic equilibrium parameters. Thus, DSC thermal profiles were analyzed to obtain apparent midpoint of transition (T_m) and calorimetric enthalpy (ΔH_{cal}). Higher values of T_m and H_{cal} are indicative of a higher stability. Native protein is considered enthalpically more stable than the denatured form, due to packing and hydrogen bonds contributions to enthalpy.

The effect of the BPs on thermal stability of protein was analyzed by DSC thermograms of proteins (1 mg/ml) in the presence of 40X (mass) of BP.

5.4.5.1 Effect of BP on LYZ T_m

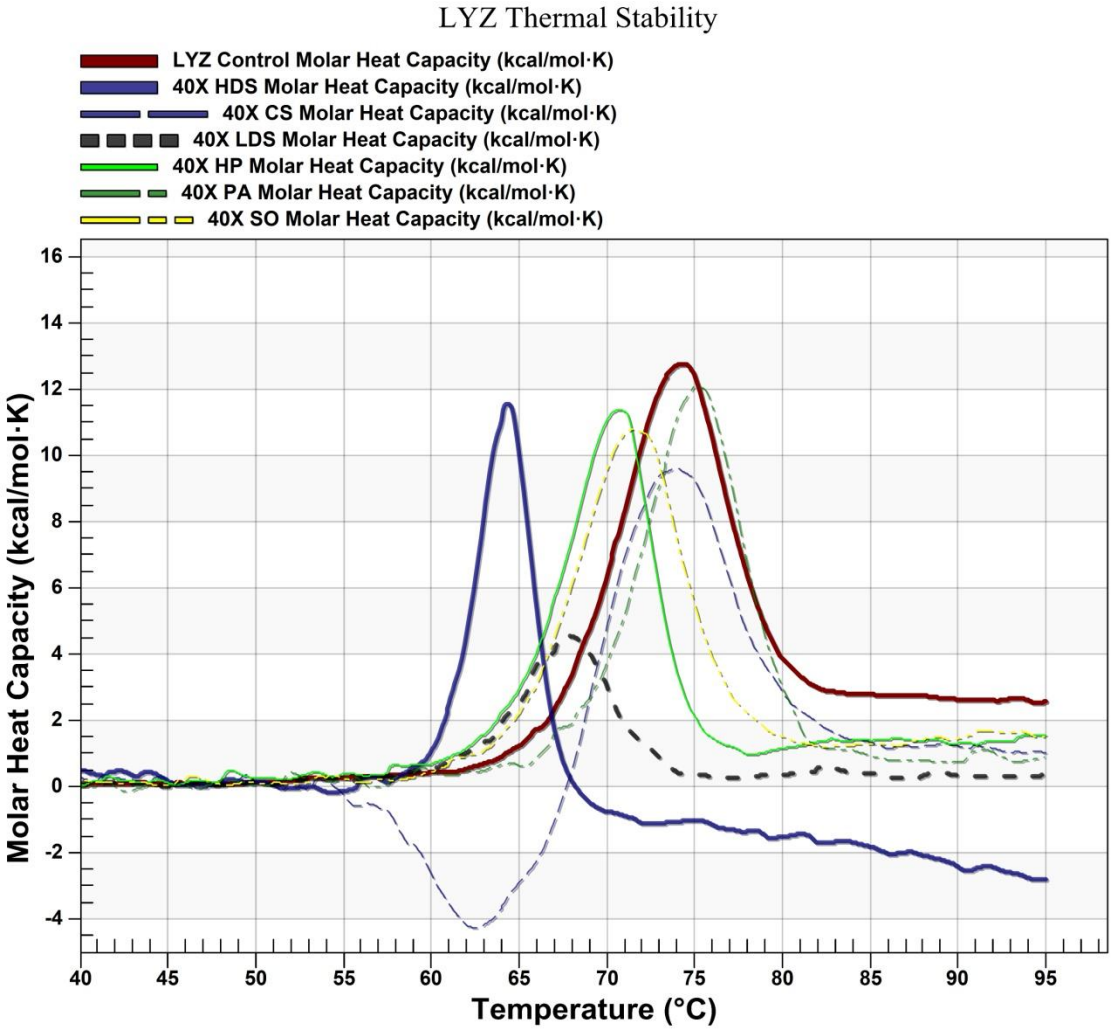

Figure 5-8 : Effect of BPs on the thermal stability of 1 mg/ ml LYZ in 10 mM phosphate buffer at pH 7(at 40 fold weigh excess of BPs).

In case LYZ, the T_m of 1 mg/ml protein in 10 mM phosphate buffer at pH 7 was ~ 74 °C (Figure 5-8). HDS, SO and HP were observed to reduce the apparent Tm of LYZ. The presence of an exothermic event before the T_m, indicates an aggregation/precipitation event prior to unfolding. LDS was found to bring about precipitation of LYZ from the solution, making the DSC prolife not useful for analysis. PA was observed to marginally improve the thermal stability of LYZ in solution.

The difference in the baseline before and after the Tm, gives an idea about the change in heat capacity (ΔC_p) brought about by the transition. ΔC_p are known to be associated with the reversibility of the transition, higher ΔC_p tend to reduce the reversibility of the transition. From the DSC profiles (Figure 5-8), the highest ΔC_p was observed in the case of LYZ, whereas the BPs observed to reduce the ΔC_p.

Table 5-2 : Analysis of LYZ DSC profiles using NanoAnalyze software[8]

Sample	Aw	Tm (°C)	ΔH (kJ/mole)
LYZ Control	0.249 ± 0.001	73.64 ± 0.02	507.7 ± 4.69
40X HDS	0.201 ± 0.001	64.21 ± 0.015	941.9 ± 9.53
40X HP	0.521 ± 0.015	70.05 ± 0.040	584.2 ± 10.03
40X PA	0.576 ± 0.009	74.86 ± 0.027	560.9 ± 5.66
40X SO	0.640 ± .007	71.20 ± .020	500.7 ± 3.651
40X LDS	NA	NA	NA
40X CS	NA	NA	NA

In the presence of HDS, ΔH_{cal} of the transition increased by ~ 440 kJ/mol, suggesting that the HDS and LYZ interacted strongly in solution. HP and PA were also observed to increase ΔH_{cal} by ~ 60-70 kJ/mol, but presence of SO did not affect the ΔH_{cal}. No analysis was feasible for the data in the presence of CS and LDS, due to precipitation/ aggregation issues.

[8] The raw DSC data was fit to the two-state scaled model, with appropriate controls. The quality of the fit was ascertained by running a statistical analysis with a 1000 trials where the parameters were varied around the fit (95 % confidence interval). Samples were run in triplicate and the data is reported as mean ± error in fit.

5.4.5.2 Effect of BP on HgH T_m

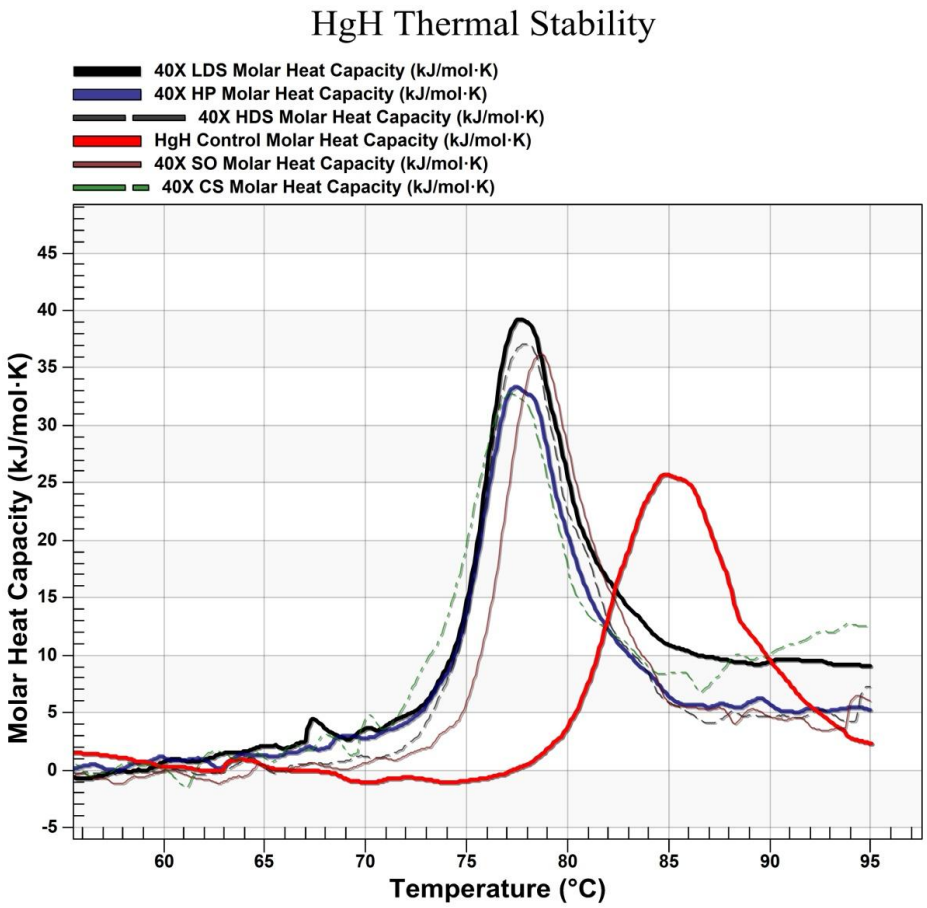

Figure 5-9 : Effect of BPs on the thermal stability of 1 mg/ ml 4mM bi-carbonate buffer at pH 8 (at 40 fold weigh excess of BPs).

1 mg/ml of hgH in 4mM bicarbonate buffer at pH 8 was observed to have an apparent Tm of ~ 85 °C (Figure 5-9). All BPs were noted to reduce this temperature, suggesting that they reduced the thermal stability of hgH in solution. Surprisingly, the apparent T_m in the presence of BPs was very similar (~ 76 - 78 °C). PA profile was not reported due to aggregation/precipitation events. From the baselines before and after the transition, ΔC_p was observed to be higher for hgH control, CS and LDS, suggesting that the transitions had a higher irreversibility, compared to other transition profiles. The hgH DSC data was

fit using the two-state scaled model in NanoAnalyze software (Table 5-3). The ΔH_{cal} was found to be increase from ~ 550 kJ/mol in the presence of BPs. The largest increase was seen in the case of LDS, where the ΔH_{cal} was reported to be ~ 755 kJ/mol. Similarly large increases in ΔH_{cal} for was observed HP and SO, suggesting that LDS, SO and HP interacted strongly to the hgH in solution. Analysis of PA profile was not feasible due to aggregation/precipitation events.

Table 5-3: Analysis of hgH DSC profiles using NanoAnalyze software[9]

Sample	**Aw**	**Tm (°C)**	**ΔH (kJ/mole)**
hgH Control	0.378 ± 0.008	85.36 ± 0.04	550.1 ± 7.45
40X HDS	0.285 ± 0.006	77.99 ± 0.028	702.8 ± 9.66
40X LDS	0.238 ± 0.015	77.95 ± 0.032	755.4 ± 11.87
40X HP	0.229 ± 0.005	77.86 ± 0.025	728.1 ± 9.85
40XCS	0.242 ± 0.001	77.40 ± 0.023	686.7 ± 9.69
40X SO	0.522 ± 0.006	78.90 ± 0.029	744.4 ± 10.78
40X PA	NA	NA	NA

[9] The raw DSC data was fit to the two-state scaled model, with appropriate controls. The quality of the fit was ascertained by running a statistical analysis with a 1000 trials where the parameters were varied around the fit (95 % confidence interval). Samples were run in triplicate and the data is reported as mean ± error in fit.

Overall, the addition of BPs to LYZ and hgH resulted in decrease of the apparent Tm in some cases. Inspite of the destabilization of the protein, it does not necessarily suggest that the presence of BPs leads to a poor formulation. Protein-BP interactions could potentially inhibit protein-protein interactions, which have been shown to cause aggregation and protein degradation. In addition, these interactions might protect the protein formulation during processing, manufacturing, handling and enhance therapeutic effect by acting as a co-factor [11, 36, 37].

5.5 Conclusions

Growth factors are known to be thermally labile, to the extent that they are known to undergo structural transitions below 40 °C possibly due to being intrinsically disordered [12, 37, 38]. While the proteins undergo a change in structure around 37 °C, a significant portion of the native structure is retained. These inductions of structural changes in the proteins upon binding to the polysaccharides in the ECM may have biological significance. Since a number of these proteins (e.g. FgF family [39]) are presented in this bound form, it is crucial to understand the interactions between the polyions and proteins in the normal and diseased state. The interactions between polysaccharides and growth factors in the ECM are commonly explained by the role of the polyionic proteoglycans on the surface of cells, to present the growth factors to their protein kinase receptors. Other roles for the interactions include chaperon like behavior, intracellular transportation and localization, stabilizing effect, etc [8, 12, 39, 40].

Our data suggests that the LYZ structure was altered by BPs in solution, especially larger BPs like HDS and SO, which could lock LYZ into a particular conformation and bring about steric hindrance. This change was observed in CD and IF data. In contrast, for hgH, not a large change in secondary structure was seen. . In addition, it was not possible to carry out structural elucidation of FgF-20 and VEGF with BPs due to the presence of Arg and polysorbote 20, respectively, to stabilize and solubilize proteins in solution. Analysis of hgH via IF was not feasible due to the poor fluorescence characteristics of hgH

The BPs used in the study demonstrate enthalpically driven binding to LYZ with significant affinity. In many cases, macromolecules that bind charged compounds are known to be entropically driven, with small ΔH values. However, numerous examples of electrostatic interactions between macromolecules and ions are reported that are driven enthalpically [41-43]. The degree of the entropy change may be related to number of binding sites on macromolecule or ligand. Protein binding to polyions has also been reported to be enthalpically driven in many cases [12-14, 34]. Multiple LYZ molecules were demonstrated to bind to the BPs, with CS having the largest number of bound LYZ.

The DSC data indicates that the addition of BPs to the protein resulted in decrease of the T_m in most cases. Inspite of the destabilization of the protein in solution, this does not necessarily suggest that the BP leads to poor formulations [12, 14]. It is important taht DSC data is dependent on the concentration and most of the pharmaceutical protein solutions are at high concentration. Protein-BP interactions could potentially inhibit

protein-protein interactions, which have been shown to cause aggregation and protein degradation. In addition, protein-BP interactions might protect the protein formulation during processing, manufacturing, handling and enhance therapeutic effect by acting as a co-factor [11, 36, 37]. Thus, BP could be explored excipients for formulating proteins, which are, known to self-associate and aggregate [37].

The existence of a vast polyanionic network at the cellular level and reports in the literature suggest that extensive polyanion-protein interactions mediate a whole range of cellular processes [37, 40, 44]. The effect of BPs/polyanions on the structure of the growth factors raises the question about the growth factors around physiological conditions, in the presence of numerous polyions. The influence of concentrated solution of polysaccharides on protein stability is hypothesized to be drive by chemical interactions and hard-core repulsion [45]. As hard-core repulsions would involve only the arrangement of molecules, they would be expected to affect the entropic component of protein stability. A vast majority of protein stability studies reported in the literature have been performed using dilute buffer with low concentration of proteins (usually < 1 gm/ml). This differs to a great extent form environment encountered by proteins within cells, where the total macromolecular concentration amounts to several hundred gms/ml [46]. The crowding leads to non-specific forces, which promote reduction in total volume and formation of compact macromolecular complexes. Such crowding behavior was found to be responsible for the stabilizing effect of dextran on cytochrome c [47]. At the macromolecular concentration needed to bring about macromolecular crowding, a substantial increase in volume occupancy was observed with a reduction in water

concentration. Excluded volume model was found to explain this stabilizing effect of dextran at very high concentration [47]. There are still a lot to understand about the effect of macromolecular crowding on the interactions between polyanions and proteins *in vivo*, especially since a majority of the work in the field fails to account for this in their work. This has important implications for understanding biologically active proteins that have little or no structure in dilute solutions [48].

Whatever the implications of polyion concentration on biological stability of proteins, the potential exists for the use of suitably selected BP like polyanion to formulate therapeutic formulations of proteins, which tend to aggregate and self associate.

5.6 References

1. Rickwod, S., M. Kleinrock, and M. Nunez-Gaviria, *The Global Use of Medicines:Outlook through 2017*, 2013, IMS Institute for Healthcare Informatics.
2. Dimitrov, D., *Therapeutic Proteins*, in *Therapeutic Proteins*, V. Voynov and J.A. Caravella, Editors. 2012, Humana Press. p. 1-26.
3. Jiskoot, W., et al., *Protein instability and immunogenicity: Roadblocks to clinical application of injectable protein delivery systems for sustained release.* Journal of Pharmaceutical Sciences, 2012. **101**(3): p. 946-954.
4. Schwendeman, S.P., et al., *Injectable controlled release depots for large molecules.* Journal of Controlled Release, 2014. **190**(0): p. 240-253.
5. Rosenberg, A., *Effects of protein aggregates: An immunologic perspective.* AAPS J, 2006. **8**(3): p. E501-E507.
6. Wang, W., et al., *Immunogenicity of protein aggregates—Concerns and realities.* International Journal of Pharmaceutics, 2012. **431**(1–2): p. 1-11.
7. Hermeling, S., et al., *Structure-Immunogenicity Relationships of Therapeutic Proteins.* Pharmaceutical Research, 2004. **21**(6): p. 897-903.
8. Gandhi, N.S. and R.L. Mancera, *The Structure of Glycosaminoglycans and their Interactions with Proteins.* Chemical Biology & Drug Design, 2008. **72**(6): p. 455-482.
9. Raman, R., V. Sasisekharan, and R. Sasisekharan, *Structural Insights into Biological Roles of Protein-Glycosaminoglycan Interactions.* Chemistry & Biology, 2005. **12**(3): p. 267-277.
10. Jain, R., *The manufacturing techniques of various drug loaded biodegradable poly (lactide-co-glycolide)(PLGA) devices.* Biomaterials, 2000. **21**(23): p. 2475-90.
11. Lai, P.-H., et al., *Acellular biological tissues containing inherent glycosaminoglycans for loading basic fibroblast growth factor promote angiogenesis and tissue regeneration.* Tissue Engineering, 2006. **12**(9): p. 2499-2508.
12. Derrick, T., et al., *Effect of polyanions on the structure and stability of repifermin (keratinocyte growth factor-2).* J Pharm Sci, 2007. **96**(4): p. 761-76.
13. Fan, H., et al., *Effects of pH and polyanions on the thermal stability of fibroblast growth factor 20.* Mol Pharm, 2007. **4**(2): p. 232-40.
14. Joshi, S.B., et al., *The interaction of Heparin/Polyanions with bovine, porcine, and human growth hormone.* Journal of Pharmaceutical Sciences, 2008. **97**(4): p. 1368-1385.
15. Jaenicke, R., *Protein Folding: Local Structures, Domains and Assemblies*, in *Methods in Protein Sequence Analysis*, H. Jörnvall, J.-O. Höög, and A.-M. Gustavsson, Editors. 1991, Birkhäuser Basel. p. 387-396.
16. Kamerzell, T.J., et al., *Protein–excipient interactions: Mechanisms and biophysical characterization applied to protein formulation development.* Advanced Drug Delivery Reviews, 2011. **63**(13): p. 1118-1159.

17. Wang, W., S. Nema, and D. Teagarden, *Protein aggregation—Pathways and influencing factors.* International Journal of Pharmaceutics, 2010. **390**(2): p. 89-99.
18. Jeong, S., *Analytical methods and formulation factors to enhance protein stability in solution.* Archives of Pharmacal Research, 2012. **35**(11): p. 1871-1886.
19. Zhao, H. and E. Topp, *Recent U.S. patents on protein drug formulation: 2000-2007.* Recent Patents on Drug Delivery Formulation, 2008. **2**(3): p. 200-208.
20. Pace, C.N., et al., *Forces contributing to the conformational stability of proteins.* Faseb J, 1996. **10**(1): p. 75-83.
21. Ohtake, S., Y. Kita, and T. Arakawa, *Interactions of formulation excipients with proteins in solution and in the dried state.* Advanced Drug Delivery Reviews, 2011. **63**(13): p. 1053-1073.
22. Maity, H., C. Karkaria, and J. Davagnino, *Effects of pH and arginine on the solubility and stability of a therapeutic protein (Fibroblast Growth Factor 20): relationship between solubility and stability.* Curr Pharm Biotechnol, 2009. **10**(6): p. 609-25.
23. Fromm, J.R., et al., *Pattern and Spacing of Basic Amino Acids in Heparin Binding Sites.* Archives of Biochemistry and Biophysics, 1997. **343**(1): p. 92-100.
24. Distler, O., et al., *The molecular control of angiogenesis.* International Reviews of Immunology, 2002. **21**(1): p. 33-49.
25. Lazarous, D.F., et al., *Comparative effects of basic fibroblast growth factor and vascular endothelial growth factor on coronary collateral development and the arterial response to injury.* Circulation, 1996. **94**(5): p. 1074-1082.
26. Rusnati, M. and M. Presta, *Extracellular angiogenic growth factor interactions: an angiogenesis interactome survey.* Endothelium, 2006. **13**(2): p. 93-111.
27. Goerges, A.L. and M.A. Nugent, *Regulation of Vascular Endothelial Growth Factor Binding and Activity by Extracellular pH*. Journal of Biological Chemistry, 2003. **278**(21): p. 19518-19525.
28. Neufeld, G., et al., *Vascular endothelial growth factor (VEGF) and its receptors.* FASEB J., 1999. **13**(1): p. 9-22.
29. Zhang, L., *Controlled Release of Angiogenic Growth Factors from Poly(Lactic-Co-Glycolic Acid) Implants for Therapeutic Angiogenesis*. 2009.
30. Greenfield, N.J., *Using circular dichroism spectra to estimate protein secondary structure.* Nat. Protocols, 2007. **1**(6): p. 2876-2890.
31. Lakowicz, J.R., *Principles of Fluorescence Spectroscopy*. 2006: Springer US.
32. Mocz, G. and J. Ross, *Fluorescence Techniques in Analysis of Protein–Ligand Interactions*, in *Protein-Ligand Interactions*, M.A. Williams and T. Daviter, Editors. 2013, Humana Press. p. 169-210.
33. Knubovets, T., et al., *Structure, thermostability, and conformational flexibility of hen egg-white lysozyme dissolved in glycerol.* Proceedings of the National Academy of Sciences, 1999. **96**(4): p. 1262-1267.
34. Kamerzell, T.J., et al., *Parathyroid hormone is a heparin/polyanion binding protein: Binding energetics and structure modification.* Protein Science, 2007. **16**(6): p. 1193-1203.

35. Remmele RL, G.W., *Differential scanning calorimetry: a practical tool for elucidating the stability of liquid biopharmaceuticals.* Pharm Tech Eur 2000(12): p. 56-60.
36. Pike, D.B., et al., *Heparin-regulated release of growth factors in vitro and angiogenic response in vivo to implanted hyaluronan hydrogels containing VEGF and bFGF*. Biomaterials, 2006. **27**(30): p. 5242-5251.
37. Jones, L.S., B. Yazzie, and C.R. Middaugh, *Polyanions and the Proteome.* Molecular & Cellular Proteomics, 2004. **3**(8): p. 746-769.
38. Dunker, A.K., et al., *Intrinsic disorder and protein function.* Biochemistry, 2002. **41**(21): p. 6573-82.
39. Plotnikov, A.N., et al., *Structural basis for FGF receptor dimerization and activation.* Cell, 1999. **98**(5): p. 641-50.
40. *Polysaccharides : Structural Diversity and Functional Versatility*, ed. S. Dumitriu. 2005, Hoboken: CRC Press.
41. Parker, M.H., C.G. Brouillette, and P.E. Prevelige, Jr., *Kinetic and calorimetric evidence for two distinct scaffolding protein binding populations within the bacteriophage P22 procapsid.* Biochemistry, 2001. **40**(30): p. 8962-70.
42. Baerga-Ortiz, A., et al., *Two different proteins that compete for binding to thrombin have opposite kinetic and thermodynamic profiles.* Protein Sci, 2004. **13**(1): p. 166-76.
43. Wintrode, P.L. and P.L. Privalov, *Energetics of target peptide recognition by calmodulin: A calorimetric study.* Journal of Molecular Biology, 1997. **266**(5): p. 1050-1062.
44. Cooper, C.L., et al., *Polyelectrolyte–protein complexes.* Current opinion in colloid & interface science, 2005. **10**(1–2): p. 52-78.
45. Benton, L.A., et al., *Unexpected Effects of Macromolecular Crowding on Protein Stability.* Biochemistry, 2012. **51**(49): p. 9773-9775.
46. Fulton, A.B., *How crowded is the cytoplasm?* Cell, 1982. **30**(2): p. 345-347.
47. Sasahara, K., P. McPhie, and A.P. Minton, *Effect of dextran on protein stability and conformation attributed to macromolecular crowding.* J Mol Biol, 2003. **326**(4): p. 1227-37.
48. Uversky, V.N., J.R. Gillespie, and A.L. Fink, *Why are "natively unfolded" proteins unstructured under physiologic conditions?* Proteins, 2000. **41**(3): p. 415-27.

CHAPTER 6 Significance and Future Directions

6.1 Significance

The data described in this thesis indicates that the biometric approach could be used to successfully ASE proteins at very high efficiency and bring about release of active proteins over 60 days [1]. The biomimetic approach provides significant advantages over traditional encapsulation paradigms. For example, a) outstanding protein stability during encapsulation is observed owing to the absence of organic solvents, high shear, and other protein-denaturing processes; b) high protein loading (~ 4-7 % w/w) and efficiency (>90%) of encapsulation is achievable suitable for pharmaceutical protein controlled release by simple mixing of blank BP-PLGA microspheres with aqueous protein solution and heating; c) appropriately chosen BPs can act as potential co-factors for the protein being delivered, greatly enhancing therapeutic effect, and reducing protein dosage and costs; d) there is a potential for controlled release of active protein over 4-8 weeks; and e) a potential to sterilize ASE microsphere formulations by gamma irradiation, allowing for bulk manufacturing for multiple growth factors or other compatible proteins [2].

This work builds upon the previous work done in our group [3, 4], by expanding our self-encapsulation paradigm for therapeutic proteins at low protein concentrations making it

possible to quickly develop and evaluate controlled release formulations. In the past, 4-10 % w/w LYZ loading was reported via passive self-encapsulation using 250 mg/ml LYZ [5], but the prohibitive cost of this approach is not very feasible for encapsulation of recombinant therapeutic proteins. In contrast, ASE of pharmaceutical proteins using the biomimetic approach described here could be brought about by simply mixing microsphere formulations with low concentration protein solutions (<10 mg/ml), to reduce losses of expensive recombinant proteins during formulation. The ease of developing and evaluating new pharmaceuticals using this approach along with the potential to bring about sterilization at the end [2], could potentiality overcome some of the issues seen with scale-up [6], and open up avenues for commercialization of new PLGA based microsphere delivery systems. The ability of BPs to act as co-factors and enhance the biological effect of the protein could potentially reduce dosage and cut costs [7-9].

The absorption data also supports the use of this approach as a new facile method to microencapsulate off-the-shelf therapeutic proteins with SM polymer excipients, suggesting that suitably selected BPs could be incorporated in materials of any shape and form, e.g., eluting stents, sutures, biodegradable implants, etc., for protein delivery.

6.2 Issues and Future Directions

One of the major issues with the development of BP-PLGA ASE microspheres was related to the change in properties of the system brought about by use of new batches of PLGA and BP. This issue is common across development done at lab scale and leads to inconstancies among the data produced. This was seen in loading and release data reported in chapter 4 (Figure 4-14).

Another concern was the possibility of BP leeching out of the BP-PLGA microsphere during the loading and release process. This was more plausible in the case of BP with a low M_w, e.g. LDS and HP. Leeching was seen in some cases with LDS, especially with the attempts to ASE anti-VEGF Fab. Due diligence is also required to ensure that the protein is stable during the loading and pore closing, due to prolonged exposure to a high temperature (for pore closure).

A better understanding of the pore closing phenomenon would allow us to improve BP-PLGA microsphere's pore closing properties. The addition of excipients and BPs would also affect PLGA pore closure, and needs to be studied in detail. Some of the BPs are hydrophilic and hygroscopic, absorbing high amounts of water and potentially acting as plasticizers. Understanding the thermodynamics and kinetics of BP-protein interactions is crucial for developing LAR products. The role of k_a and M_w of BP on protein binding and retention inside the microsphere needs to be better understood to develop better formulations with desired release kinetics. One way to gain better insight would be to

determine the interactions and concentrations of BPs and proteins inside the micro-pores of the PLGA microspheres. Efforts should also be directed towards investigating the effect of BP and its distribution on the pore structure of the PLGA polymer. For example, we need to understand how to control the co-distribution of BPs and encapsulated protein, which would be important for developing formulations with optimal release kinetics and minimal protein residue in the polymer matrix.

6.3 References

1. Shah, R.B. and S.P. Schwendeman, *A biomimetic approach to active self-microencapsulation of proteins in PLGA.* Journal of Controlled Release, 2014. **196**(0): p. 60-70.
2. Desai, K.-G., S. Kadous, and S. Schwendeman, *Gamma Irradiation of Active Self-Healing PLGA Microspheres for Efficient Aqueous Encapsulation of Vaccine Antigens.* Pharmaceutical Research, 2013. **30**(7): p. 1768-1778.
3. Reinhold, S.E., et al., *Self-Healing Microencapsulation of Biomacromolecules without Organic Solvents.* Angewandte Chemie International Edition, 2012. **51**(43): p. 10800-10803.
4. Desai, K.-G.H. and S.P. Schwendeman, *Active self-healing encapsulation of vaccine antigens in PLGA microspheres.* Journal of Controlled Release, 2013. **165**(1): p. 62-74.
5. Reinhold, S.E. and S.P. Schwendeman, *Effect of polymer porosity on aqueous self-healing encapsulation of proteins in PLGA microspheres.* Macromolecular Bioscience, 2013. **13**(12): p. 1700-10.
6. Brown, L.R., *Commercial challenges of protein drug delivery.* Expert Opinion on Drug Delivery, 2005. **2**(1): p. 29-42.
7. Pike, D.B., et al., *Heparin-regulated release of growth factors in vitro and angiogenic response in vivo to implanted hyaluronan hydrogels containing VEGF and bFGF.* Biomaterials, 2006. **27**(30): p. 5242-5251.
8. Jones, L.S., B. Yazzie, and C.R. Middaugh, *Polyanions and the Proteome.* Molecular & Cellular Proteomics, 2004. **3**(8): p. 746-769.
9. Lai, P.-H., et al., *Acellular biological tissues containing inherent glycosaminoglycans for loading basic fibroblast growth factor promote angiogenesis and tissue regeneration.* Tissue Engineering, 2006. **12**(9): p. 2499-2508.